VARIABILITY IN COASTAL SHARK POPULATIONS ACROSS MULTIPLE SPATIOTEMPORAL SCALES

Martin Tomas Benavides

A dissertation submitted to the faculty at the University of North Carolina at Chapel Hill in partial fulfillment of the requirements for the degree of Doctor of Philosophy in the Department of Marine Sciences in the College of Arts and Sciences.

Chapel Hill
2020

Approved by:

F. Joel Fodrie

Charles Peterson

Stephen Fegley

Johanna Rosman

Nathan Bacheler

ABSTRACT

Martin Tomas Benavides: Variability in coastal shark populations across multiple spatiotemporal scales
(Under the direction of F. Joel Fodrie)

Variability across spatiotemporal scales has been recognized by ecologists as a fundamental issue in understanding ecosystem dynamics. Sharks emerged as a conservation concern as their populations declined and their influence on marine ecosystem dynamics became apparent. Efforts to better manage and understand shark populations and their response to anthropogenic pressures have been hindered by a lack of understanding of patterns across multiple scales of time and space. This dissertation aimed to describe patterns of variability in coastal shark populations across multiple spatiotemporal scales.

Chapter 1 exploits a 45-year time series of shark monitoring to describe patterns of seasonality in the coastal shark community in Onslow Bay, North Carolina, and how seasonality shifted over long timescales (interannual-decadal). Seasonal turnover in coastal shark community composition was correlated with temperature changes, with spring/autumn species appearing first and subsequently being replaced by summer species before appearing again in autumn; both transitions occurred at approximately 25 °C. On interannual scales, this seasonal pattern was overshadowed by increases in abundance of the Atlantic sharpnose shark (*Rhizoprionodon terraenovae*), a non-seasonal species caught during all months of sampling. Chapter 2 utilizes the long-term data set to investigate within-species size structure over four decades. My analyses suggest declining trends in size for all species analyzed, with the strongest evidence for size

declines in two small coastal shark species, Atlantic sharpnose shark and blacknose shark (*Carcharhinus acronotus*). These results provide insight on assemblage-level responses to anthropogenic pressure via environmental or genetic mechanisms.

Chapter 3 employs acoustic telemetry to decipher bonnethead shark (*Sphyrna tiburo*) movement and behavior (e.g., residency and habitat use) over multiple spatiotemporal scales. My results suggest individual bonnethead sharks show fidelity across years to specific areas within estuaries in North Carolina and Georgia during seasonal residency and have affinity for areas nearest inlets. Finally, Chapter 4 evaluates shark detection probabilities from aerial drone surveys and how these were affected by environmental conditions in a temperate estuary. Shark detection from drone surveys was most influenced by depth, wind speed, and time of day; the highest detection probabilities occurred at shallow depth, low wind speed, and mid-day flight times.

ACKNOWLEDGEMENTS

Many people influenced this work, too many to make an exhaustive list possible. First and foremost, I would like to thank my advisor and mentor Joel Fodrie, whose incisive intellect and patient guidance I depended on to complete this process. I thank my committee members Pete Peterson, Steve Fegley, Johanna Rosman, and Nate Bacheler for their thoughtful comments that helped focus my dissertation research and develop my thinking as a scientist. I thank my collaborators Matt Kenworthy, Jeb Byers, Dave Johnston, Amy Yarnall, and Giada Bargione for their critical assistance with fieldwork and data analysis for my dissertation chapters. I thank others who have been immensely helpful in the field or with data sharing/processing, specifically Danielle Keller, Shelby Ziegler, Max Tice-Lewis, Mayor Rett Newton, Julian Dale, Jacob Krause, Connor Neagle, Austin Moore, and Cameron Luck.

Over the years many have contributed to the UNC-IMS shark survey program and without them this dissertation would not have been possible, above all Dr. Frank Schwartz, whose visionary efforts established the survey and oversaw it for nearly its entirety. I also thank Captains John Purifoy and Stacy Davis who ran the survey trips during my tenure at UNC-IMS, as well as the UNC-IMS shop crew who ran the gear: Glenn Safrit, Claude Lewis, and Phil Herbst. There were also innumerous undergraduate students, interns, and outside volunteers who assisted me, for which I am deeply grateful.

I was funded for most of my graduate tenure at UNC-IMS through a doctoral scholarship awarded to me by the Peruvian National Council for Science and Technology (CONCYTEC),

without which this research would not have been possible. I am also grateful to the UNC Department of Marine Sciences for their support during the admissions process and providing funding during the last year of my dissertation research. Specifically, I would like to thank Marc Alperin, who was instrumental in navigating the admissions process, which was perhaps uniquely challenging for me due to my scholarship. The UNC-IMS shark survey was funded in its early years by the Carolina Power & Light Company and throughout by the University of North Carolina. I am also grateful to the North Carolina Aquarium Society for funding my research on bonnethead movement and drone surveys. I thank the Atlantic Cooperative Telemetry Network and the FACT Network, and the many members of these networks who shared acoustic telemetry data with me that greatly increased the spatial coverage of my bonnethead tracking efforts.

Finally, I thank my family, who provided endless love and support that helped me through this experience.

TABLE OF CONTENTS

LIST OF TABLES

LIST OF FIGURES

LIST OF ABBREVIATIONS AND SYMBOLS

BOFFFF	Big old fat fecund female fish
CPUE	Catch per unit effort
df	Degrees of freedom
FL	Fork length
FLa	Florida
GA	Georgia
$L_{90\%}$	90^{th} percentile of fork length
N	Number or sample size
NC	North Carolina
NIR	Near-infrared filter
nMDS	Non-metric multidimensional scaling
NOAA	National Oceanic and Atmospheric Administration
p	Probability value
r^2	Coefficient of determination
RE	Red-edge filter
RGB	Regular filter
SC	South Carolina
SE	Standard error
SST	Sea surface temperature
TL	Total length
UNC-IMS	University of North Carolina Institute of Marine Sciences
UAS	Unoccupied aircraft system

US	United States
X^2	Chi-square value
Z	Z value

INTRODUCTION

Biological oceanographers have long been aware of the importance of understanding variability across a spectrum of spatiotemporal scales as a fundamental issue in marine ecological dynamics, first illustrated by Stommel (1963). In deed the concept of pattern and scale in understanding organismal and environmental variability has become a unifying concept in ecology (Haury et al. 1978; Steele 1978; Vance and Doel 2010). An integrated approach to understanding marine ecosystem dynamics emerged, one that coupled the study of biological and physical processes of the oceans across scales (Legendre and Demers 1984). For example, in Legendre (1981), the alternation of stabilization and destabilization of the water column was proposed as a hydrodynamic mechanism conducive to enhancing primary productivity in an estuarine system, accounting for the variability documented on annual scales, such as the spring bloom and subsequent phytoplankton growth (Gilmartin 1964), as well as small-scale turbulence (Savidge 1981). Importantly, however, this tight coupling of biological processes to physical processes for phytoplankton appears to break down at longer timescales (interannual to multidecadal), suggesting the increased variability on these timescales is under the control of other physical mechanisms or perhaps biological mechanisms such as zooplankton grazing (Barton et al. 2015).

For zooplankton, the pattern appears to be somewhat opposite, showing increases in variability relative to their resource (phytoplankton) at the finer scales (Mackas et al. 1985;

Weber et al. 1986; Levin 1992). Steele (1978) used the time and space scales of lifespan as a simplistic representation of relevant scales for trophic levels, including phytoplankton, zooplankton and fish. While useful for illustrating the conceptual problem of observational scale in resolving pattern at successively higher trophic levels, this simplistic depiction may not always be an accurate representation of true trophic dynamics of the system, which could cause the coupling of physical forcing and biological response to occur on widely divergent scales (Denman 1994). Moreover, as recognized by Haury et al. (1978) through the use of a variable time scale in the definition of ambit for long-lived organisms, pattern and its relationship to physical processes will vary depending on the temporal scale of the biological process of interest (e.g., daily foraging, annual migrations, lifetime distribution). For instance, in their study of scale dependent processes of marine birds, Hunt and Schneider (1987) showed that the distribution of birds on meso- to mega-scales (100 - 3,000 km+) is closely related to the presence and periodicity of upwelling systems (Brown 1979). Conversely, on the coarse-scale (1 – 100 km), concentrations of seabirds appear to be poorly correlated with conditions related to upwelling water masses (see Abrams and Griffiths 1981), with patchiness hypothesized to be related to species-specific responses such as prey preferences and foraging strategy (Schneider and Duffy 1985).

Sharks are one group of long-lived marine megafauna that have life history adaptations, such as slow growth and late maturity, that make them vulnerable to overexploitation and bycatch mortality (Musick 1999). This group has been given increasing conservation attention as populations have declined and due to their role as apex predators structuring marine food webs. In marine ecosystems, sharks can also serve as important indicators for responses to ecological disturbance as a result of their trophic position and relatively sensitive life history characteristics

(Fulton et al. 2005). Efforts to assess shark populations have been hindered by a paucity of quantitative information and the challenge of reconciling information on a number of relevant spatiotemporal scales to represent species dynamics accurately (Dulvy et al. 2008; Pilling et al. 2009). Understanding patterns in variability of shark populations across a spectrum of spatiotemporal scales is critical if we are to properly assess and conserve these species; this variability may also serve as a record of ecosystem responses to increasing anthropogenic pressures occurring over a range of scales in time and space. Only one published study has explicitly looked at variability across a broad range of spatiotemporal scales in a shark species, *Cetorhinus maximus*, which examined correlations of surface sightings with environmental parameters and found basking shark distribution to be determined largely by zooplankton abundance at local scales, whereas at larger scales it was significantly correlated with thermal boundaries characteristic of tidal and shelf-break fronts (Cotton et al. 2005).

Sharks are a group of large, mobile, and generally uncommon species that can make predicting absolute densities from any single survey approach nearly impossible. An increasing array of emergent technologies can be used in combination with traditional survey approaches to provide new insights in investigations of almost every aspect of shark biology (Carrier et al. 2018). Moreover, each survey approach is particularly suited for sampling at specific scales in time and space. By combining survey approaches there is the potential to synthesize information across spatiotemporal scales. As an example, traditional fishing surveys, suited for gathering long-term data at specific locations, can be combined with acoustic or satellite tracking data that provide potentially greater spatial coverage.

This dissertation investigated patterns in variability of coastal shark populations across multiple spatiotemporal scales using a combination of observational studies and manipulative

field experiments. Chapters 1 & 2 both utilize the long-term dataset from the University of North Carolina at Chapel Hill Institute of Marine Sciences (UNC-IMS) shark survey. Chapters 3 & 4 use acoustic telemetry and drone surveys, respectively, as part of a two-year effort to study bonnethead sharks (*Sphyrna tiburo*) in both North Carolina (NC) and Georgia (GA) estuaries. Chapter 1 focuses on seasonal patterns of the coastal shark community and how these patterns changed on decadal timescales. Chapter 2 focuses on within-species size changes at interannual and decadal timescales. Chapter 3 examines the residency and distribution of bonnethead sharks along the southeast United States (US) Atlantic coastline over multiple spatiotemporal scales. Finally, Chapter 4 assesses detection probabilities from drone surveys for sharks in temperate estuaries and the effects of different environmental variables on these detection probabilities.

REFERENCES

Abrams, R., and A. Griffiths. 1981. Ecological structure of the pelagic seabird community in the Benguela Current region. Marine Ecology Progress Series 5:269–277.

Barton, A. D., M. S. Lozier, and R. G. Williams. 2015. Physical controls of variability in north Atlantic phytoplankton communities. Limnology and Oceanography 60(1):181–197.

Brown, R. G. B. 1979. Seabirds of the Senegal Upwelling and Adjacent Waters. Ibis 121(3):283–292.

Carrier, J. C., M. R. Heithaus, and C. A. Simpfendorfer, editors. 2018. Shark research: emerging technologies and applications for the field and laboratory. CRC Press, Boca Raton, FL.

Cotton, P. A., D. W. Sims, S. Fanshawe, and M. Chadwick. 2005. The effects of climate variability on zooplankton and basking shark (Cetorhinus maximus) relative abundance off southwest Britain. Fisheries Oceanography 14(2):151–155.

Denman, K. L. 1994. Scale-determining biological-physical interactions in oceanic food webs. Pages 377–402 *in* P. S. Giller, A. G. Hildrew, and D. G. Raffaelli, editors. Aquatic ecology: scale, pattern and process. Blackwell Scientific Publications, Oxford.

Dulvy, N. K., J. K. Baum, S. Clarke, L. J. V. Compagno, E. Cortés, A. Domingo, S. Fordham, S. Fowler, M. P. Francis, C. Gibson, J. Martínez, J. A. Musick, A. Soldo, J. D. Stevens, and S. Valenti. 2008. You can swim but you can't hide: the global status and conservation of oceanic pelagic sharks and rays. Aquatic Conservation: Marine and Freshwater Ecosystems 18(5):459–482.

Fulton, E. A., A. D. M. Smith, and A. E. Punt. 2005. Which ecological indicators can robustly detect effects of fishing? ICES Journal of Marine Science 62(3):540–551.

Gilmartin, M. 1964. The primary production of a British Columbia fjord. Journal of the Fisheries Research Board of Canada 21(3):505–538.

Haury, L. R., J. A. McGowan, and P. H. Wiebe. 1978. Patterns and processes in the time-space scales of plankton distributions. Pages 277–327 *in* J. H. Steele, editor. Spatial Pattern in Plankton Communities. Springer, Boston, MA.

Hunt, G. L., and D. C. Schneider. 1987. Scale dependent processes in the physical and biological environment of seabirds. Pages 7–41 *in* J. P. Croxall, editor. Seabird Feeding Ecology. Cambridge University Press, Cambridge.

Legendre, L. 1981. Hydrodynamic control of marine phytoplankton production: the paradox of stability. Pages 191–207 *in* J. C. J. Nihoul, editor. Ecohydrodynamics: Proceedings of the 12th International Liège Colloquium on Ocean Hydrodynamics. Elseiver Oceanography Series Volume 32.

Legendre, L., and S. Demers. 1984. Towards dynamic biological oceanography and limnology. Canadian Journal of Fisheries and Aquatic Sciences 41:2–19.

Levin, S. A. 1992. The problem of pattern and scale in ecology: the Robert H. MacArthur Award lecture. Ecology 73(6):1943–1967.

Mackas, D. L., K. L. Denman, and M. R. Abbott. 1985. Plankton patchiness: biology in the physical vernacular. Bulletin of Marine Science 37(2):653–674.

Musick, J. A. 1999. Ecology and conservation of long-lived marine animals. American Fisheries Society Symposium 23:1–10.

Pilling, G. M., P. Apostolaki, P. Failler, C. Floros, P. A. Large, B. Morales-Nin, P. Reglero, K. I. Stergiou, and A. C. Tsikliras. 2009. Assessment and management of data-poor fisheries. Pages 280–305 *in* A. Payne, J. Cotter, and T. Potter, editors. Advances in Fisheries Science: 50 years on from Beverton and Holt. Blackwell Publishing, Ltd, Oxford.

Savidge, G. 1981. Studies of the effects of small-scale turbulence on phytoplankton. Journal of the Marine Biological Association of the United Kingdom 61(02):477. Cambridge University Press.

Schneider, D., and D. Duffy. 1985. Scale-dependent variability in seabird abundance. Marine Ecology Progress Series 25:211–218.

Steele, J. H. 1978. Some Comments on Plankton Patches. Pages 1–20 *in* J. H. Steele, editor. Spatial Pattern in Plankton Communities. Springer, Boston, MA.

Stommel, H. 1963. Varieties of oceanographic experience. Science 139(3555):572–576.

Vance, T., and R. E. Doel. 2010. Graphical methods and cold war scientific practice: the Stommel diagram's intriguing journey from the physical to the biological environmental sciences. Historical Studies in the Natural Sciences 40(1):1–47.

Weber, L. H., S. Z. El-Sayed, and I. Hampton. 1986. The variance spectra of phytoplankton, krill and water temperature in the Antarctic Ocean south of Africa. Deep Sea Research Part A, Oceanographic Research Papers 33(10):1327–1343.

CHAPTER 1: TEMPORAL PATTERNS OF COASTAL SHARK COMMUNITY STRUCTURE IN ONSLOW BAY, NORTH CAROLINA

Introduction

Understanding how biological communities are organized in time and space and how these patterns are related across scales is perhaps one of the most fundamental challenges for both theoretical and applied ecology (Levin 1992). With increasing global change brought about by anthropogenic pressures such as overexploitation and climate change, being able to detect shared patterns of variation in biological communities and extrinsic influences is an important first step in predicting consequences of these influences (McGowan 1990). Due to their ability to provide historical context or baselines, long-term data sets provide unique insight for disentangling the effects of anthropogenic effects operating on both global scales (e.g., climate change) and local or regional scales (e.g., overfishing), as well as segregating these effects from natural changes (Mieszkowska et al. 2014). Discerning the effects of human pressures, often coupled across scales, is complicated, as illustrated by recent studies suggesting a synergistic effect of climate and exploitation, with top predator removal and concurrent climate change causing complex and cascading top-down effects (Kirby et al. 2009; Planque et al. 2010). In marine ecosystems, sharks could serve as important indicators for system-wide responses to ecological disturbance as a result of their trophic position and relatively sensitive life history characteristics (Fulton et al. 2005).

Most shark species show patterns of seasonal migrations as a life history adaptation, which is thought to be related to reproduction, shifting prey distributions, and seasonal changes in water

temperatures (Springer 1967; Bres 1993; Heithaus 2004; Knip et al. 2010; Schlaff et al. 2014). For coastal shark species in the Atlantic, these migrations can range up to 3,800 km, a distance traveled by the dusky shark (*Carcharhinus obscurus*) between the waters off of Long Island, New York and the southwestern Gulf of Mexico (Casey and Kohler 1991). Of the 33 species of Atlantic sharks tagged as part of the National Marine Fisheries Service's Cooperative Shark Tagging Program between 1962-1993, only the Greenland shark (*Somniosus microcephalus*) showed no evidence of migration from tag recaptures (Kohler et al. 1998). Understanding coastal shark migrations, and in particular the seasonal windows associated with these migrations, is critical to proper implementation of stock management (Bonfil 1997). Unfortunately, in many instances this information is lacking, depriving management agencies of the information required to coordinate local and regional management efforts (Speed et al. 2010).

Establishing temporal patterns in coastal shark community structure across seasonal, interannual, and decadal scales can be used as a baseline for evaluating the effects of anthropogenic disturbances, such as climate change and fishing pressure, as well as aid in predicting the consequences of these disturbances to inform future management decisions. To that end, I used data from a 46-year shark monitoring program to explore temporal patterns of coastal shark community composition through a combination of univariate and multivariate analyses. The objectives of this study were to 1) investigate temporal patterns in coastal shark community structure of Onslow Bay, North Carolina across seasonal, interannual and decadal scales, and 2) examine any correlations of community structure with temperature changes throughout the survey period.

Methods

Field Sampling

To assess temporal variation in coastal shark community assemblage, I used species-specific time series data generated during the course of a 1973-2018 fishery independent shark survey in Onslow Bay. The survey was conducted by the University of North Carolina at Chapel Hill's Institute of Marine Sciences (UNC-IMS) and since its inception, the UNC-IMS shark survey has employed standardized longline sampling gear at two fixed stations in Onslow Bay: 4 km (34.6338°N, 76.6306°W, 15 m depth) and 13 km (34.5512°N, 76.6237°W, 17 m depth) southeast of Beaufort Inlet. During each deployment at each station, a 7.6 mm braided nylon longline extended 1 km, with gangion lines attached to the mainline at every 10 m (N = 100). Each gangion consists of a 1.8 m long, #2-chain leader and a 9/0 Mustad tuna J hook. Polyball buoys are attached between every 10 gangions (100-m separation), allowing the longline gear to fish the entire water column at each station.

In addition to standardized gears and stations, consistent deployment methods have been used since the first sets were made in 1973. Survey trips are conducted biweekly, between April and November each year, on 10-15-m research vessels operated by UNC-IMS. A demersal trawl is used at the start of each survey day to collect bait (e.g., spot *Leiostomus xanthurus*, Atlantic croaker *Micropogonias undulatus*), which are attached subsequently through the operculum onto hooks (one fish per hook). Longline deployment occurs between 0800 and 1300 hours, with the gear soaking for one hour during each set. Efforts are made to deploy at each station on each scheduled survey day (weather dependent), and the inshore set is typically, but not always, made first. Environmental variables (sea surface temperature [SST], wind conditions, tide, and sea state) are recorded for each set. All captured sharks are identified to species, sexed, and measured

for fork length (FL) and total length to the nearest mm. Live individuals are outfitted with an external dart tag and returned to the water (~90% of catch). The survey is conducted under UNC-IMS Institutional Animal Care and Use Committee protocol 19-137.0.

Data Analysis

I selected 12 of the 21 shark species caught in the survey for seasonality analyses generally based on large overall sample sizes (N > 100 individuals captured): blacknose shark (*Carcharhinus acronotus*), spinner shark (*Carcharhinus brevipinna*), silky shark (*Carcharhinus falciformis*), finetooth shark (*Carcharhinus isodon*), blacktip shark (*Carcharhinus limbatus*), dusky shark, sandbar shark (*Carcharhinus plumbeus*), smooth dogfish (*Mustelus canis*), Atlantic sharpnose shark (*Rhizoprionodon terraenovae*), and scalloped hammerhead shark (*Sphyrna lewini*). Two species had lower sample sizes (bull shark *Carcharhinus leucas,* N = 26; tiger shark *Galeocerdo cuvier,* N = 46), but were added due to being large coastal sharks of general public interest. For each focal species, I evaluated catch per unit effort (CPUE) from all samples with non-zero catch (due to zero-inflation) as a function of day of year, as well as SST measurements taken during the survey, to reveal any seasonal trends or correlation with SST in the catch data. Visual inspection of abundances allowed me to categorize species for seasonality as spring/autumn (bimodal annual peaks in CPUE with absence during summer months) or summer (single annual peak in CPUE during summer months). Monthly mean CPUE values were computed for each of the 12 focal species across all years, and the maximum value identified for each species. I used these maxima to generate a ratio for each month, which was the proportion of the maximum monthly mean CPUE that each month represented. This ratio ranged from 0 to 1, with 0 representing a month where no sharks were caught and 1 representing the month with

the maximum mean CPUE value. This index was examined across the 12 focal species to look for patterns of seasonal succession or turnover in community assemblage.

To better understand how temperatures might be associated with different months of the year, I explored mean SST as a function of month. I also fit Gaussian curve models to CPUE data as a function of SST, using the 'nls2sol' algorithm from the Port library (https://netlib.sandia.gov/port/), to determine how the appearance or disappearance of particular species might be related to seasonal temperature changes. These models were used to calculate the inflection points (mean $\pm$ 1 standard deviation) to infer temperatures associated with periods of entrance and exit for each species. Only the lower-temperature inflection point was utilized for non-seasonal and summer seasonal species since they both entered and exited during colder temperatures. Conversely, for spring/autumn seasonal species, both inflection points were utilized, since they first exited as waters warmed in summer, returning again in milder autumn months before their final exit. Model fit was assessed visually and using *p*-values of *t*-tests for model parameters (mean, standard deviation). Models that failed to converge, surpassed a *p*-value of 0.1 for any parameter, or failed to accurately represent the data based on visual inspection (i.e., where a majority of data points fell outside the range of the Guassian curve) were not utilized.

Catch data for all 21 species caught in the survey were aggregated into a species by set matrix with CPUE values calculated for each set and species as sharks per 100 hooks. I further aggregated samples by day (i.e., both inshore and offshore sets) as well as by year, separately, as mean CPUE values, to analyze seasonal and interannual community structure and potential correlation with SST. I chose to include only days in which two longline sets were conducted and a SST measurement was taken for daily aggregations, to remove the effects of differences in

effort between days and allow for correlation with SST. For both daily and yearly aggregations I calculated mean SST across longline sets within each grouping, for use in correlation analyses.

The daily and annual mean CPUE data were then examined by non-metric multidimensional scaling (nMDS) analyses using the R package vegan (Oksanen et al. 2019), to examine patterns of community dissimilarity across multiple timescales free of assumptions of normality or other specific underlying distributions that constrain many other multivariate analyses. I performed a Wisconsin double standardization on the data, which first standardized CPUE values by each species' observed maximum, followed by sample (i.e., daily or annual aggregations) total maximum. This allowed for a uniform basis for comparison, such that values for each species indicated relative contribution to the sample aggregate, in relation to its maximum contribution in the entire series (Bray and Curtis 1957). I excluded extremely rare species (i.e., 3 individuals or less over the entire survey interval, leaving a total of 15 species), which have considerably lower information content and could become over-weighted by the standardization, causing spurious results (Cao et al. 2001). I then constructed a dissimilarity matrix using the Bray-Curtis distance metric, which is widely used in analysis of community data, due to its robustness and ability to capture important assemblage relationships having ecological relevance (Faith et al. 1987; Clarke et al. 2006). To further examine potential drivers of seasonal variation, I calculated and plotted species weighted average scores onto the daily nMDS plot, as well as fitting a vector for which changes in SST are most correlated with the ordination structure. Each data point was color coded by day of year to examine potential seasonal patterns. For the annual nMDS plot I defined clusters with 10% similarity, to examine where breaks in community structure occurred on interannual scales.

To examine for changes in seasonal community assemblage on decadal time scales, I parsed CPUE data, using the clusters from my annual mean CPUE nMDS analysis. These data were then aggregated as mean CPUE, binned by month, and frequency of occurrence was calculated for each species as the proportion of the total monthly mean CPUE across species. All statistical analyses were performed in R (R Core Team 2016).

Results

The UNC-IMS shark survey database consisted of a total of 596 trips with 1,134 longline sets made using 142,505 baited hooks and 9,266 individual sharks captured across 21 species (Table 1.1). Atlantic sharpnose shark, blacknose shark, dusky shark, and blacktip shark were numerically dominant in terms of raw abundance, representing 77% of the catch (Atlantic sharpnose shark – 40%, blacknose shark – 16%, dusky shark – 11%, blacktip shark – 10%). Individuals from the 21 species caught in the survey ranged in size from 215-2860 mm in FL and represented eight distinct management groupings (Table 1.2).

The majority of the 12 focal species caught in the survey exhibited a summer seasonal pattern (single annual peak in CPUE during summer months): blacknose shark, blacktip shark, bull shark, finetooth shark, scalloped hammerhead shark, spinner shark, and tiger shark. Four of the remaining species were bimodal in abundance with spring/autumn peaks: dusky shark, sandbar shark, silky shark, and smooth dogfish. Only Atlantic sharpnose shark was categorized as non-seasonal (Table 1.3; Figure 1.1). Overall, the pattern of seasonality in CPUE indices among the 12 focal species was characterized by early catches (April-May) of spring/autumn species, along with Atlantic sharpnose shark, before the appearance of summer species in June.

Spring/autumn species were mostly absent from catches during July and August, before reappearing in September or October (Figure 1.2).

Monthly mean temperatures first climbed from 17.6 °C in April to 28 °C in August, before dropping back to 18.7 °C by November (Figure 1.3). Patterns of CPUE as a function of SST were similar among species, with all focal species exhibiting unimodal distributions of CPUE, although the temperature at which these peaks occurred, as well the distribution of points along the temperature axis varied (Figure 1.4). Entrance and exit periods for spring/autumn species were associated with temperatures of 14.2-17.2 °C for first entrance and last exit, as well as 21.3-26.4 °C for first exit and second entrance ($p < 0.01$), although the model for silky shark was rejected upon visual inspection of model fit to data. Summer species (excluding bull shark and tiger shark) displayed entrance and exit temperatures of 19-27.3 °C, although model fit was not statistically clear in the case of blacktip shark and spinner shark ($p < 0.1$). Models for tiger shark and bull shark were rejected due to failure to converge and lack of statistical clarity ($p > 0.5$), respectively (Table 1.3).

Community structure based on multivariate analysis of daily mean CPUE resulted in temporal patterns on both seasonal (shapes of points) and interannual (color of points) time scales, which could be related to specific species based on weighted average scores (Figure 1.5). Temperature was clearly correlated with dissimilarity in community structure along the first and second order axes ($r^2 = 0.37$; $p = 0.001$; Figure 1.5). For community structure based on multivariate analysis of annual mean CPUE there were two clusters defined at the 10% similarity level, which was the level of similarity that gave the most informative split between clusters, since greater similarity resulted in single- or two-year clusters only. The first cluster included the years 1973-1989, while the second cluster included the years 1990-2018 (Figure 1.6).

Community assemblage was dominated by spring/autumn and summer species during the early years of the survey that corresponded to the first nMDS cluster group (1973-1989). During the years corresponding to the second nMDS cluster (1990-2018) Atlantic sharpnose shark became the dominant species in all months except April, which was still dominated by smooth dogfish (Figure 1.7).

Discussion

This study analyzed the longest running shark survey program conducted on the US Atlantic coast to characterize temporal patterns in a diverse assemblage of sharks across multiple time scales and establish a baseline for future studies. Moreover, my analyses show that community structure is correlated with temperature changes on seasonal and perhaps interannual time scales. These data also provide a window into long-term change in the coastal shark community of Onslow Bay, showing an already altered baseline and the potential for future shifts in seasonal community composition as a result of climate change.

Coastal shark community structure is correlated to temperature on seasonal time scales. The statistical clarity ($p < 0.005$) of SST vector fitting to nMDS structure for daily mean CPUE values indicates that temperature is correlated with seasonal changes in community structure (Figure 1.5). Species scores for the 12 focal species in the daily nMDS plot also appeared to separate into groups along the axis for SST in a manner consistent with seasonal categories or temperature preferences (Table 1.3; Figure 1.5). For example, summer species (i.e., blacknose shark, blacktip shark, bull shark, finetooth shark, scalloped hammerhead shark, spinner shark, tiger shark) were grouped together at higher x and lower y values, which correlates with higher SST values. Temperature has been implicated as a driving force for structuring coastal shark

community structure and distribution patterns, which this study supports (Ulrich et al. 2007; Froeschke et al. 2010; Ward-Paige et al. 2015; Plumlee et al. 2018).

CPUE annual patterns of the 12 focal species revealed a transition between spring/autumn and summer species at a threshold of approximately 25 °C. The patterns revealed in the individual species scatterplots of CPUE as a function of time (day of year), as well as the monthly CPUE indices for all 12 species, suggest there is clearly definable seasonal turnover in the community assemblage (Figures 1.1 & 1.2). This appears to be correlated to temperature, as indicated by the calculations of periods of entrance and exit for each species as a function of SST, which align with the range of monthly mean temperatures during months that each species is observed (Table 1.3; Figures 1.1 & 1.3). Furthermore, the range of temperatures associated with periods of first exit in spring/autumn species (21.3-26.4 °C) roughly coincides with the range of temperatures associated with periods of entrance for summer species (19-27.3 °C), with a majority of the species turnover having taken place when temperatures reach 25-26 °C (Table 1.3). Whereas previous work found that spring/autumn species (e.g., sandbar sharks) remained throughout summer months, I found that they were absent, which could be caused by differing sampling methodologies, with other studies sampling estuarine waters (Schwartz 2003; Ulrich et al. 2007; Drymon et al. 2010). Temperature thresholds have been hypothesized to stimulate migration in coastal sharks, often to or from nursery areas in estuarine waters, which may explain the discrepancy in results for sandbar sharks (e.g., Grubbs et al. 2007; Heupel 2007).

Here, I document long-term changes to the coastal shark community, taking place across multiple temporal scales, while also highlighting the potential for future shifts in community structure as a result of climate change. Interannual community composition analyses suggest that perhaps species that have increased in abundance (i.e., Atlantic sharpnose shark) during the

survey period could continue to be numerically dominant (Figures 1.6 & 1.7). Two other meta analyses of survey data from these regions found population increases in Atlantic sharpnose shark on decadal timescales and attributed these to mesopredatory release as a result of the overfishing of large coastal sharks and implementation of bycatch reduction devices, mechanisms which could explain the dominance of this species (Myers et al. 2007; Peterson et al. 2017). In that context, the results of this study underscore the need for future, targeted studies to resolve potential causes of the rise in Atlantic sharpnose shark populations. Concurrently, I suggest clues to predicting future shifts as a result of climate change can be found on seasonal time scales, where if observed seasonal migration onsets/endpoints correlated with temperature changes continue to hold, I would hypothesize that all species would begin to show up slightly earlier in the year and stay later as water temperatures warm earlier and stay warm later. This could favor summer species to become more numerically dominant, as they expand their seasonal presence.

Several assumptions guided the interpretation of my results related to CPUE as a measure of shark abundance. CPUE has been called into question as a measure of abundance, particularly from commercial and recreational fisheries. The use of standardized fishery-independent data from a research survey, however, as in this study, is less susceptible to biases associated with fishery-dependent CPUE data (Harley et al. 2001). Catchability, which is the coefficient relating CPUE to abundance, has also been shown to vary over time and may be related to various environmental variables, including water temperature (Ward 2008). While I acknowledge this may influence estimates of abundance, it is unlikely that this variability would be driving the seasonal patterns since examining monthly percent presence for each species showed similar seasonal patterns to those reported here. Due to the large number of samples with zero catch for

each species I chose to remove zero-catch data when examining seasonal patterns in the 12 focal species. I also used the delta approach, however, modeling presence/absence and abundance data separately and then combining these estimates (sensu Serafy et al. 2007), and seasonal patterns were nearly identical to those reported here when incorporating zero-catch data.

By describing patterns of community structure of coastal sharks in Onslow Bay across temporal timescales, the present study both provides a baseline for future studies and evidence of long-term shifts that could inform future management efforts. Peterson et al. (2017) suggested past management efforts may have led to a recovery of coastal sharks that were overexploited; in that context, the temporal patterns of coastal shark community structure documented here serve as a record by which to judge ongoing recovery. My study is also an important first step in monitoring future assemblage shifts to tease apart the influences of harvest and climate change.

REFERENCES

Bonfil, R. 1997. Status of shark resources in the southern Gulf of Mexico and Caribbean: implications for management. Fisheries Research 29(2):101–117.

Bray, J. R., and J. T. Curtis. 1957. An ordination of the upland forest communities of southern Wisconsin. Ecological Monographs 27(4):325–349.

Bres, M. 1993. The behaviour of sharks. Reviews in Fish Biology and Fisheries 3(2):133–159.

Cao, Y., D. P. Larsen, and R. S.-J. Thorne. 2001. Rare species in multivariate analysis for bioassessment: some considerations. Journal of the North American Benthological Society 20(1):144–153.

Casey, J. G., and N. E. Kohler. 1991. Long distance movements of Atlantic sharks. Pages 87–91 *in* S. H. Gruber, editor. Discovering sharks, 1st edition. American Littoral Society, Highlands, NJ.

Clarke, K. R., P. J. Somerfield, and M. G. Chapman. 2006. On resemblance measures for ecological studies, including taxonomic dissimilarities and a zero-adjusted Bray–Curtis coefficient for denuded assemblages. Journal of Experimental Marine Biology and Ecology 330(1):55–80.

Drymon, J. M., S. P. Powers, J. Dindo, B. Dzwonkowski, and T. A. Henwood. 2010. Distributions of sharks across a continental shelf in the northern Gulf of Mexico. Marine and Coastal Fisheries 2(1):440–450.

Faith, D. P., P. R. Minchin, and L. Belbin. 1987. Compositional dissimilarity as a robust measure of ecological distance. Vegetatio 69(1–3):57–68.

Froeschke, J., G. Stunz, and M. Wildhaber. 2010. Environmental influences on the occurrence of coastal sharks in estuarine waters. Marine Ecology Progress Series 407:279–292.

Fulton, E. A., A. D. M. Smith, and A. E. Punt. 2005. Which ecological indicators can robustly detect effects of fishing? ICES Journal of Marine Science 62(3):540–551.

Grubbs, R. D., J. A. Musick, C. L. Conrath, and J. G. Romine. 2007. Long-term movements, migration, and temporal delineation of a summer nursery for juvenile sandbar sharks in the Chesapeake Bay region. American Fisheries Society Symposium 50:87–107.

Harley, S. J., R. A. Myers, and A. Dunn. 2001. Is catch-per-unit-effort proportional to abundance? Canadian Journal of Fisheries and Aquatic Sciences 58: 1760–1772.

Heithaus, M. R. 2004. Predator-prey interactions. Pages 487–521 *in* J. C. Carrier, J. A. Musick, and Heith, editors. Biology of sharks and their relatives. CRC Press LLC, Boca Raton, FL.

Heupel, M. R. 2007. Exiting Terra Ceia Bay: examination of cues stimulating migration from a summer nursery area. American Fisheries Society Symposium 50:265–280.

Kirby, R. R., G. Beaugrand, and J. A. Lindley. 2009. Synergistic effects of climate and fishing in a marine ecosystem. Ecosystems 12(4):548–561.

Knip, D., M. Heupel, and C. Simpfendorfer. 2010. Sharks in nearshore environments: models, importance, and consequences. Marine Ecology Progress Series 402:1–11.

Kohler, N. E., J. G. Casey, and P. A. Turner. 1998. NMFS cooperative shark tagging program, 1962-93: an atlas of shark tag and recapture data. Marine Fisheries Review 60(2):1.

Levin, S. A. 1992. The problem of pattern and scale in ecology: the Robert H. MacArthur Award lecture. Ecology 73(6):1943–1967.

McGowan, J. A. 1990. Climate and change in oceanic ecosystems: the value of time-series data. Trends in Ecology and Evolution 5(9):293–299. Elsevier Current Trends.

Mieszkowska, N., H. Sugden, L. B. Firth, and S. J. Hawkins. 2014. The role of sustained observations in tracking impacts of environmental change on marine biodiversity and ecosystems. Philosophical Transactions of the Royal Society A 372:20130339.

Myers, R. A., J. K. Baum, T. D. Shepherd, S. P. Powers, and C. H. Peterson. 2007. Cascading effects of the loss of apex predatory sharks from a coastal ocean. Science 315(5820):1846–1850.

NMFS. 2006. Final Consolidated Atlantic Highly Migratory Species Fishery Management Plan. National Oceanic and Atmospheric Administration, National Marine Fisheries Service,

Office of Sustainable Fisheries, Highly Migratory Species Management Division, Silver Spring, MD.

Oksanen, J., F. G. Blanchet, M. Friendly, R. Kindt, P. Legendre, D. McGlinn, P. R. Minchin, R. B. O'Hara, G. L. Simpson, P. Solymos, M. H. H. Stevens, E. Szoecs, and H. Wagner. 2019. vegan: community ecology package. https://cran.r-project.org/package=vegan.

Peterson, C. D., C. N. Belcher, D. M. Bethea, W. B. Driggers, B. S. Frazier, and R. J. Latour. 2017. Preliminary recovery of coastal sharks in the south-east United States. Fish and Fisheries 18(5):845–859.

Planque, B., J. M. Fromentin, P. Cury, K. F. Drinkwater, S. Jennings, R. I. Perry, and S. Kifani. 2010. How does fishing alter marine populations and ecosystems sensitivity to climate? Journal of Marine Systems 79(3–4):403–417.

Plumlee, J. D., K. M. Dance, P. Matich, J. A. Mohan, T. M. Richards, T. C. TinHan, M. R. Fisher, and R. J. D. Wells. 2018. Community structure of elasmobranchs in estuaries along the northwest Gulf of Mexico. Estuarine, Coastal and Shelf Science 204:103–113.

R Core Team. 2016. R: A language and environment for statistical computing. http://www.r-project.org.

Schlaff, A. M., M. R. Heupel, and C. A. Simpfendorfer. 2014. Influence of environmental factors on shark and ray movement, behaviour and habitat use: a review. Reviews in Fish Biology and Fisheries 24(4): 1089–1103.

Schwartz, F. J. 2003. Sharks, skates, and rays of the Carolinas. The University of North Carolina Press, Chapel Hill, North Carolina.

Serafy, J. E., M. Valle, C. H. Faunce, and J. Luo. 2007. Species-specific patterns of fish abundance and size along a subtropical mangrove shoreline: an application of the delta approach. Bulletin of Marine Science 80(3): 609–624.

Speed, C. W., I. C. Field, M. G. Meekan, and C. J. A. Bradshaw. 2010. Complexities of coastal shark movements and their implications for management. Marine Ecology Progress Series 408:275–293.

Springer, S. 1967. Social organization of shark populations. Pages 149–174 *in* P. W. Gilbert, R. F. Matthewson, and D. P. Rall, editors. Sharks, skates, and rays. The John Hopkins Press, Baltimore, MD.

Ulrich, G. F., C. M. Jones, W. B. Driggers, J. M. Drymon, D. Oakley, and C. Riley. 2007. Habitat utilization, relative abundance, and seasonality of sharks in the estuarine and nearshore waters of South Carolina. American Fisheries Society Symposium 50:125–139.

Ward, P. 2008. Empirical estimates of historical variations in the catchability and fishing power of pelagic longline fishing gear. Reviews in Fish Biology and Fisheries 18:408–426.

Ward-Paige, C. A., G. L. Britten, D. M. Bethea, and J. K. Carlson. 2015. Characterizing and predicting essential habitat features for juvenile coastal sharks. Marine Ecology 36(3):419–431.

Table 1.1: Summary of effort, date range, temperature and species-specific catch for each year of UNC-IMS survey. Temperature is shown as mean + 1 standard error. Catch is listed as raw catch for each species.

Year	Survey trips	Longline sets	Hooks	Date range (day of year)	Temperature (°C)	Atlantic sharpnose	Bigeye thresher	Blacknose	Blacktip	Bull	Dusky	Finetooth
1973	6	11	980	170-276	NA	9	0	40	26	3	6	0
1974	9	17	1660	108-284	NA	5	0	21	15	1	70	0
1975	15	26	2527	122-322	18	17	0	62	50	3	123	0
1976	15	26	2192	106-307	20.7 + 1.2	7	0	37	29	0	52	0
1977	16	30	2868	109-314	23.8 + 1.3	20	0	134	34	1	78	1
1978	14	26	2382	102-311	22.1 + 0.8	31	0	61	39	0	12	1
1979	15	29	3129	93-303	23.4 + 0.7	31	0	71	22	4	32	3
1980	15	29	4953	94-288	22.3 + 1.2	60	0	85	83	0	93	0
1981	16	31	4267	105-300	23.2 + 1	31	0	29	12	0	75	1
1982	16	32	5533	110-328	22.8 + 1	16	0	65	33	4	116	2
1983	16	31	5175	111-319	23.2 + 0.9	69	0	33	62	2	51	2
1984	17	34	5340	110-304	24.6 + 0.6	44	0	79	83	1	81	0
1985	16	30	4624	122-301	24.5 + 0.6	77	0	43	23	0	18	0
1986	15	29	4601	104-314	21.1 + 2.1	50	0	24	40	0	35	0
1987	13	25	4369	117-292	26.8 + 0.9	81	0	48	80	0	54	2
1988	17	42	6217	109-291	25 + 0.8	151	0	127	50	0	31	6
1989	16	36	6370	100-289	25 + 0.7	67	0	40	25	0	33	17
1990	15	29	4655	106-302	26 + 0.6	60	0	15	2	0	3	0
1991	14	27	3925	105-302	25.7 + 0.8	86	0	31	29	2	13	0
1992	12	23	3080	118-301	24.3 + 0.9	121	0	45	7	0	0	4
1993	11	21	3090	137-299	27.2 + 0.6	126	0	49	13	1	4	3
1994	15	30	4102	108-304	NA	78	0	32	33	0	11	46
1995	15	29	3803	115-299	25.9 + 0.7	148	0	42	20	1	0	3
1996	12	23	3013	120-288	25.7 + 0.7	82	0	46	31	0	1	9
1997	13	22	2702	119-301	24.3 + 1.1	85	0	12	11	0	3	5
1998	13	24	3140	110-306	24.5 + 0.9	129	1	8	9	0	0	0
1999	11	22	2700	116-299	24 + 0.7	87	0	3	6	0	2	0
2000	13	24	2961	108-300	22.8 + 1.1	117	0	4	12	0	1	0
2001	10	19	1866	135-295	25.5 + 0.7	104	0	11	2	0	1	0
2002	12	24	2870	126-299	25.9 + 0.5	133	0	9	3	0	4	0
2003	11	22	2224	118-286	24.3 + 0.6	138	0	3	1	0	1	0
2004	10	18	1805	117-296	24.7 + 0.7	111	0	5	3	0	10	0
2005	11	21	2118	118-297	24.6 + 1.1	104	0	8	5	0	0	6
2006	14	27	2711	114-299	24.3 + 0.7	119	0	11	2	0	1	1
2007	13	24	2416	116-302	24.3 + 0.7	125	0	25	8	0	3	2
2008	8	15	1506	119-294	23 + 0.8	90	0	2	2	1	1	0
2009	9	15	1497	121-300	24.3 + 0.9	64	0	8	2	0	0	0
2010	11	18	1822	125-285	25.4 + 0.7	89	0	13	2	1	5	0
2011	13	25	2529	111-305	24.1 + 0.9	79	0	16	11	1	5	0
2012	14	25	2514	108-313	23.3 + 0.9	64	0	15	8	0	2	0
2013	10	18	1799	127-295	23.6 + 0.9	93	0	9	4	0	0	0
2014	12	20	2000	133-302	24.9 + 0.6	83	0	22	4	0	0	0
2015	13	23	2283	38-310	24.1 + 1.1	112	0	8	0	0	2	0
2016	14	22	2195	113-306	26.3 + 0.7	112	0	13	1	0	2	0
2017	10	17	1699	108-311	25.4 + 0.8	81	0	6	1	0	0	0
2018	10	23	2293	121-331	26.9 + 0.7	104	0	2	2	0	0	0

Great hammer head	Lemon	Night	Nurse	Sand tiger	Sand -bar	Scalloped hammer-head	Silky	Smooth dogfish	Smooth hammer head	Spin-ner	Spiny dog-fish	Tig-er	White
0	1	0	0	0	0	16	0	0	1	0	0	2	0
0	0	2	2	0	0	9	0	42	0	4	0	1	1
2	0	0	0	0	6	34	0	2	1	6	0	2	0
0	0	0	0	0	2	30	0	20	0	2	0	0	0
1	0	0	0	0	33	36	0	44	0	12	0	1	0
0	0	0	0	1	29	21	0	43	0	20	3	1	0
0	1	0	0	0	36	27	1	62	0	27	5	9	0
0	0	0	0	0	1	45	1	54	0	9	0	4	0
0	0	0	0	0	3	34	0	69	0	2	0	1	0
0	0	0	0	0	4	23	19	27	0	8	0	2	0
0	0	0	0	0	43	34	31	36	0	7	0	1	0
0	0	0	0	0	17	40	12	32	0	2	0	2	0
0	0	0	0	0	19	10	3	4	0	1	0	2	0
0	0	0	0	0	10	14	25	1	0	3	0	3	0
0	0	0	0	0	43	19	16	30	0	12	0	3	0
0	0	0	0	0	17	37	30	6	0	10	0	0	0
0	0	0	0	0	15	4	18	21	1	11	2	0	0
0	0	0	0	0	0	1	5	20	0	0	0	1	0
0	0	0	0	0	2	1	4	7	0	12	1	0	0
0	0	0	0	0	2	1	1	4	0	5	0	0	0
0	0	0	0	0	2	3	1	4	0	4	0	1	0
0	0	0	0	0	24	3	4	2	1	12	0	0	0
1	0	0	0	0	1	0	1	7	0	7	0	0	0
0	0	0	0	0	1	3	2	3	0	14	0	0	0
1	0	0	0	0	3	0	0	0	0	7	0	0	0
0	0	0	0	0	3	1	8	2	0	4	0	1	0
0	0	0	0	0	2	1	0	0	0	9	0	0	0
0	0	0	0	0	1	4	1	3	0	6	0	0	0
0	0	0	0	0	0	1	0	0	0	2	0	0	0
0	0	0	0	0	0	2	1	1	0	0	0	1	0
0	0	0	0	0	0	2	6	3	0	6	0	0	0
0	0	0	0	0	0	2	0	6	0	3	0	0	0
0	0	0	0	0	0	4	2	5	0	5	0	0	0
0	0	0	0	0	1	13	3	6	0	8	0	0	0
0	0	0	0	0	0	8	1	2	0	2	0	1	0
0	0	0	0	0	1	6	0	2	0	0	0	0	0
0	0	0	0	1	0	0	0	0	0	0	0	0	0
0	0	0	0	1	0	2	2	0	4	1	0	0	0
0	0	0	0	0	0	10	1	0	0	10	0	0	0
0	0	0	0	0	0	3	0	0	0	3	0	0	0
0	0	0	0	0	0	12	0	0	0	2	0	0	0
0	0	0	0	0	0	3	0	1	0	11	0	1	0
0	0	0	0	0	0	5	0	1	0	0	1	1	0
0	0	0	0	0	0	3	0	0	0	6	0	3	0
0	0	0	0	0	0	4	0	0	0	0	0	1	0
0	0	0	0	0	2	4	0	1	0	2	0	1	0

Table 1.2: Summary of coastal shark species; longline CPUE (mean ± standard error); FL = fork length, f = female, m = male; management grouping according to NMFS 2006; individuals for which sex was not recorded were omitted for sex ratio calculations.

Species	N	CPUE (sharks/100 hooks)	FL Range (mm)	Sex Ratio (f:m)	Management
Atlantic sharpnose	3690	2.734 + 0.114	215-1315	1689:1936	Non-blacknose small coastal
Bigeye thresher	1	0.001 + 0.001	2860	1:0	Prohibited
Blacknose	1472	0.988 + 0.072	270-1850	289:175	Blacknose
Blacktip	940	0.58 + 0.045	320-2000	343:549	Aggregated large coastal
Bull	26	0.018 + 0.004	390-2370	2:9	Aggregated large coastal
Dusky	1035	0.697 + 0.09	215-2550	283:220	Prohibited
Finetooth	114	0.068 + 0.017	740-1350	15:41	Non-blacknose small coastal
Great hammerhead	5	0.004 + 0.002	1640-2390	1:3	Hammerhead
Lemon	2	0.002 + 0.001	2160	0:1	Aggregated large coastal
Night	2	0.002 + 0.059	NA	1:0	Prohibited
Nurse	2	0.001 + 0.001	1660-2073	0:2	Aggregated large coastal
Sand tiger	3	0.003 + 0.002	1550-1980	0:2	Prohibited
Sandbar	323	0.231 + 0.031	455-2290	283:220	Aggregated large coastal (research only)
Scalloped hammerhead	535	0.374 + 0.03	590-3048	229:270	Hammerhead
Silky	199	0.11 + 0.02	280-1600	108:89	Aggregated large coastal
Smooth dogfish	573	0.487 + 0.07	290-1500	16:9	Smoothhound
Smooth hammerhead	8	0.006 + 0.003	840-1900	3:2	Hammerhead
Spinner	277	0.204 + 0.023	600-2110	79:53	Aggregated large coastal
Spiny dogfish	12	0.01 + 0.005	640-950	12:0	Spiny dogfish
Tiger	46	0.032 + 0,006	710-2510	4:1	Aggregated large coastal
White	1	0.001 + 0.001	NA	1:0	Prohibited

Table 1.3: Summary of seasonality (summer or spring/autumn), first entrance/exit sea surface temperature (SST) for each of the 12 focal species, and second entrance/exit for sprin/autumn seasonal species. Species for which no convergence was found or for which model fit was deemed inappropriate were removed from entrance SST and exit SST calculations.

Species	Seasonality	1st entrance/exit SST (°C)	2nd entrance/exit SST (°C)
Atlantic sharpnose shark	3 season	15.2	NA
Blacknose shark	summer	25	NA
Blacktip shark	summer	25.6	NA
Bull shark	summer	NA	NA
Dusky shark	spring/autumn	17.2	25.4
Finetooth shark	summer	27.3	NA
Sandbar shark	spring/autumn	17	26.4
Scalloped hammerhead shark	summer	21.6	NA
Silky shark	spring/autumn	NA	NA
Smooth dogfish	spring/autumn	14.2	21.3
Spinner shark	summer	19	NA
Tiger shark	summer	NA	NA

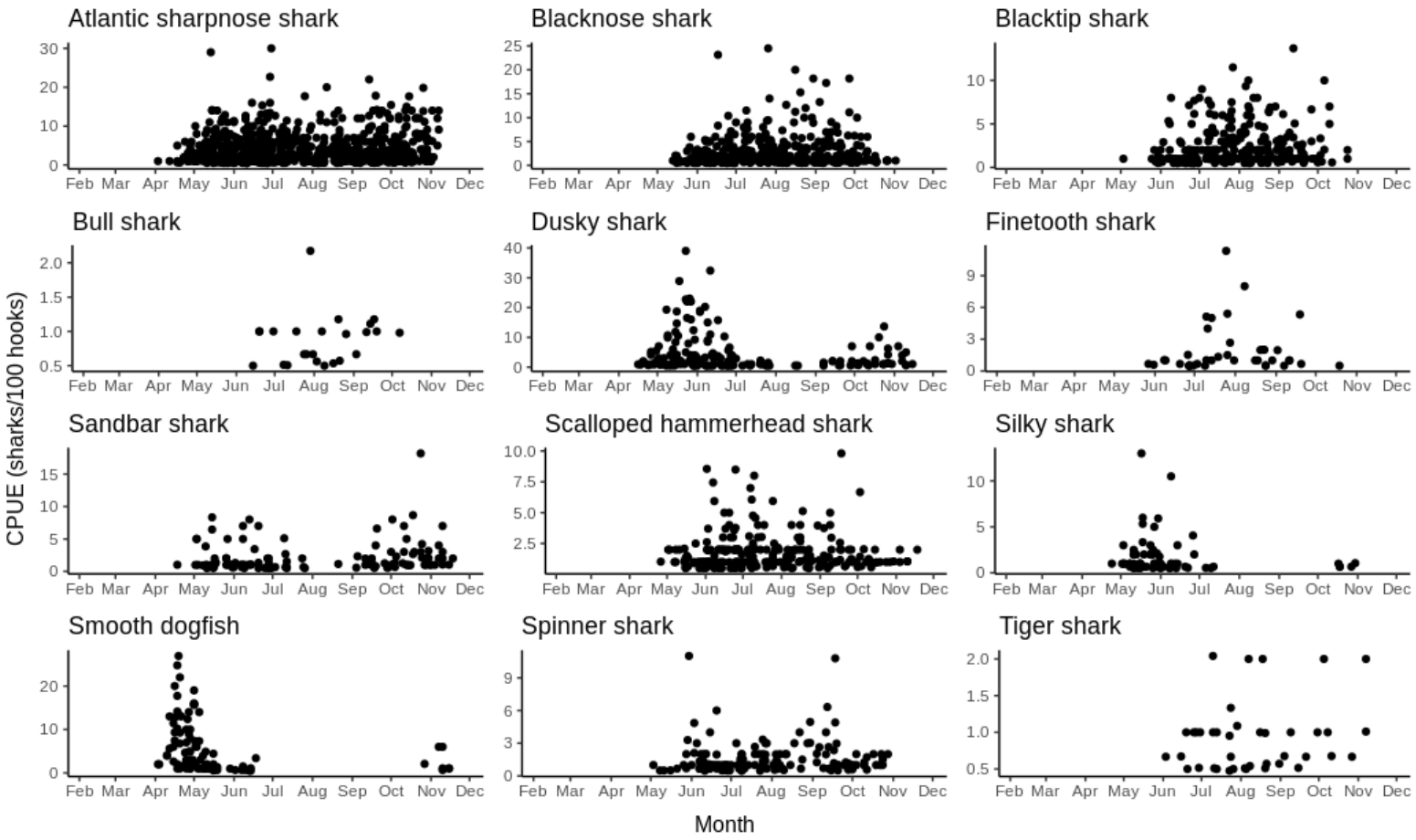

Figure 1.1: Scatterplots of CPUE by day of year for each of the 12 focal species. Axis for day of year has been converted to monthly scale to aid in interpretation.

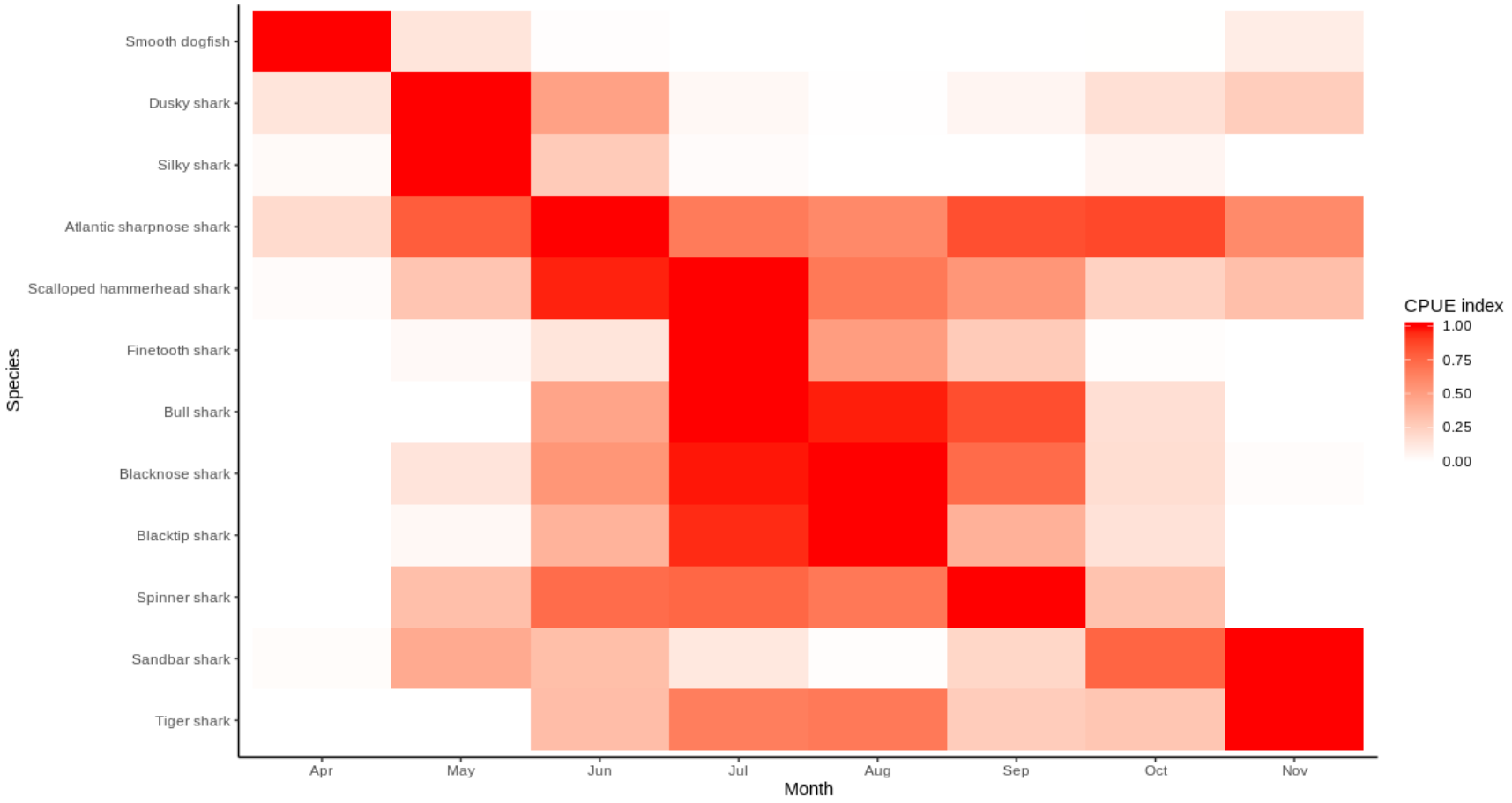

Figure 1.2: Heat map of CPUE index for each of 12 focal species across survey months. Index is calculated as monthly mean CPUE/ maximum of monthly mean CPUE values for each species.

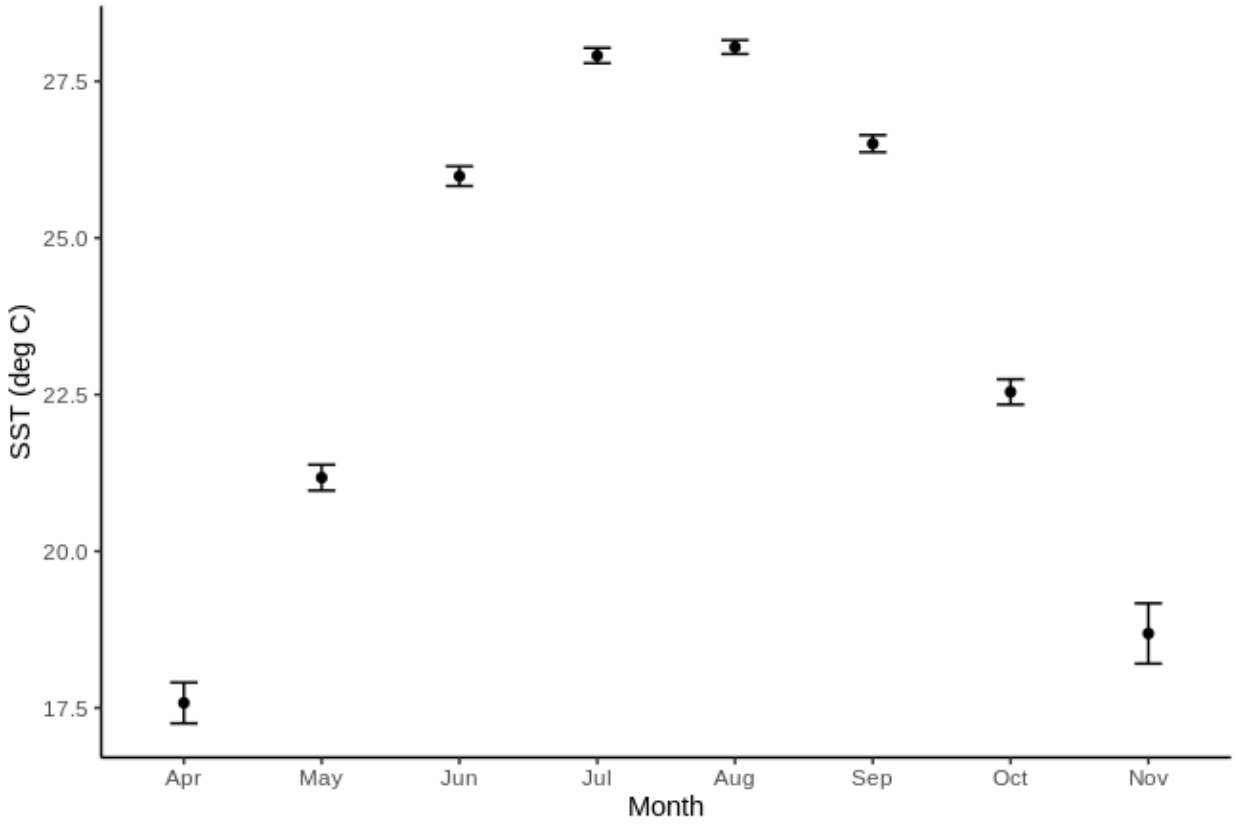

Figure 1.3: Mean SST records aggregated by month. Values are shown as mean $\pm$ 1 standard error.

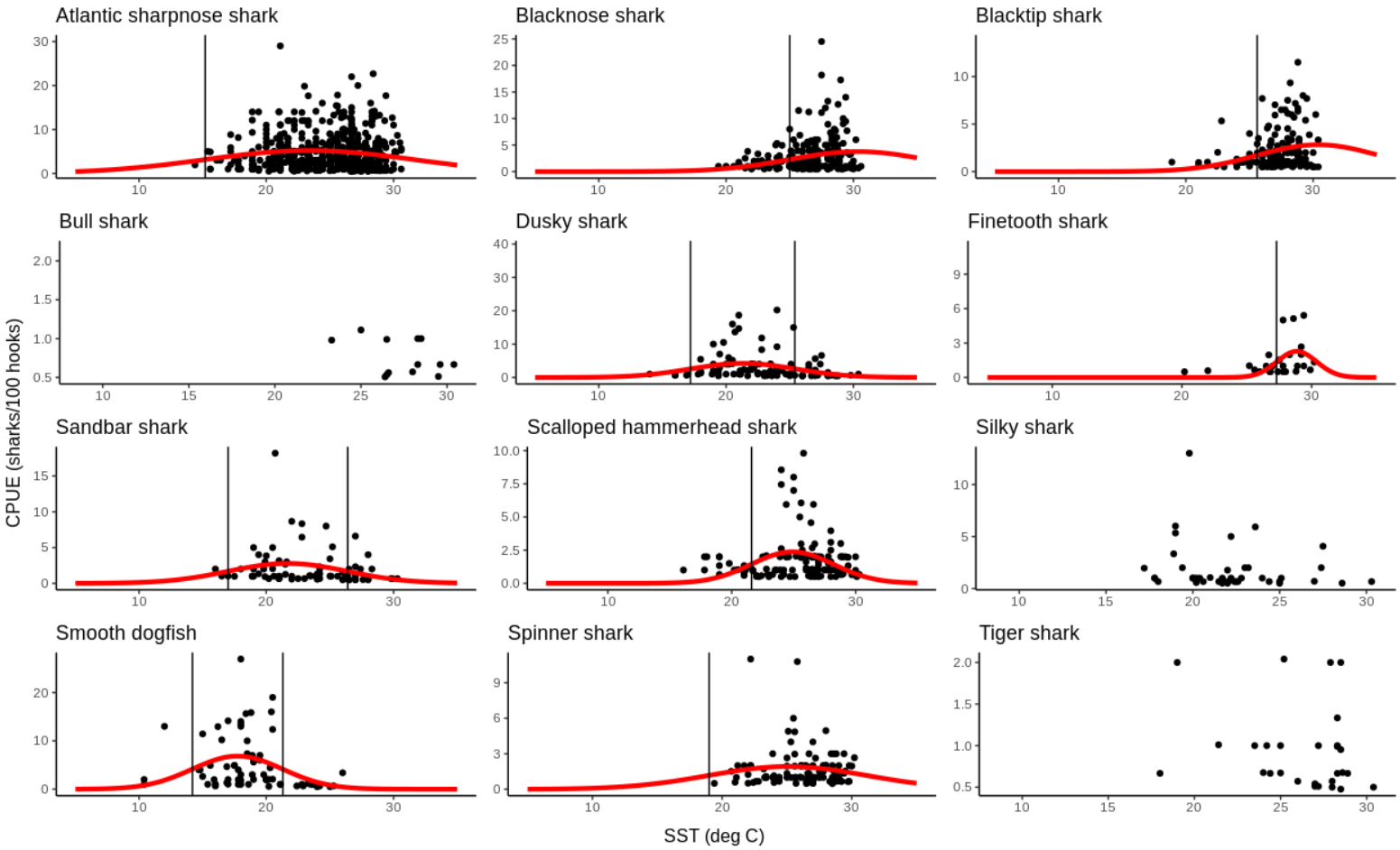

Figure 1.4: Scatterplots of CPUE by SST for each of the 12 focal species with guassian curve model fits and entrance/exit temperature calculations plotted as vertical lines. Species for which no convergence was found or for which model fit was deemed inappropriate are shown simply as scatterplots.

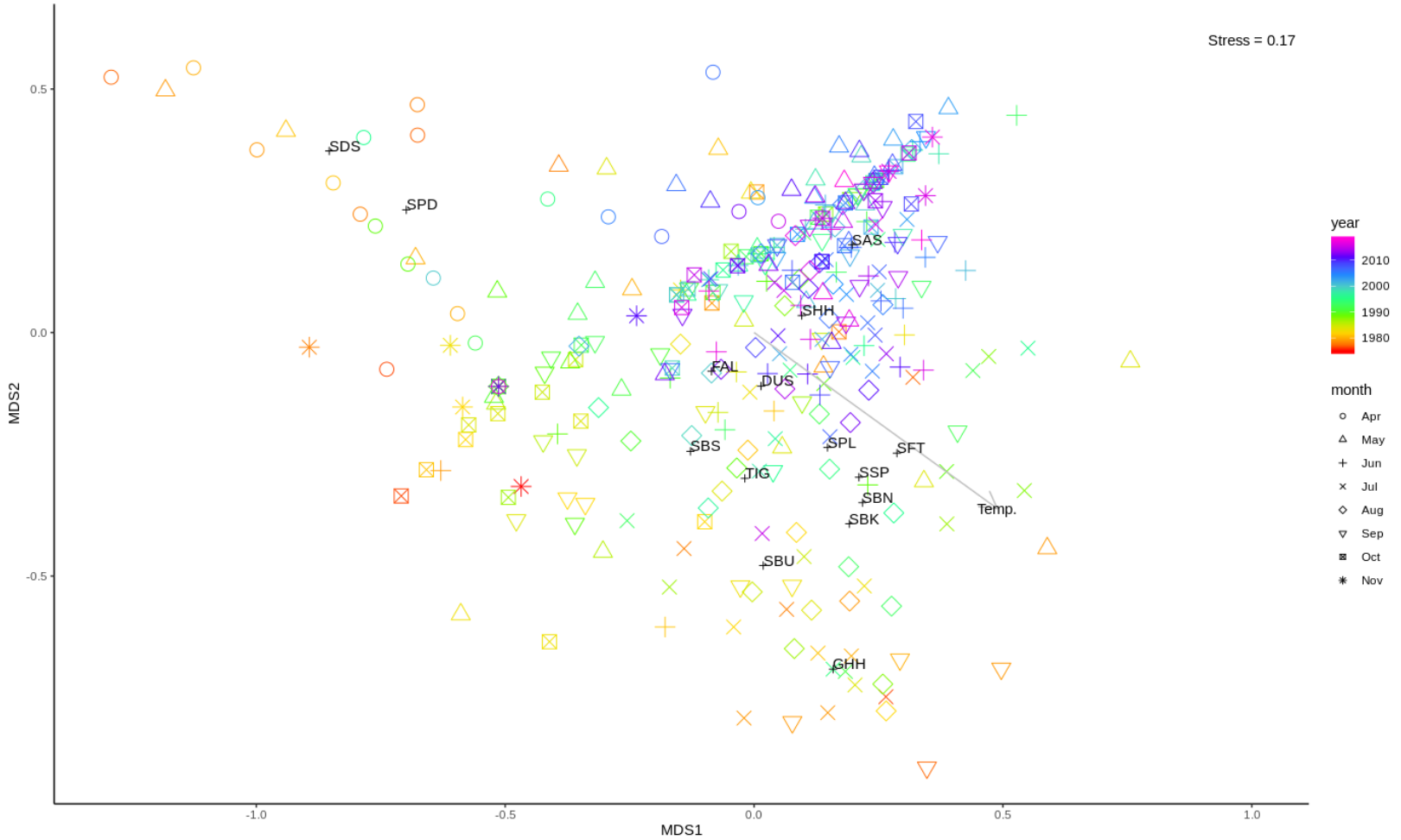

Figure 1.5: nMDS plot of daily mean CPUE and fitted vector for SST (Temp.). Three letter codes indicate weighted average points for each species. Colors represent year, while shapes represent month. Species codes (N = 15): DUS, dusky shark (*Carcharhinus* obscurus); FAL, silky shark (*Carcharhinus* falciformis); GHH, great hammerhead shark (*Sphyrna* mokarran); SAS, Atlantic sharpnose shark (*Rhizoprionodon terraenovae*); SBK, blacktip shark (*Carcharhinus limbatus*); SBN, blacknose shark (*Carcharhinus acronotus*); SBS, sandbar shark (*Carcharhinus plumbeus*); SBU, bull shark (*Carcharhinus leucas*); SDS, smooth dogfish (*Mustelus canis*); SFT, finetooth shark (*Carcharhinus isodon*); SHH, smooth hammerhead (*Sphyrna zygaena*); SPD, spiny dogfish (*Squalus acanthias*); SPL, scalloped hammerhead shark (*Sphyrna lewini*), SSP, spinner shark (*Carcharhinus brevipinna*); TIG, tiger shark (*Galeocerdo cuvier*).

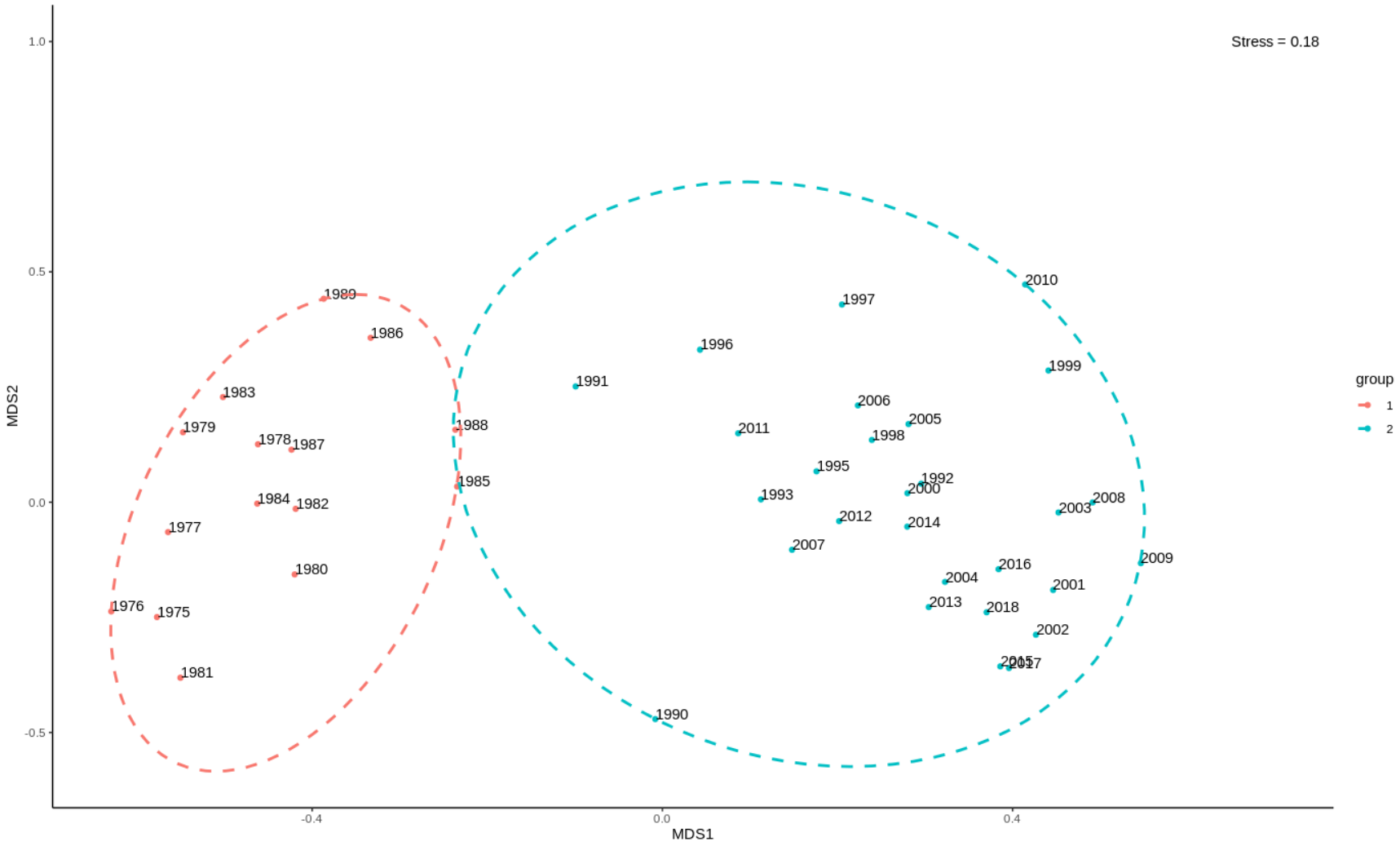

Figure 1.6: nMDS plot of annual mean CPUE. Colors represent clusters drawn at 10% similarity.

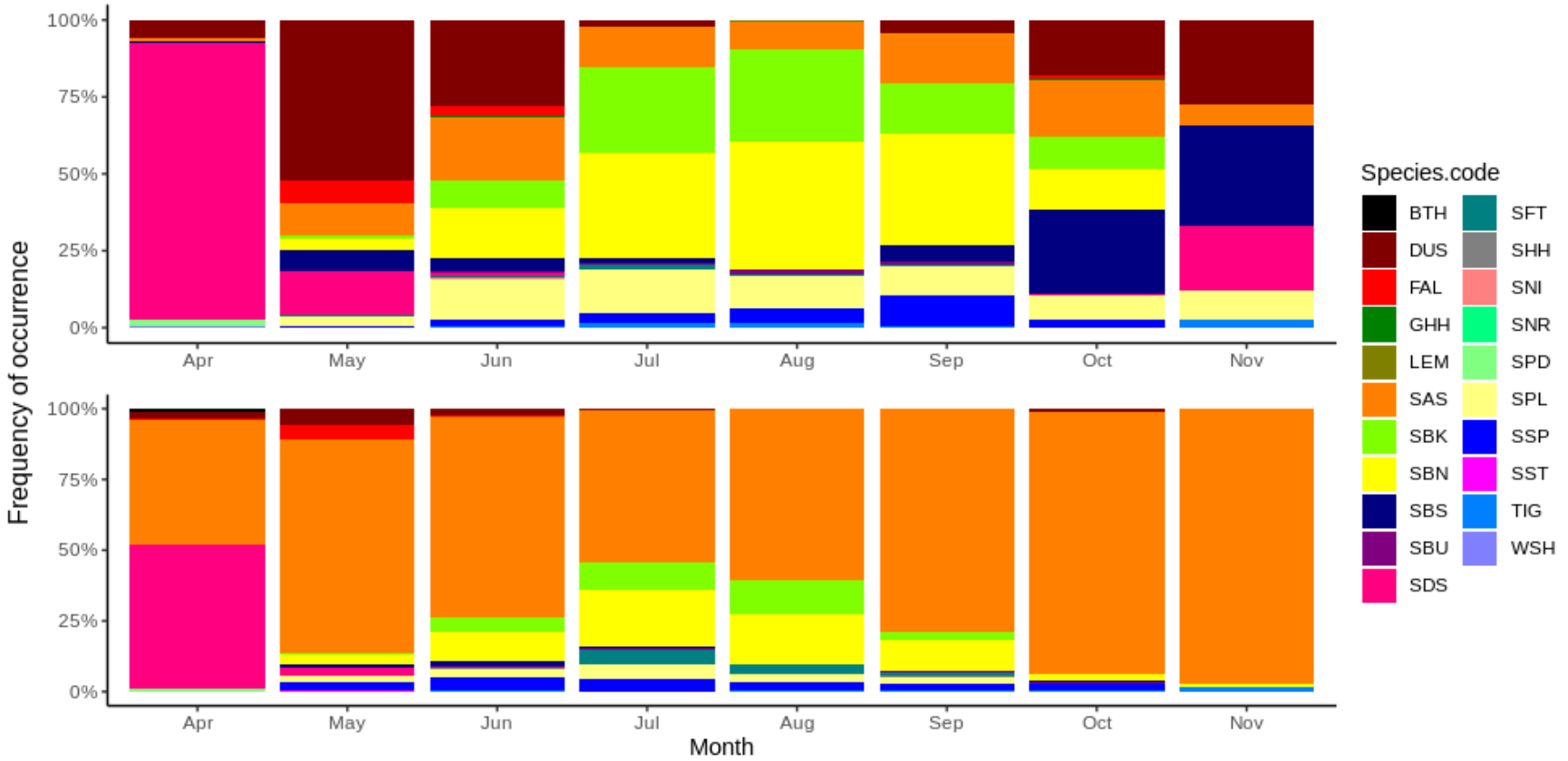

Figure 1.7: Stacked bar plots showing frequency of occurrence for mean CPUE values of each species aggregated by month. Top bar plot corresponds to annual mean nMDS cluster group 1 (1973-1989), while bottom bar plot corresponds to annual mean nMDS cluster group 2 (1990-2018). Species codes (N = 21): BTH, bigeye thresher (*Alopias superciliosus*); DUS, dusky shark (*Carcharhinus* obscurus); FAL, silky shark (*Carcharhinus* falciformis); GHH, great hammerhead shark (*Sphyrna* mokarran); LEM, lemon shark (*Negaprion brevirostris*); SAS, Atlantic sharpnose shark (*Rhizoprionodon terraenovae*); SBK, blacktip shark (*Carcharhinus limbatus*); SBN, blacknose shark (*Carcharhinus acronotus*); SBS, sandbar shark (*Carcharhinus plumbeus*); SBU, bull shark (*Carcharhinus leucas*); SDS, smooth dogfish (*Mustelus canis*); SFT, finetooth shark (*Carcharhinus isodon*); SHH, smooth hammerhead (*Sphyrna zygaena*); SNI, night shark (*Carcharhinus signatus*); SNR, nurse shark (*Ginglymostoma cirratum*); SPD, spiny dogfish (*Squalus acanthias*); SPL, scalloped hammerhead shark (*Sphyrna lewini*), SSP, spinner shark (*Carcharhinus brevipinna*); TIG, tiger shark (*Galeocerdo cuvier*); WSH, white shark (*Carcharodon carcharias*).

CHAPTER 2: SIZE CHANGES WITHIN A SOUTHEAST UNITED STATES COASTAL SHARK ASSEMBLAGE

Introduction

Fishing can cause substantial changes within exploited fish populations, both as a result of selective removal of target species and bycatch of non-target species. Size-selective harvesting (either targeted or bycatch fishes, which is the process of differentially removing larger individuals of a particular species due to gear design (e.g., net mesh size) or management directive (e.g., minimum size limits), has been documented across diverse fishes, often leading to a reduction in mean or maximum observed body size within a stock (Fenberg and Roy 2008). Truncation of size structure towards smaller individuals is troubling on both economic and ecological levels. Growth overfishing - the harvesting of fish before they reach their growth potential - results in decreased yield-per-recruit, was the first form of overfishing to be conceptually resolved, and has been a concern throughout post World War II fisheries (Beverton and Holt 1957). Furthermore, some analysts have suggested that maintaining "old-growth" age structure is as important as spawning biomass levels in determining the sustainability of fished stocks (Berkeley et al. 2004). In particular, big old fat fecund female fish (BOFFFFs) are thought to disproportionately contribute to recruitment potential of a stock via both offspring quantity and quality, as well as diversity of larval source locations since fish can segregate spatially based on size. Both of these factors can help to stabilize the population dynamics of harvested species (Birkeland and Dayton 2005; Hixon et al. 2014).

There are multiple, somewhat competing mechanistic hypotheses regarding the response of fished species to harvest pressure vis-à-vis population-level size structure. Darwinian fisheries science has focused on the potential of harvest pressure to select for traits such as reduced growth or earlier size- or age-at-maturity (Law 2007). In size-selective fisheries targeting large individuals, fish growing more quickly or reproducing at larger sizes and older ages may be captured before successfully contributing to the spawning population, greatly reducing their individual fitness relative to slower growers or earlier reproducers (Ratner and Lande 2001; Conover and Munch 2002). Over evolutionary scales, this could truncate the size structure of an exploited population towards smaller fish. Alarmingly, these potential evolutionary consequences may be hard to reverse with the relaxation of fishing pressure due to hysteresis, or a lag associated with relatively weak selection differentials in the opposing direction (Allendorf and Hard 2009). While evolutionary dynamics may drive fished populations towards smaller individuals, environmental selection within exploited stocks could have the opposite effect on fish. Reduction of stock abundance can cause a release from intraspecific competition, resulting in greater per-capita availability of resources and increased growth, as has also been documented in a number of marine fishes (Heino and Godo 2002). These latter observations support the hypothesis that such density-dependent growth could lead to an increase in body size of individuals through time via compensatory processes in harvested populations (Hilborn and Minte-vera 2008).

The response of a harvested species/stock regarding individual life history vital rates and population-level size structure ultimately depends on the case-specific nature of density-dependent resource competition, genetic correlates or heritabilities of relevant traits, and the intensity (including temporal consistency) of size-selective harvest (Law 2007). Common among

fished taxa/stocks, however, is the fundamental need to document patterns in size-based indicators over appropriate timescales (i.e., years to decades) to guide us in understanding the dynamics and root mechanisms of size-structure shifts (Shin et al. 2005). Sharks are an interesting and important test case for evaluating changes in size structure, as there are a mix of factors that might buffer or exacerbate harvest-driven changes. Within this group, many species are defined by relatively *K*-selected life histories (i.e., slower growth, larger maximum size, longer maximum age, lower fecundity), and as such are vulnerable to overfishing (Stevens et al. 2000). The effects of maternal investment on offspring in sharks has received relatively limited attention and has yet to be fully explored; however, there is evidence suggesting that maternal size can affect both offspring quantity (litter size) and quality (fitness) (Carlson and Baremore 2003; Hussey et al. 2010; Baremore and Passerotti 2013). Gears used to harvest sharks include those that are likely to be size selective (i.e., gill nets), but also some that are potentially less so (i.e., long lines) (Hovgård and Lassen 2000; ASMFC 2008). Because shark species are challenging to distinguish, management is often – but not always (e.g., blacknose shark *Carcharhinus acronotus*) - conducted at multispecies levels, such as the large coastal shark (seven species) and small coastal shark (3 species) complexes. These are jointly managed by the Atlantic States Marine Fisheries Commission in state waters (0-3 miles from shore) and the National Oceanic and Atmospheric Administration (NOAA) Fisheries Highly Migratory Species Management Division in the Exclusive Economic Zone (3-200 miles from shore) along the southeast United States (US) (ASMFC 2008). As a result, these multispecies commercial fisheries operate without minimum size limits that often drive size-selective fisheries. Finally, pressure on 'great sharks', such as bull shark *Carcharhinus leucas* and tiger shark *Galeocerdo cuvier*, has been hypothesized to have resulted in "mesopredator release" of smaller sharks and

rays, which could further complicate the patterns of size structure within some fished species such as blacknose shark (sensu Myers et al. 2007).

With these dynamics in mind, we used a decades-running survey of the coastal shark assemblage in Onslow Bay, North Carolina, to document temporal patterns of population size structure among 12 commonly captured species. Our overarching goal was to evaluate the null hypothesis that size-structure has not changed appreciably over time, on a species-by-species basis. Observed patterns are discussed in the context of management strategies, potential genetic and environmental drivers of size structure within fished populations, and purported "mesopredator release".

Methods

Field sampling

To examine trends in size structure within coastal shark populations, we used species-specific time series size data generated during the course of a 1972-present fishery independent shark survey in Onslow Bay, North Carolina. The survey was conducted by the University of North Carolina at Chapel Hill's Institute of Marine Sciences (UNC-IMS) and since its inception, the UNC-IMS shark survey has employed standardized longline sampling gear at two fixed stations in Onslow Bay: 4 km (34.6338°N, 76.6306°W, 15 m depth) and 13 km (34.5512°N, 76.6237°W, 17 m depth) southeast of Beaufort Inlet. During each deployment at each station, the 7.6 mm braided nylon longline extends 1 km, with gangion lines attached to the mainline at every 10 m (N = 100). Each gangion consists of a 1.8 m long, #2-chain leader and a 9/0 Mustad tuna J hook. Polyball buoys are attached between every 10 gangions (100-m separation), allowing the longline gear to effectively fish the entire water column at each station.

In addition to standardized gears and stations, consistent deployment methods have been used since the first sets were made in 1972. Survey trips were conducted biweekly, between April and November each year, on 10-15-m research vessels operated by UNC-IMS. A demersal trawl was used at the start of each survey day to collect bait (e.g., spot *Leiostomus xanthurus*, Atlantic croaker *Micropogonias undulatus*), which were attached through the operculum on hooks (one fish per hook). Longline deployment occurred between 0800 and 1300 hours, with the gear soaked for one hour during each set. Efforts were made to deploy at each station on each survey day (weather dependent), and the inshore set was typically, but not always, made first. Upon gear recovery, all captured sharks were identified to species, sexed, and measured for fork length (FL) and total length (TL) to the nearest mm. Live individuals were outfitted with an external dart tag and returned to the water (~90% of catch). To date, more than 500 survey trips have been conducted, > 1,000 longline sets have been made, > 100,000 baited hooks have been set, and > 10,000 individual shark captures across 21 species have contributed to the UNC-IMS shark survey database. The survey is conducted under UNC-IMS Institutional Animal Care and Use Committee protocol 19-137.0.

Data Analysis

We selected 12 of the 21 shark species caught in the survey for analyses based on overall sample sizes, management context, and conservation interest: blacknose shark, spinner shark *Carcharhinus brevipinna,* silky shark *Carcharhinus falciformis,* finetooth shark *Carcharhinus isodon,* bull shark, blacktip shark *Carcharhinus limbatus,* dusky shark *Carcharhinus obscurus,* sandbar shark *Carcharhinus plumbeus,* tiger shark, smooth dogfish *Mustelus canis,* Atlantic sharpnose shark (*Rhizoprionodon terraenovae*), and scalloped hammerhead (*Sphyrna lewini*).

For each focal species, separately, we binned data by year, combining individuals across all months and both stations to describe the entire surveyed population. We utilized FL data as this measurement was the most consistently collected across the entire survey, and we focused on data collected during 1975 – 2018 since data from the first three survey years reported abundance and TL more heavily, rather than FL. For each species*year, we then used three different size indices to obtain a more holistic and robust assessment of potential size changes over time: mean FL, median FL, and an index of maximum FL ($L_{90\%}$ or 90th percentile of FL).

The advantage of using the mean is it provides a weighted center to the distribution and allows the application of parametric assumptions. The advantage of using the median is it is not sensitive to outliers. The advantage of using the 90th percentile is it is more sensitive to changes in the maximum values. These three metrics complement each other nicely as mean and median provide two measures of changes to the overall size distribution, one sensitive to outliers and the other insensitive, while $L_{90\%}$ quantifies the abundance of large individuals, relative to smaller individuals (Shin et al. 2005). We used R package Hmisc to implement the Harrell-Davis quantile estimator for our calculation of $L_{90\%}$, which is more robust at lower sample sizes and extreme percentiles than standard quantile calculations (Harrell and Davis 1982). Only species × years with three or more specimens captured and measured were included in the $L_{90\%}$ calculations.

We used linear regressions on each species and size metric (except $L_{90\%}$ for bull shark and tiger shark, which lacked sufficient sample sizes) to assess the strength and ecological significance of relationships between year and shark size. Confidence intervals (CI; 95% level) were also computed for all linear regressions to better quantify certainty for each model. We used R package estimatr to implement a heteroscedasticity-consistent standard error estimator (HC3)

for computing confidence intervals and p-values for regression models, which is relatively insensitive to data heteroscedasticity (Hayes and Cai 2007).

Using linear regression models and associated confidence intervals, we estimated the magnitude of long-term size increases or decreases for each species and each FL index. Firstly, we determined the difference between the regression model value for the first and last year in which each species was captured, both in raw change as well as percent difference. Secondly, as a conservative measure of size change, we estimated a minimum potential difference in sizes (mm and %) between the first and last year in which a species was recorded using the regression confidence intervals (i.e., using lower and upper CIs as appropriate to find the smallest potential difference between early and late records for apparent decreases in size). Finally, as an indicator of maximum potential changes in size (mm and %) over time, (as a "worst-case scenario" in instances of apparent declines in size), we again compared regression confidence intervals between the first and last year in which each species was captured, but rather than selecting for the smallest potential change based on lower/upper CIs of early and late records, instead identified the largest potential change through time based on CIs.

As a last measure of species-specific size-structure through time, we calculated the number of individuals for each species × year in 200 mm size class bins. Two-hundred-mm bins appeared to provide valuable resolution for all species and was therefore used across all analyses. Due to the relative rarity of individuals over 2000 mm, we collapsed all bins above this value into a single size class. We also calculated mean catch per unit effort (CPUE) for each species across years to provide context regarding how population size/density and size structure may be related. We computed CPUE for each species × year as the number of sharks caught per 100 hooks set.

The power of our analytical approach is in the availability of a 40-year dataset on shark sizes across multiple species, despite some sample size limitations. To emphasize the ecological significance of the patterns we observed, our inferences were drawn from a suite of information that includes effect sizes (i.e., mean differences over time), confidence intervals, and measures of statistical clarity (Nakagawa and Cuthill 2007). Importantly, given the multiple size metrics we considered, it would be conceptually problematic within a species to default to "statistically significant" changes for one size metric, but "statistically insignificant" changes for another metric based solely on any arbitrary alpha (Amrhein et al. 2017; Hurlbert et al. 2019). All statistical analyses and plotting of data were conducted in R (R Foundation, Vienna, Austria).

Results

Survey results indicated > 9% relative decreases in $L_{90\%}$ for all 10 species for which linear regression models were run (relative changes based on absolute trendlines; Figure 2.1). The largest relative declines were seen in sandbar shark (35%; 541 mm) and spinner shark (28%; 399 mm) (Table 2.1). We found the strongest statistical support ($p < 0.04$) for $L_{90\%}$ declines in four species: blacknose shark (10%; 115 mm), dusky shark (23%; 297 mm), smooth dogfish (17%; 178 mm), and Atlantic sharpnose shark (10%; 88 mm) (Table 2.1). Using a conservative approach to account for intra- and interannual variability in observations, we still recorded small, but notable declines in $L_{90\%}$ for blacknose shark (3%; 32 mm), smooth dogfish (2%; 24 mm), and Atlantic sharpnose shark (5%; 45 mm) (Table 2.1). Using a "worst-case scenario" framework, relative declines in $L_{90\%}$ among species ranged between 15-63%, with five species potentially exhibiting > 45% relative decreases in $L_{90\%}$ over time (Table 2.1).

Patterns in mean FL over time followed similar overall trends: 10 of 12 species were characterized by FLs that trended over time toward smaller average sizes (Figure 2.2). Exceptions included tiger shark and bull shark. Tiger shark were defined by the almost complete absence of catches from 1990 through 2010 – with the exception of three small (< 1000 mm FL) individuals – bracketed by the occurrence of relatively large individuals (1500-2500 mm FL) in the survey during the 1970's-1980s and 2010s (Figure 2.2). Except for one small (390 mm FL) bull shark captured in 2008, which had significant leverage in the regression analysis, individuals routinely measured ~2000 mm FL throughout the survey. Using trendline patterns among species other than tiger shark and bull shark, the largest relative decline in mean FL was observed for sandbar shark (20%; 214 mm), while the range of declines across all other species was 2-17% (Table 2.1). The strongest statistical support ($p = 0.001$) for a mean FL decline was found in blacknose shark, which declined by 11% (116 mm) (Table 2.1). Blacknose shark was also the only species characterized by a potential decline (4%; 41 mm) in mean FL using a relatively conservative approach (Table 2.1). Using a "worst-case scenario", mean FL declined 12-55% across 10 species (largest decline for sandbar shark), with average sizes potentially shrinking by > 32% in seven of those species (Table 2.1).

Median sizes also trended toward smaller fish for nine of 12 species (Figure 2.3). For tiger shark and bull shark, mean and median FL values/patterns were virtually identical due to low overall sample sizes. Unlike mean FL, median FL values for spinner shark did not appear to change appreciably over time. Among the nine sharks with declining trendlines, changes in median FL ranged from 2-18%. Again, blacknose shark exhibited the best statistical support for a decline in median FL ($p = 0.008$) of 10% (104 mm) (Table 2.1), and viewed conservatively, only blacknose shark showed a potential decline in median FL (2%; 21 mm) (Table 2.1). Potential

declines in median FL ranged from 13-51% in a “worst-case scenario” among species other than spinner shark, tiger shark, or bull shark. As with mean FL, largest potential declines in median Fl were suggested for sandbar shark, with four species expressing > 31% reductions in median FL over time (Table 2.1).

Several sharks exhibited obvious reductions in catches of individuals within the largest size class of that particular species through time, including blacknose shark, silky shark, blacktip shark, sandbar shark, smooth dogfish and scalloped hammerhead (Figure 2.4). Across these species, the loss of largest individuals was generally evident sometime during the 1990s, mirroring declines in overall CPUEs for those species over the same period. Atlantic sharpnose shark was also characterized by the loss of the largest size class (800-1000 mm FL) by the end of the survey period, but with a couple of important nuances. (1) Catches of 800-1000-mm FL individuals appeared highest in the years between 1980-2005, whereas for other species, highest catches of the largest size class tended to occur between 1975-1995. And (2) Atlantic sharpnose shark was the only species that showed an increasing trend in annual mean CPUE (all size classes combined), from one shark per 100 hooks in the 1970s to seven sharks per 100 hooks by the 2000s (Figure 2.4).

Discussion

Expanding on previous analyses that suggest the loss of “great sharks” from the coastal ocean over the last several decades (Myers et al. 2007; Powers et al. 2013), our analyses suggest that within-species size changes over time may be pervasive throughout the entire coastal shark assemblage visiting Onslow Bay (Table 2.1). Indeed, survey results indicated decreases in size structure among members of the Large Coastal Shark complex (blacktip shark, bull shark, silky

shark, spinner shark, tiger shark), Small Coastal Shark complex (Atlantic sharpnose shark, finetooth shark), Hammerhead Shark complex (scalloped hammerhead), Smoothhound complex (smooth dogfish), Harvest-Prohibited complex (dusky shark), Research-Only-Harvest species (sandbar shark) and individually managed species (blacknose shark). Below, we consider how observed decreases in sizes across species fit in the context of management, genetic versus environmental drivers of size structure within fished populations, and purported "mesopredator release."

We readily acknowledge that the nature of this long-term, two-station, observational dataset presents some logistical challenges for applying standard statistical approaches to assess changes in size structure among species. We have attempted to respect these constraints by evaluating multiple metrics of size structure for thoroughness, as well as using a 'totality of evidence' approach regarding size trends, confidence intervals, and statistical clarity to draw ecological inferences. We also conclude that there is important meaning at the assemblage level in the consistency of trends across species over decadal time scales. Across all 12 species for which we evaluated mean and median sizes (and all 10 species assessed using $L_{90\%}$), we recorded decreasing sizes through time based on the raw sign of fitted slopes. The probability of recording consistently negative slopes across 12 species – presuming size-structure was actually stable across species (i.e., a coin flip between the raw sign of slope being positive versus negative for each species [excluding zero slope]) – is only < 0.05% (< 1-in-4,000). Therefore, we conclude that the interpretation of across-assemblage decreases in sizes is likely robust.

For nine species we evaluated, decreases in size over time co-occurred with long-term declines in catch rates in the IMS shark survey (Figure 2.4). Although shark-species-specific harvest records are patchy before the mid-1990s, we do speculate that fishing pressure was a

significant contributor to both the size and catch patterns we observed. At the assemblage level, commercial landings for sharks included in this study in the NOAA Fisheries South Atlantic region rose during the 1970s- 1980s to a peak of 4,324 metric tons in 1994 (NOAA 2019). Since that peak, landings have declined by ten-fold at the assemblage level, with similar declines in harvest for many species. Exceptions include blacknose shark and blacktip shark, which showed modest increases in landings, as well as Atlantic sharpnose shark, for which the pattern was reversed (landings increased by ten-fold). These recent, lower landings are presumed to result from harvest-induced reductions in shark abundances as well as reductions in allowable catches (Final Consolidated Atlantic Highly Migratory Species Fishery Management Plan; NMFS 2006). Notably, the mid-1990s peak in catches, and rapid decline in landings since, corresponds to the loss of the largest size classes of blacknose shark, silky shark, blacktip shark, sandbar shark, smooth dogfish, and scalloped hammerhead (Figure 2.4).

While there is compelling evidence that tighter harvest management over the last two decades has begun to reserve trends in shark abundance towards recovery over the last few years (Peterson et al. 2017), the IMS survey data – particularly size-class breakdowns – would suggest these positive trends have largely not been manifest yet in intraspecific size structure. However, we do note that over the last five years, mean size of spinner shark, blacktip shark, dusky shark, tiger shark, and scalloped hammerhead potentially suggest the very earliest signs of increase – a pattern that deserves continued monitoring and inspection (Figure 2.2). Dusky shark has been prohibited from harvest since 2000 (SEDAR 2011), and therefore could be expected to be among the species to grow in mean size over time (sensu Fenberg and Roy 2008). Other species in this group belong to the Large Coastal Shark or Hammerhead Shark complexes, perhaps indicative of the effectiveness of these management units as a conservation framework.

Across management units, the consistent patterns of size decreases among species may also suggest something about mechanisms by which fishing impacts size structure. Shark management complexes generally operate without minimum size limits, thereby reducing the potential for this to drive size-selective fishing. Therefore, perhaps coastal shark population size shifts could be driven by the selectivity of fishing gear (Stevens et al. 2000), which often target larger individuals. Furthermore, recreational fisheries for Large Coastal Sharks and Hammerhead Shark complexes do operate with minimum size requirements, while commercial fisheries for "ridgeback" Large Coastal Sharks operated with a minimum size from 1999-2003 (NMFS 2006). If minimum size regulations were a primary driver of reductions in mean body size, it makes little sense that species within these management units would be showing the most notable signs of potential increase over the last few survey years. Finally, the lack of recovery in either catch rates or sizes of sandbar shark since the mid-1990s, despite its status as a research-only-harvest species, invokes several possibilities: (1) the life-history of this species does not allow recovery under current, presumably modest, rates of research harvest; (2) environmental conditions have shifted and do not support rapid recovery of this species; and (3) the life history of this species does not allow recovery under current, poorly quantified, rates of non-target bycatch mortality (Crowder and Murawski 1998).

Regarding the dynamics of genetic versus environmental drivers of size structure within fished populations, our data indicate, at a minimum, that compensatory processes within the life history of sharks do not appear broadly capable of completely counteracting the effects of fishing on population size structure (Stevens et al. 2000). This, however, does not preclude the possibility that individual growth rates have increased for some species experiencing significant decreases in abundance over time (e.g., blacknose shark, blacktip shark, dusky shark). In this

context – simply reversed – Atlantic sharpnose shark was the lone species in our survey defined by increases in catch rates over time. Carlson and Baremore (2003) reported that Atlantic sharpnose shark exhibited increased juvenile growth rates in response to population declines, suggesting this may be a mechanism for density-dependent regulation. Thus, higher intraspecific competition for resources (i.e., lower growth rates) rather than just fishing pressure, could explain some of the decreases in sizes we observed for Atlantic sharpnose shark (sensu Cushing 1995).

While the assemblage-level decreases in size we observed may simply reflect the long-term press of continually removing the large(r) individuals from the stock, the opportunity for selective forces to impact shark populations and potential shark recovery appears present (Walker 1998). We are unable to arbitrate between these different and potentially co-occurring mechanisms within our analyses. Rather, the results presented here represent an important first step by documenting size-based indicators over appropriate timescales (i.e., years to decades), which should guide further exploration into the dynamics and root mechanisms of size-structure shifts. Despite the logistic challenges of examining sharks in the context of Darwinian fisheries (e.g., generation times of sharks, handling sharks for controlled experiments), we suggest this is an important area of investigation given the particular life histories and management approaches within this guild.

Size decreases reported in this study represent possible changes in recruitment, given empirical evidence of maternal investment in sharks, and its relationship to maternal size/age. In teleost fish, BOFFFFs are known to contribute disproportionately to offspring growth and survival, with older or larger rockfishes showing increased maternal provisioning, in the form of enlarged oil globule volume of offspring (Sogard et al. 2008). The volume of oil globule present

at parturition was the larval trait that most highly correlated with larval performance in black rockfish, with larvae from cohorts with the largest oil globules displaying a three-fold increase in growth rate and two-fold increase in survival rate (Berkeley et al. 2004). Maternal provisioning in sharks appears to occur via enlarged livers of offspring, with neonatal carcharhinid sharks showing a declining trend in liver mass (as well as overall body mass) shortly after parturition, presumably the excess liver reserves provide a maternal head-start for offspring to use in the first weeks of life (Hussey et al. 2010). Hussey et al. (2010) also found a clear relationship between pup mass and maternal size, with mean pup mass increasing with maternal size, although there was evidence for a decline at the largest mother lengths.

There has been increasing interest in the "rise of the mesopredator," in which the loss of apex predators is accompanied by the expansion in density or distribution of middle-rank predators (i.e., mesopredator release Prugh et al. 2009). This has led to concerns of potential food-web-level trophic cascades (Polis 1994), defined as inverse patterns of abundance at successive trophic levels that are transmitted down the food web (Brashares et al. 2010). Myers et al. (2007) found sharp declines in abundance for species of "great sharks" (> 2 m; e.g., bull shark, dusky shark, sandbar shark, tiger shark), using the UNC-IMS survey data, which they attributed to direct exploitation. Myers et al. (2007) linked this decline in great sharks to the abundance of characteristically smaller species such as Atlantic sharpnose shark. While our findings are not in direct conflict with the results of Myers et al. (2007) our results do suggest that the direct effects of fishing may be more pervasive throughout the shark assemblage, rather than focused on just the largest species with subsequent cascading impacts. In particular, Atlantic sharpnose shark (acknowledging potential density-dependent drivers of size shifts), blacknose shark, finetooth shark, and smooth dogfish are all relatively small-bodied, and aptly described as mesopredators.

For all four of these species, long-term trends suggest decreases in size, which runs counter to the notion of top-down "release." Combined with the long-term declines in catch rates of blacknose shark and smooth dogfish, these results suggest that mesopredators also experience population responses to ("top-down") fishing pressure. Indeed, Blacknose shark exhibited perhaps the clearest shift over time, with all of the indices examined showing declines of ~10% throughout the survey period with high statistical confidence (Table 2.1), as well as relatively lower proportions of larger size classes in later years of the survey (Figure 2.4).

This study provides a baseline for future coastal shark size structure comparison, while also serving as a critical step for considering how shark populations may have responded to fishing via environmental versus genetic mechanisms. Over the next few decades, there is perhaps a unique opportunity to monitor size structure in populations of coastal sharks in the Fisheries Southeast regional as managers attempt to reverse past overharvest (Peterson et al. 2017). As in other fishery stocks, size structure is a critical component of monitoring and an indicator of stock health and resilience in the context of harvest pressure (Berkeley et al. 2004) and other, compounding perturbations (e.g., bottom disruption of resources [Duplisea et al. 2002], climate change syndromes [Morley et al. 2017]).

REFERENCES

Allendorf, F. W., and J. J. Hard. 2009. Human-induced evolution caused by unnatural selection through harvest of wild animals. Proceedings of the National Academy of Sciences 106(Supplement 1):9987–9994.

Amrhein, V., F. Korner-Nievergelt, and T. Roth. 2017. The earth is flat ($p > 0.05$): significance thresholds and the crisis of unreplicable research. PeerJ 5:e3544.

ASMFC. 2008. Interstate fishery management plan for Atlantic coastal sharks. Atlantic States Marine Fisheries Commission, Washington, D.C.

Baremore, I. E., and M. S. Passerotti. 2013. Reproduction of the blacktip shark in the Gulf of Mexico. Marine and Coastal Fisheries 5(1):127–138.

Berkeley, S. A., C. Chapman, and S. M. Sogard. 2004. Maternal age as a determinant of larval growth and survival in a marine fish, Sebastes melanops. Ecology 85(5):1258–1264.

Beverton, R. J. H., and S. J. Holt. 1957. On the dynamics of exploited fish stocks. Fisheries Investigations Series 2(19). Ministry of Agriculture, Fisheries and Food, London, U.K.

Birkeland, C., and P. K. Dayton. 2005. The importance in fishery management of leaving the big ones. Trends in Ecology & Evolution 20(7):356–358.

Brashares, J., L. Prugh, C. J. Stoner, and C. Epps. 2010. Ecological and conservation implications of mesopredator release. Pages 221–240 *in* John Terborgh and J. A. Estes, editors. Trophic Cascades: Predators, Prey, and the Changing Dynamics of Nature. Island Press, Washington, D.C.

Carlson, J. K., and I. E. Baremore. 2003. Changes in biological parameters of Atlantic sharpnose shark Rhizoprionodon terraenovae in the Gulf of Mexico: evidence for density-dependent growth and maturity? Marine and Freshwater Research 54(3):227.

Conover, D. O., and S. B. Munch. 2002. Sustaining fisheries yields over evolutionary time scales. Science 297(5578):94–96.

Crowder, L. B., and S. A. Murawski. 1998. Fisheries bycatch: implications for management. Fisheries 23(6):8–17. Wiley.

Cushing, D. H. 1995. Population production and regulation in the sea: a fisheries perspective. Cambridge University Press, New York, NY.

Duplisea, D. E., S. Jennings, K. J. Warr, and T. A. Dinmore. 2002. A size-based model of the impacts of bottom trawling on benthic community structure. Canadian Journal of Fisheries and Aquatic Sciences 59(11):1785–1795.

Fenberg, P. B., and K. Roy. 2008. Ecological and evolutionary consequences of size-selective harvesting: how much do we know? Molecular Ecology 17(1):209–220.

Harrell, F. E., and C. E. Davis. 1982. A new distribution-free quantile estimator. Biometrika 69(3):635–640.

Hayes, A. F., and L. Cai. 2007. Using heteroskedasticity-consistent standard error estimators in OLS regression: an introduction and software implementation. Behavior Research Methods 39(4):709–722.

Heino, M., and R. O. Godo. 2002. Fisheries-induced selection pressures in the context of sustainable fisheries. Bulletin of Marine Science 70(2):639–656.

Hilborn, R., and C. V. Minte-vera. 2008. Fisheries-induced changes in growth rates in marine fisheries: are they significant? Bulletin of Marine Science 83(1):95–105.

Hixon, M. A., D. W. Johnson, and S. M. Sogard. 2014. BOFFFFs: on the importance of conserving old-growth age structure in fishery populations. ICES Journal of Marine Science 71(8):2171–2185.

Hovgård, H., and H. Lassen. 2000. Manual on estimation of selectivity for gillnet and longline gears in abundance surveys. FAO Fisheries Technical Paper No. 397. Rome.

Hurlbert, S. H., R. A. Levine, and J. Utts. 2019. Coup de grâce for a tough old bull: “statistically significant” expires. The American Statistician 73(sup1):352–357.

Hussey, N. E., S. P. Wintner, S. F. J. Dudley, G. Cliff, D. T. Cocks, and M. A. MacNeil. 2010. Maternal investment and size-specific reproductive output in carcharhinid sharks. Journal of Animal Ecology 79(1):184–193.

Law, R. 2007. Fisheries-induced evolution: present status and future directions. Marine Ecology-Progress Series 335:271–277.

Morley, J. W., R. D. Batt, and M. L. Pinsky. 2017. Marine assemblages respond rapidly to winter climate variability. Global Change Biology 23(7):2590–2601.

Myers, R. A., J. K. Baum, T. D. Shepherd, S. P. Powers, and C. H. Peterson. 2007. Cascading effects of the loss of apex predatory sharks from a coastal ocean. Science 315(5820):1846–1850.

Nakagawa, S., and I. C. Cuthill. 2007. Effect size, confidence interval and statistical significance: a practical guide for biologists. Biological Reviews 82(4):591–605.

NMFS. 2006. Final Consolidated Atlantic Highly Migratory Species Fishery Management Plan. National Oceanic and Atmospheric Administration, National Marine Fisheries Service, Office of Sustainable Fisheries, Highly Migratory Species Management Division, Silver Spring, MD.

NOAA. 2019. Annual commercial landing statistics. https://foss.nmfs.noaa.gov/.

Peterson, C. D., C. N. Belcher, D. M. Bethea, W. B. Driggers, B. S. Frazier, and R. J. Latour. 2017. Preliminary recovery of coastal sharks in the south-east United States. Fish and Fisheries 18(5):845–859.

Polis, G. A. 1994. Food webs, trophic cascades and community structure. Australian Journal of Ecology 19(2):121–136.

Powers, S. P., F. J. Fodrie, S. B. Scyphers, J. M. Drymon, R. L. Shipp, and G. W. Stunz. 2013. Gulf-wide decreases in the size of large coastal sharks documented by generations of fishermen. Marine and Coastal Fisheries 5(1):93–102.

Prugh, L. R., C. J. Stoner, C. W. Epps, W. T. Bean, W. J. Ripple, A. S. Laliberte, and J. S. Brashares. 2009. The rise of the mesopredator. BioScience 59(9):779–791.

Ratner, S., and R. Lande. 2001. Demographic and evolutionary responses to selective harvesting in populations with discrete generations. Ecology 82(11):3093–3104.

SEDAR. 2011. Sedar 21 - HMS Dusky Shark Stock Assessment Report. SEDAR, North Charleston, SC. http://sedarweb.org/docs/sar/Dusky_SAR.pdf.

Shin, Y. J., M. J. Rochet, S. Jennings, J. G. Field, and H. Gislason. 2005. Using size-based indicators to evaluate the ecosystem effects of fishing. ICES Journal of Marine Science 62(3):384–396.

Sogard, S., S. Berkeley, and R. Fisher. 2008. Maternal effects in rockfishes Sebastes spp.: a comparison among species. Marine Ecology Progress Series 360:227–236.

Stevens, J. D., R. Bonfil, N. K. Dulvy, and P. A. Walker. 2000. The effects of fishing on sharks, rays, and chimaeras (chondrichthyans), and the implications for marine ecosystems. ICES Journal of Marine Science 57(3):476–494.

Walker, T. I. 1998. Can shark resources be harvested sustainably? A question revisited with a review of shark fisheries. Marine and Freshwater Research 49(7):553–572.

Table 2.1: Coefficient of determination and probability value, as well as decline, conservative decline and extreme decline (as defined in Methods section), in both millimeters and percentage, for each size index and species analyzed.

Species:	Atlantic sharpnose	Blacknose	Blacktip	Bull	Dusky
$L_{90\%}$					
R^2	0.51	0.19	0.06	NA	0.11
p	< 0.001	0.002	0.299	NA	0.04
decline (mm)	88	115	141	NA	297
decline (%)	10	10	10	NA	23
conservative decline (mm)	45	32	NA	NA	NA
conservative decline (%)	5	3	NA	NA	NA
extreme decline (mm)	132	199	440	NA	654
extreme decline (%)	15	17	29	NA	45
mean FL					
R^2	0.01	0.28	0.01	0.17	0.04
p	0.603	0.001	0.574	0.41	0.382
decline (mm)	18	116	49	559	95
decline (%)	2	11	4	27	10
conservative decline (mm)	NA	41	NA	NA	NA
conservative decline (%)	NA	4	NA	NA	NA
extreme decline (mm)	93	192	240	2073	330
extreme decline (%)	12	18	20	85	32
median FL					
R^2	0.12	0.2	< 0.01	0.18	< 0.01
p	0.078	0.008	0.836	0.403	0.766
decline (mm)	49	104	19	569	32
decline (%)	6	10	2	27	4
conservative decline (mm)	NA	21	NA	NA	NA
conservative decline (%)	NA	2	NA	NA	NA
extreme decline (mm)	107	188	222	2080	267
extreme decline (%)	13	18	21	85	26

Finetooth	Sandbar	Scalloped hammerhead	Silky	Smooth dogfish	Spinner	Tiger
0.1	0.35	0.06	0.15	0.23	0.14	NA
0.647	0.096	0.266	0.115	0.007	0.177	NA
133	541	294	83	178	399	NA
12	35	19	9	23	28	NA
NA	NA	NA	NA	2	NA	NA
NA	NA	NA	NA	0	NA	NA
804	1219	905	215	333	1035	NA
56	63	49	22	30	61	NA
0.23	0.07	0.03	0.03	0.06	< 0.01	< 0.01
0.164	0.337	0.328	0.197	0.22	0.762	0.943
166	214	131	66	149	45	NA
15	20	11	8	17	4	NA
NA	NA	NA	NA	NA	NA	NA
NA	NA	NA	NA	NA	NA	NA
430	693	439	200	421	377	857
35	55	33	22	43	33	42
0.24	0.05	0.02	0.03	0.07	< 0.01	< 0.01
0.154	0.35	0.323	0.205	0.165	0.997	0.924
171	193	117	65	166	NA	35
16	18	10	8	18	NA	2
NA	NA	NA	NA	NA	NA	NA
NA	NA	NA	NA	NA	NA	NA
434	643	397	201	436	352	988
35	51	31	22	44	31	47

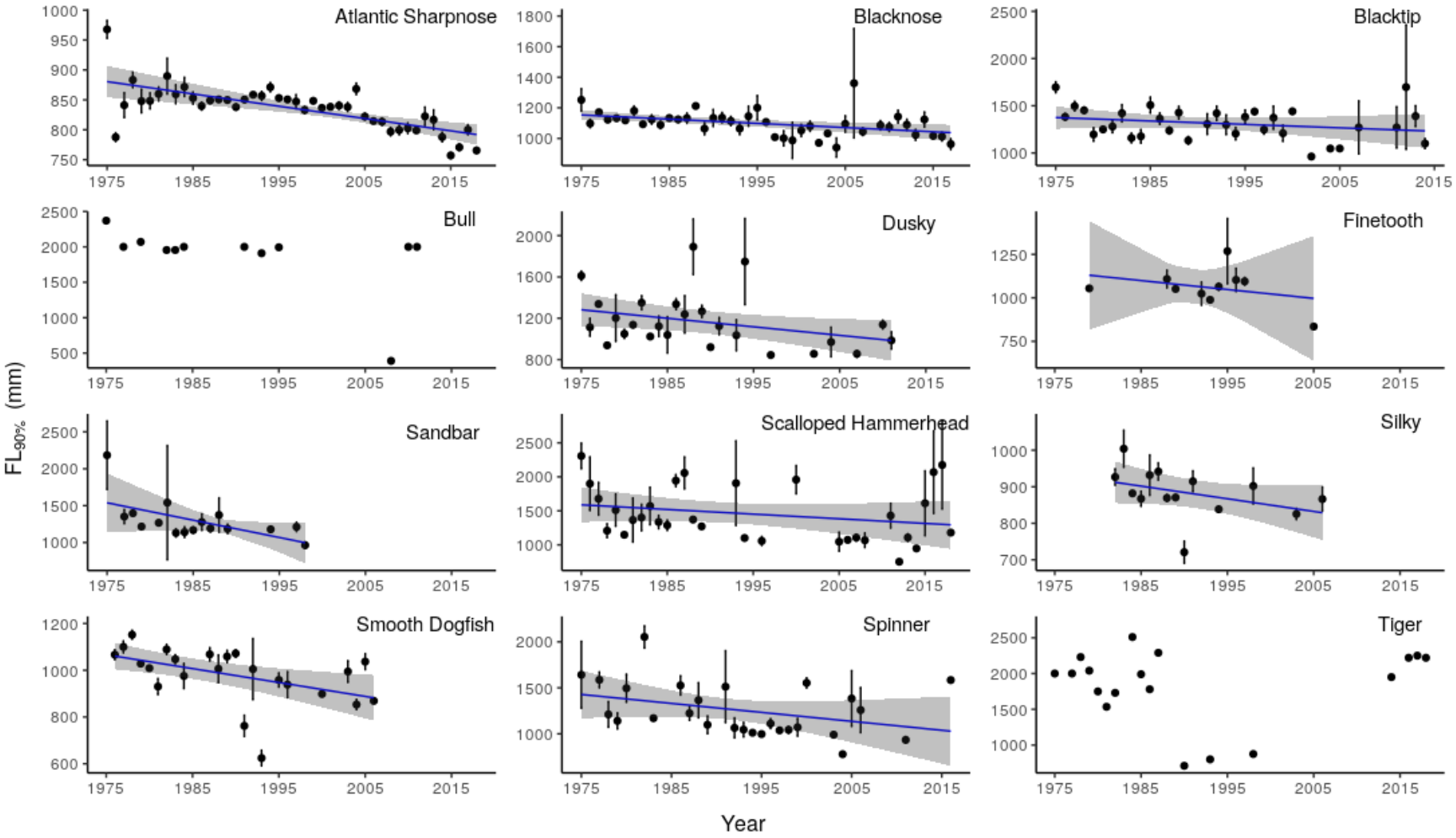

Figure 2.1: Index of maximum FL $\pm$ 1 standard error with linear regression models and 95% confidence intervals for each species.

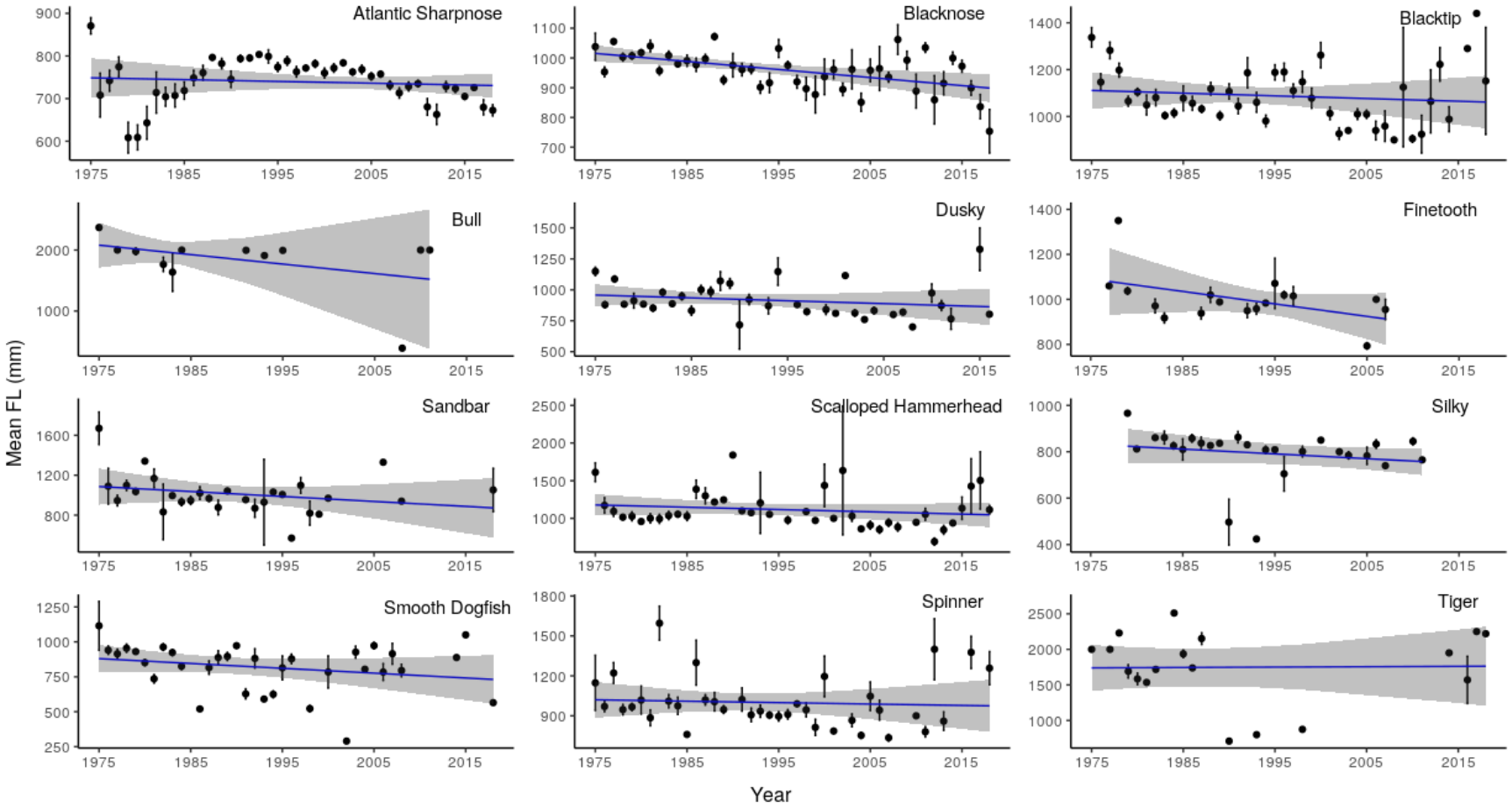

Figure 2.2: Mean FL ± 1 standard error with linear regression models and 95% confidence intervals for each species.

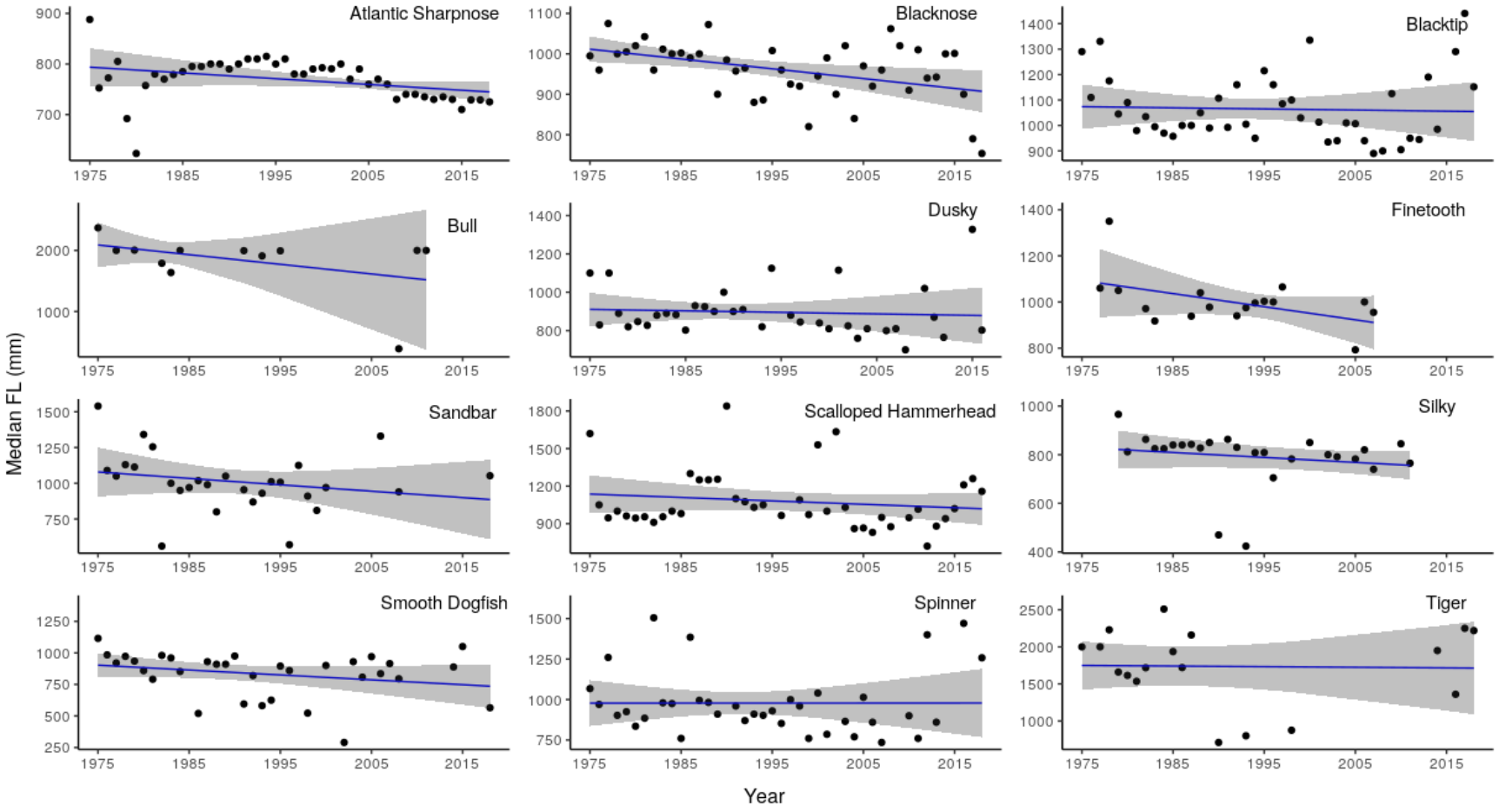

Figure 2.3: Median FL $\pm$ 1 standard error with linear regression models and 95% confidence intervals for each species.

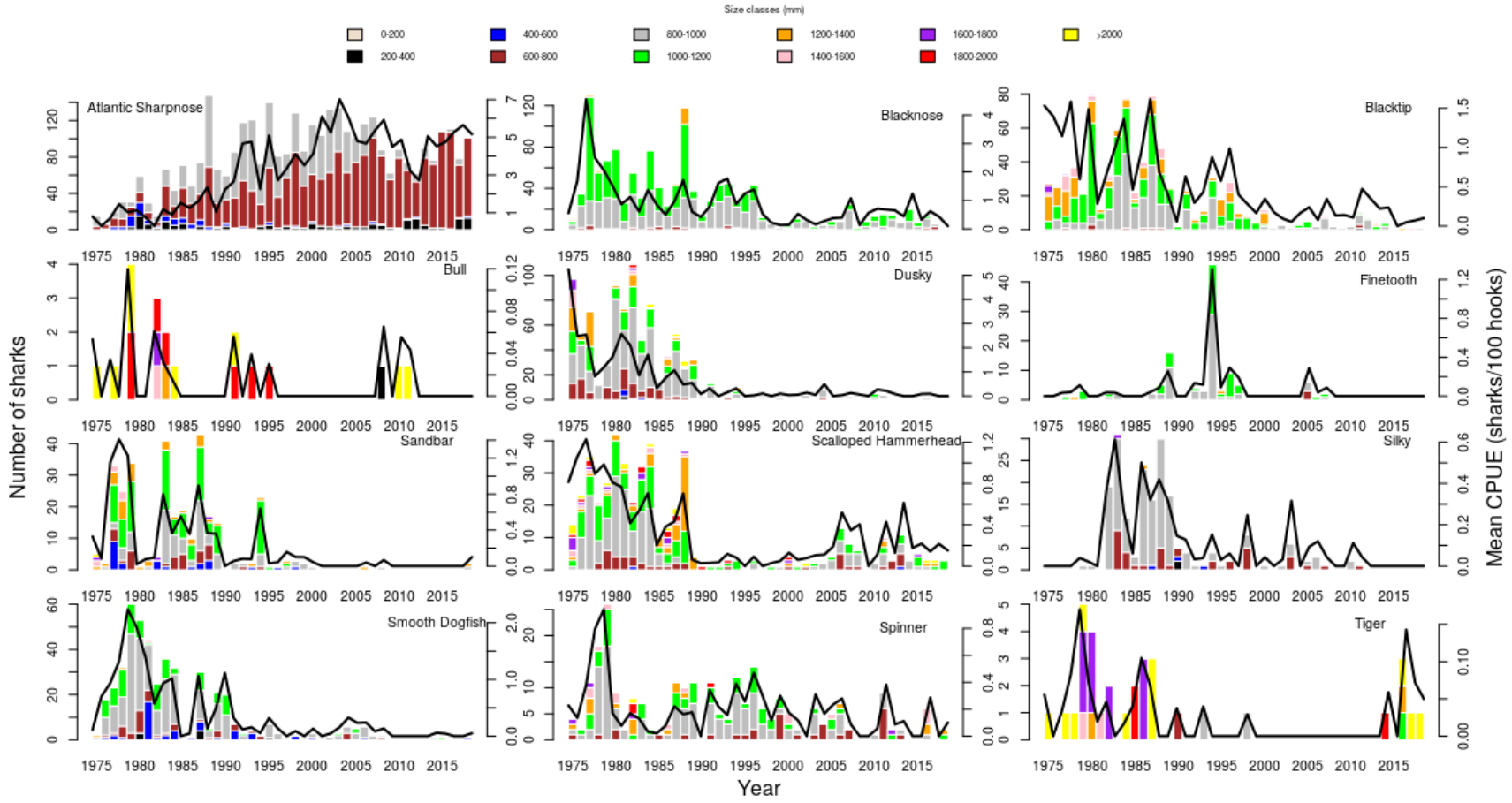

Figure 2.4: Stacked barplots displaying annual length frequency distribution, with mean CPUE shown as a line plot.

CHAPTER 3: SEASONAL RESIDENCY AND MOVEMENT PATTERNS OF BONNETHEAD SHARKS (*SPHYRNA TIBURO*) IN NORTH CAROLINA AND GEORGIA ESTUARIES

Introduction

Many animals perform seasonal and life-history dependent movements related to foraging or reproduction, knowledge of which is crucial for predicting population and community dynamics (Morales et al. 2010). In fish, these movements can occur over a range of scales, such as among habitats, through coastal estuaries, or between management regions, as individuals attempt to maximize growth, survival, or reproductive success (i.e., fitness) (Mason and Brandt 1996). For many estuarine-associated species, tracking seasonal movements or migrations of fishes capable of transiting between offshore spawning/resting and inshore foraging habitats is critical for defining stock concepts and quantifying vital rates (Cadrin and Secor 2009). Most stock assessment models are unable to account for the fitness costs or benefits arising from movement or due to differences in habitat quality, resulting in fairly course resolution of location- and population- specific vital rates (i.e., growth, survivorship, fecundity). Understanding how movement and habitat utilization (together referred to as behavior) affects population ecology of fishes is important as we move toward ecosystem-based approaches for managing coastal resources (Crowder and Norse 2008).

Bonnethead sharks (*Sphyrna tiburo*) appear seasonally in southeast United States (US) Atlantic coast estuaries, including in North Carolina (NC) and Georgia (GA), and are potentially important predators on other key estuarine species such as blue crabs (*Callinectes sapidus*) and

red drum (*Sciaenops ocellatus*) (Cortés et al. 1996). Although demography, social behaviors, and estuarine habitat use of bonnethead sharks has been studied in the Gulf of Mexico and along Florida (e.g., Myrberg and Gruber 1974; Cortés and Parsons 1996; Heupel et al. 2006), comparatively little work has been undertaken north of Florida, where climate change may contribute to increases in bonnethead occurrence as warming waters will likely expand the range of suitable habitat farther north along the US Atlantic coastline. Previous work has detected latitudinal variation in growth rates of bonnethead sharks (Carlson and Parsons 1997; Lombardi-Carlson et al. 2003), as well as regional differences in age and growth (Frazier et al. 2014), highlighting the importance of understanding movement patterns throughout the entire range of this species. A recent tagging study on female bonnethead sharks in South Carolina found evidence of site fidelity to specific estuaries for this species, a pattern that remains to be confirmed from other locations within the northern extent of their range (Driggers et al. 2014).

I employed acoustic telemetry to quantify the behavior of bonnethead sharks across spatiotemporal scales relevant to seasonal residency and migration patterns to better inform management of coastal habitats and resources. Due to the relative paucity of studies for this species north of Florida, this study also aims to expand the geographical range over which these seasonal patterns have been described. The objectives of this study were three-fold: 1) determine the seasonal residency period and return rates for bonnethead sharks in two spatially-distant estuaries (NC and GA) to assess site fidelity of bonnethead sharks to specific estuaries regionally, 2) identify areas of highest affinity for bonnethead sharks within these estuaries, and 3) evaluate migration patterns to reveal migration routes and potential overlap between individuals from these estuaries.

Methods

Field sampling

To monitor bonnethead shark residency and distribution in NC and GA inshore waters, two separate diffuse arrays of VR2W hydrophones (Vemco, Nova Scotia, Canada) were deployed between June 2015 and September 2016. The VR2W is an omni-directional hydrophone with a detection range of approximately 350 m in these systems based on cursory onsite tests. The NC array consisted of 78 hydrophones placed in and around Beaufort Inlet: Morehead City shipping channel, Carrot Island, Middle Marsh, North River Marsh, Haystacks Marsh, Bogue Sound and Back Sound, which are waterways and marsh complexes between Beaufort Inlet and the lower estuary regions of the Newport and North Rivers (Figure 3.1). The GA array consisted of 8 hydrophones placed in and around several marsh creeks within lower Wassaw Sound including Romerly Creek, Bull River, and Tybee Cut, as well as the lower Wilmington and Skidaway Rivers surrounding Skidaway Island (Figure 3.2). Acoustic arrays were maintained from 2015 – 2019 in GA and 2016 – 2018 in NC.

A total of 21 bonnethead sharks in NC and 16 in GA were captured for this study. Bonnethead sharks were captured using either hook and line, gill netting, cast net (1 individual), or bottom trawl (1 individual) from June 2015 through August 2017. Because bonnethead sharks segregate by sex, with those exhibiting seasonal residency in estuaries comprised almost entirely of females, all but a single bonnethead shark captured offshore by bottom trawl were females. A 50 mm external “roto” tag (Premier 1 Supplies, Iowa, USA) was attached to the first dorsal fin of each shark. External tags had Vemco V13 acoustic transmitters affixed to them using marine epoxy, which ensured transmitters would remain attached to external tags. These ‘coded’ transmitters were set to transmit a signal from each shark (using a train of pings unique to each

individual tag) randomly once every 3-5 minutes, throughout the life of the tag (~ 4 years). I chose to use external attachment as this reduced the handling time for each shark and is perhaps much less invasive than surgery, thus likely increasing the survival rate for the encounter. Tagged sharks were observed prior to being released to assess condition, with bonnethead sharks exhibiting extreme distress retained to re-deploy tags, avoiding tracking of individuals likely to expire. Information on location, date and time captured, sex and size were collected for each tagged bonnethead shark (Tables 3.1 & 3.2).

Data analysis

To examine seasonal residency patterns, I looked for extended periods without detections to estimate periods of ingress and egress to and from the estuaries surrounding these periods of absence, which would define seasonal residency periods. Within periods of seasonal residency in the NC array I used hydrophones surrounding Beaufort Inlet to identify shorter-term excursion events outside of the inlet during more seasonal residency periods. An excursion was defined as any detection(s) occurring outside of Beaufort Inlet, with detections occurring within the estuary both before and afterwards. For excursions from the NC estuary, I also quantified the time elapsed between the last detection within Beaufort Inlet and the first detection occurring within Beaufort Inlet subsequent to outside detections, as the time spent outside of the estuaries during ocean excursions. For the GA array, the large embayment as well as hydrophone placement did not allow for examination of ocean excursions during seasonal residency periods. To further examine patterns of movement in relation to Beaufort Inlet and how these varied by distance from the inlet, I evaluated detection density as a function of distance from the inlet in 1,000 m increments, starting from 500 m distance as this was the distance for the hydrophone located

closest to the inlet. The number of hydrophones within each 1,000 m bin was also quantified to more fully evaluate how hydrophone density influenced the pattern of detection density by distance from inlet.

I used non-metric multidimensional scaling (nMDS) in the R package vegan (Oksanen et al. 2019) to examine hydrophone station visits by individual sharks and determine similarity in location of movement patterns across individuals. I generated a matrix with each hydrophone on the x-axis, ordered in decreasing longitude, and each shark on the y-axis. This matrix was filled in using the number of detections for each shark, at each hydrophone, standardized by total detections for each shark, such that each value represented the relative contribution of each hydrophone to an individual shark's overall pattern of detections (Bray and Curtis 1957). I then constructed a dissimilarity matrix using the Bray-Curtis distance metric, which is widely used in analysis of ecological data due to its robustness and ability to capture important relationships having ecological relevance (Faith et al. 1987; Clarke et al. 2006). I performed cluster analysis on the nMDS ordination, defining clusters with 10% similarity, to examine potential groupings of sharks based on hydrophone station visits. I also calculated weighted average scores for each hydrophone station to examine how visits to particular hydrophone stations influenced ordination structure among or between groupings or individuals. Due to the large number of hydrophone stations in the NC array (N = 68), I selected the 5% of hydrophone stations with the highest correlation to ordination axes using the R package goeveg (Goral and Schellenberg 2018). All statistical analyses were performed in R (R Core Team 2016).

To determine if bonnethead sharks exhibited site fidelity to specific estuaries as has been documented previously in Florida (FLa) and South Carolina (SC), return rates were calculated for both arrays as the number of sharks returning each consecutive year after tagging. I also

evaluated detections from other arrays that were shared with me from areas in SC, GA, and FLa: Myrtle Beach (SC), Charleston (SC), Savannah (GA), Ossabaw Sound (GA), Gray's Reef National Marine Sanctuary (GA), Brunswick (GA), St. Mary's River (FLa), Cape Canaveral (FLa), and Pensacola (FLa), to determine broader regional patterns of residency and movement when sharks left the arrays in NC and GA. Number of detections outside of array where each shark was tagged were quantified and detection location (state) as well as range of dates detected outside were recorded for each bonnethead shark. This also allowed me to evaluate if sharks moved up the coast together as one big mixing stock, or if the GA-tagged sharks have a stop point that's consistently south of the NC tagged sharks, by comparing the states visited by NC-tagged sharks and GA-tagged sharks to see which states overlapped and which states differed between these groups.

Results

I recorded a total of 34,423 detections within the NC array and 43,204 detections from the GA array. In NC, an average of 1,639 $\pm$ 292 (SE) detections per shark were recorded from the 21 tagged sharks. In GA there was an average of 2,880 $\pm$ 869 detections per shark recorded for 15 of 16 tagged sharks. NC sharks visited 19 $\pm$ 2 out of 78 total hydrophones, on average, whereas GA sharks visited an average of 2 out of 8 total hydrophones. In NC sharks were recorded within the array between 2 and 133 days from when they were tagged (excluding time between egress of tagging year and ingress the following year) with an average of 41 $\pm$ 8 days at liberty (Table 3.1). In GA sharks were recorded within the array between 0 and 395 days from when they were tagged with an average of 84 $\pm$ 24 days at liberty (Table 3.2).

Bonnethead sharks left the NC array between July 20th and November 19th in the year they were tagged, with half of tagged sharks having left by September 3rd. The sharks that returned to the NC array arrived between March 16th and June 5th of the following year, with half of the sharks returning by May 17th (Figure 3.3). In the GA array, bonnethead sharks left between June 17th and November 21st on the year tagged, with half of tagged sharks having left by August 29th. The sharks that returned to the GA array arrived between March 17th and May 2nd the year following tagging, with half of the sharks returning by April 26th (Figure 3.4). Assuming no tag loss, transmitter failure, or shark death, one quarter of bonnethead sharks tagged in this study returned to NC, with 5 of 20 sharks tagged in 2016 returning in 2017 (Figure 3.3). In GA, 19% of tagged bonnethead sharks returned (once again assuming no tag loss, transmitter failure, or shark death), with 2 of 8 sharks tagged in 2015 returning in 2016 and 1 of the 8 sharks tagged in 2016 returning in 2017 (Figure 3.4). During their residency within the NC array, bonnethead sharks made an average of 8 $\pm$ 2 excursions outside of Beaufort Inlet, with an average duration of 7.5 $\pm$ 2 hr (Table 3.3).

Detection density in the NC array was concentrated in and around Beaufort Inlet, with the maximum number of detections per 1,000 m bin within the NC array of 21,411 occurring between 500-1,500 m from Beaufort Inlet. When normalized by the number of hydrophones, the maximum number of detections was 1,946, also occurring between 500-1,500 m from Beaufort Inlet (Figure 3.5). The maximum number of hydrophones per 1,000 m bin was 15, occurring between 6,500 and 7,500 m from Beaufort Inlet (Figure 3.6).

There were three groupings or clusters with more than one shark defined at the 10% similarity level in the NC array. The three clusters were associated with Beaufort and Morehead City Channels, northeast Middle Marsh, or North River Channel, based on hydrophone weighted

average scores (Figure 3.7). In the GA array there were four groupings or clusters defined at the 10% similarity level, associated with Bull River, west and central Romerly Creek, Tybee Cut, and Priest Landing (Figure 3.8).

Thirteen of the 21 bonnethead sharks tagged in the NC array were detected outside of that array between the dates of 08/27/16 and 05/19/18. All 13 bonnethead sharks were detected in SC, 11 of them were detected in GA, and six were detected in FLa (Table 3.4). Ten of the 16 bonnethead sharks tagged in the GA array were detected outside of that array between the dates of 07/22/15 and 02/13/17. Nine of these bonnethead sharks were detected in GA and four were detected in FLa (Table 3.5). Whereas both NC-tagged sharks and GA-tagged sharks were detected in both GA and FLa, GA-tagged sharks were not found north of GA, where only NC-tagged sharks were detected.

Discussion

This study further documents the site fidelity of bonnethead sharks to specific estuaries on intra- and inter-annual time scales and builds upon previous studies in the region by revealing individual patterns of within-estuary habitat use during seasonal residency. Moreover, by identifying critical habitat for bonnethead sharks within estuaries, my results contribute novel information important to the management of this species. These data also serve to arbitrate in the hypotheses established in previous studies of bonnethead sharks related to seasonal foraging habitat, countergradient variation in growth rate, population connectivity along the southeastern US Atlantic Coast, and social transmission of migratory routes.

Approximately 25% of bonnethead sharks tagged in this study were observed to return to NC or GA estuaries across years, suggesting that at least some individuals of this species

establish annual migration patterns of returning to the same estuaries (Figures 3.3 & 3.4). Fidelity rates for bonnethead sharks returning to estuaries may be higher since two acoustic transmitters attached to individuals caught within the NC array were returned to us by fishermen, who indicated they found the transmitters within their fishing gear (i.e., gillnets), revealing the potential for tag shedding or fishing mortality. Driggers et al. (2014) documented patterns of intra- and inter-annual site fidelity of bonnethead sharks to specific estuaries in South Carolina using mark-recapture, finding some individuals returned to the same estuary multiple times, up to 9 years subsequent to tagging. Results of the present study support this finding.

Bonnethead sharks in both NC and GA displayed affinity to specific areas within estuaries in which they were seasonal residents, suggesting the potential for intraspecific habitat partitioning during periods of seasonal residency (Figures 3.7 & 3.8). These results contrast with those of other acoustic telemetry studies, which found that bonnethead sharks did not return to specific areas within estuaries (Heupel et al. 2006; Smith 2012). Heupel et al. (2006) deployed a smaller hydrophone array in one portion of Charlotte Harbor, Florida, therefore it is possible that on a larger scale bonnethead sharks exhibit site fidelity to specific areas of Charlotte Harbor estuary, since three sharks did return to use similar areas within their array. Smith (2012) deployed yet a smaller hydrophone array in Romerly Marsh Creek, GA and utilized a cordless drill to drill holes in the first dorsal fin of bonnethead sharks for transmitter attachment, which may have led to higher mortality rates for the 9 bonnethead sharks tagged as the author acknowledged that 2 of these sharks were observed to have slight bleeding from the holes and were not detected post-release.

In NC and GA estuaries, bonnethead sharks showed a preference for areas that were near an inlet or mouth. There was a concentration of detections at sites nearest Beaufort Inlet, suggesting

that the inlet is an important feature, restricting bonnethead shark movement within the estuary during seasonal residency (Figure 3.5). In Gulf of Mexico estuaries, bonnethead shark captures were highest near tidal inlets, suggesting the distribution pattern observed in this study is characteristic for this species (Froeschke et al. 2010). Proximity to inlets may be related to foraging; bonnethead sharks are known to feed primarily on blue crabs, making up greater than 70% of the diet for bonnethead sharks by net weight and occurrence (Cortés et al. 1996). Female blue crabs migrate from low salinity estuarine regions to high salinity regions near the ocean, specifically areas surrounding Beaufort Inlet in North Carolina, using ebb-tide transport, to release larvae during summer months (Carr et al. 2004). This study therefore provides further evidence to support the hypothesis that bonnetheads use southeast US estuaries as seasonal foraging habitat, exploiting energetically-rich ovigerous blue crabs to meet higher energetic demands associated with reproduction (Driggers et al. 2014).

The frequent ocean excursions performed by female bonnethead sharks in NC suggest that while they are seasonal residents to estuaries, they transit between inshore and offshore habitats to maximize fitness. This may be related to foraging as well, in the Gulf of Mexico increased signatures of offshore primary production were found in mature bonnethead sharks using stable isotope analysis and it was suggested this was related to foraging on blue crabs migrating offshore to spawn (Plumlee and Wells 2016). Towards the end of their seasonal residency, female bonnethead sharks could also be migrating offshore for reproduction, since mating wounds have been found in southeastern US Atlantic bonnethead sharks in September and October (Gonzalez De Acevedo 2014).

By comparing seasonal residency patterns between estuaries at different latitudes, this study highlights the possibility of countergradient variation in bonnethead sharks, or the inverse

relationship between growth rates and length of growing season, determined by latitude (Conover 1990). Bonnethead sharks appear to arrive earlier to GA estuaries and remain later into the year, with many being detected either within the GA array or in other arrays in GA well into the fall and in late winter/early spring (Table 3.5; Figure 3.4), suggesting that seasonal migration patterns vary in timing by latitude of summer feeding grounds. This finding, combined with the fidelity to specific estuaries previously described, indicates that bonnethead sharks that are seasonal residents in Georgia are able to exploit foraging habitat for extended periods of time each year, providing a longer growing season. Previous studies have suggested that bonnethead sharks exhibit clinal variation in size and growth rate, with larger and faster growing individuals, particularly females, occurring at higher latitudes (Parsons 1993; Carlson and Parsons 1997). This was hypothesized to be related to countergradient variation, with faster growth rates acting as a mechanism for individuals at higher latitudes to compensate for shorter growing seasons (Lombardi-Carlson et al. 2003). While this study did not measure growth rates, average sizes for bonnethead sharks tracked in NC and GA estuaries were within 2 cm when compared between these two regions, suggesting that differences in growing season did not affect sizes overall and the possibility for a tradeoff that allows for both groups to maximize fitness (Tables 3.1 & 3.2).

My results also indicate connectivity among populations of bonnethead sharks along the southeastern US Atlantic coast. Bonnethead sharks tagged within the NC array were detected in the GA array, and both NC and GA sharks were detected in the same arrays during their overwintering periods, which suggests that there is possible gene flow between populations along the Atlantic coast (Tables 3.4 & 3.5). Both NC and GA bonnethead sharks were only detected in arrays along the Atlantic coast, with the exception of one shark tagged in GA (GA04), which crossed into the eastern Gulf of Mexico (Table 3.5). This finding is supported by

differences in life-history parameters between bonnethead sharks along the southeast US Atlantic coast and the Gulf of Mexico, suggesting that these should be considered separate stocks (Frazier et al. 2014). Escatel-Luna et al. (2015) also found evidence of barriers to gene flow between US Atlantic waters and the Gulf of Mexico, contrasted with a lack of genetic differences along the Atlantic coast of Florida, which the present study supports. The occurrence of genetically distinct populations along the US Atlantic coast and the northern Gulf of Mexico was also found in another small coastal shark, the blacknose shark (*Carcharhinus acronotus*), as well as several other marine fishes, and has been attributed to surface currents in the Florida Straits or the absence of suitable habitat along the southern Florida coast (Gold and Richardson 1998; Gold et al. 2002, 2009; Portnoy et al. 2014). The fact that one bonnethead shark from the present study was able to traverse the Florida Straits suggests that to do so is possible, however this event was relatively infrequent and occurred outside of the months associated with mating in this species (Sep – Nov; Gonzalez De Acevedo 2014), anecdotally supporting the hypothesis of this feature acting as a barrier to gene flow.

Conversely, the lack of overlap in migration structure between bonnethead sharks that are seasonal residents in NC and GA suggests that migrations are social behaviors that could serve to partition seasonal foraging habitat. Bonnethead sharks in NC and GA both migrated south during months when they were not seasonal residents and overlapped in the waters of GA and FLa, at least some of which subsequently returned, however only NC sharks were detected north of GA, in SC and NC (Table 3.4). Combined with the site-fidelity to specific areas within estuaries reported in this study, this is indicative of individual bonnethead sharks perhaps performing migrations in groups, where migration routes could be transmitted socially, as has been hypothesized in a previous study (Driggers et al. 2014). Several bonnethead sharks captured in

the present study were encountered in aggregations, with up to 8 individuals being tagged in the same location, on the same day, which further supports the idea of social transmission of behavior in this species (Table 3.1).

This study is the first to document the site fidelity of bonnethead sharks to specific areas within estuaries on intra- and inter-annual time scales. By identifying critical foraging habitat within estuaries, these results also provide information crucial to effective management of this species and perhaps entire southeast US estuarine systems using ecosystem-based management due to the strong trophic link to a key estuarine species (i.e., blue crab). These data also build upon previous lines of research on bonnethead shark life history and population connectivity, while generating novel hypotheses. Specifically, bonnethead shark proximity to inlets during seasonal residency in estuaries is hypothesized to be related to blue crab foraging and differences in timing of bonnethead shark seasonal migration are hypothesized to be associated with countergradient variation in growth rates as a result of differences in length of growing season by latitude. These hypotheses must be resolved by future, targeted behavioral and life history studies of bonnethead sharks along the southeast US Atlantic coast.

REFERENCES

Bray, J. R., and J. T. Curtis. 1957. An ordination of the upland forest communities of southern Wisconsin. Ecological Monographs 27(4):325–349.

Cadrin, S. X., and D. H. Secor. 2009. Accounting for spatial population structure in stock assessment: past, present, and future. Pages 405–426 *in* R. J. Beamish and B. J. Rothschild, editors. The Future of Fisheries Science in North America. Springer US.

Carlson, J. K., and G. R. Parsons. 1997. Age and growth of the bonnethead shark, Sphyrna tiburo, from northwest Florida, with comments on clinal variation. Environmental Biology of Fishes 50(3):331–341.

Carr, S. D., R. A. Tankersley, J. L. Hench, R. B. Forward, and R. A. Luettich. 2004. Movement patterns and trajectories of ovigerous blue crabs Callinectes sapidus during the spawning migration. Estuarine, Coastal and Shelf Science 60(4):567–579.

Clarke, K. R., P. J. Somerfield, and M. G. Chapman. 2006. On resemblance measures for ecological studies, including taxonomic dissimilarities and a zero-adjusted Bray–Curtis coefficient for denuded assemblages. Journal of Experimental Marine Biology and Ecology 330(1):55–80.

Conover, D. O. 1990. The relation between capacity for growth and length of growing season: evidence for and implications of countergradient variation. Transactions of the American Fisheries Society 119(3):416–430.

Cortés, E., C. a Manire, and R. E. Hueter. 1996. Diet, feeding habits, and diel feeding chronology of the bonnethead shark, Sphyrna tiburo, in southwest Florida. Bulletin of Marine Science 58(November 1993):353–367.

Cortés, E., and G. R. Parsons. 1996. Comparative demography of two populations of the bonnethead shark (Sphyrna tiburo). Canadian Journal of Fisheries and Aquatic Sciences 53(4):709–718.

Crowder, L., and E. Norse. 2008. Essential ecological insights for marine ecosystem-based management and marine spatial planning. Marine Policy 32(5):772–778.

Driggers, W. B., B. S. Frazier, D. H. Adams, G. F. Ulrich, C. M. Jones, E. R. Hoffmayer, and M. D. Campbell. 2014. Site fidelity of migratory bonnethead sharks Sphyrna tiburo (L. 1758)

to specific estuaries in South Carolina, USA. Journal of Experimental Marine Biology and Ecology 459:61–69.

Escatel-Luna, E., D. H. Adams, M. Uribe-Alcocer, V. Islas-Villanueva, and P. Díaz-Jaimes. 2015. Population genetic structure of the bonnethead shark, Sphyrna tiburo, from the western north Atlantic Ocean based on mtDNA sequences. Journal of Heredity 106(4):355–365.

Faith, D. P., P. R. Minchin, and L. Belbin. 1987. Compositional dissimilarity as a robust measure of ecological distance. Vegetatio 69(1–3):57–68.

Frazier, B. S., W. B. Driggers, D. H. Adams, C. M. Jones, and J. K. Loefer. 2014. Validated age, growth and maturity of the bonnethead Sphyrna tiburo in the western North Atlantic Ocean. Journal of Fish Biology 85(3):688–712.

Froeschke, J., G. Stunz, and M. Wildhaber. 2010. Environmental influences on the occurrence of coastal sharks in estuarine waters. Marine Ecology Progress Series 407:279–292.

Gold, J. R., E. Pak, and D. A. DeVries. 2002. Population structure of king mackerel (Scomberomorus cavalla) around peninsular Florida, as revealed by microsatellite DNA. Fishery Bulletin 100(3):491–509.

Gold, J. R., and L. R. Richardson. 1998. Population structure in greater amberjack, Seriola dumerili, from the Gulf of Mexico and the western Atlantic Ocean. Fishery Bulletin 96(4):767–778.

Gold, J. R., E. Saillant, N. D. Ebelt, and S. Lem. 2009. Conservation genetics of gray snapper (Lutjanus griseus) in U.S. waters of the northern Gulf of Mexico and western Atlantic Ocean. Copeia 2009(2):277–286.

Gonzalez De Acevedo, M. I. 2014. Reproductive biology of the bonnethead (Sphyrna tiburo) from the southeastern US Atlantic coast. University of North Florida.

Goral, F., and J. Schellenberg. 2018. goeveg: functions for community data and ordinations. https://cran.r-project.org/package=goeveg.

Heupel, M. R., C. A. Simpfendorfer, A. B. Collins, and J. P. Tyminski. 2006. Residency and movement patterns of bonnethead sharks, Sphyrna tiburo, in a large Florida estuary. Environmental Biology of Fishes 76(1):47–67.

Lombardi-Carlson, L., E. Cortés, G. Parsons, and C. Manire. 2003. Latitudinal variation in life-history traits of bonnethead sharks, *Sphyrna tiburo*, (Carcharhiniformes : Sphyrnidae) from the eastern Gulf of Mexico. Marine & Freshwater Research 54:875–883.

Mason, D. M., and S. B. Brandt. 1996. Effects of spatial scale and foraging efficiency on the predictions made by spatially-explicit models of fish growth potential. Environmental Biology of Fishes 45:283–298.

Morales, J. M., P. R. Moorcroft, J. Matthiopoulos, J. L. Frair, J. G. Kie, R. A. Powell, E. H. Merrill, and D. T. Haydon. 2010, July 27. Building the bridge between animal movement and population dynamics. Royal Society.

Myrberg, A. a, and S. H. Gruber. 1974. The behavior of the bonnethead shark, Sphyrna tiburo. Copeia 1974(2):358–374.

Oksanen, J., F. G. Blanchet, M. Friendly, R. Kindt, P. Legendre, D. McGlinn, P. R. Minchin, R. B. O'Hara, G. L. Simpson, P. Solymos, M. H. H. Stevens, E. Szoecs, and H. Wagner. 2019. vegan: community ecology package. https://cran.r-project.org/package=vegan.

Parsons, G. R. 1993. Age determination and growth of the bonnethead shark Sphyrna tiburo: a comparison of two populations. Marine Biology 117(1):23–31.

Plumlee, J., and R. Wells. 2016. Feeding ecology of three coastal shark species in the northwest Gulf of Mexico. Marine Ecology Progress Series 550:163–174.

Portnoy, D. S., C. M. Hollenbeck, C. N. Belcher, W. B. Driggers, B. S. Frazier, J. Gelsleichter, R. D. Grubbs, and J. R. Gold. 2014. Contemporary population structure and post-glacial genetic demography in a migratory marine species, the blacknose shark, Carcharhinus acronotus. Molecular Ecology 23(22):5480–5495.

R Core Team. 2016. R: A language and environment for statistical computing. http://www.r-project.org.

Smith, D. T. 2012. The utilization of spatial analyses to assess the distribution of shark populations off Georgia along with acoustic telemetry to track the bonnethead Sphyrna tiburo in a small coastal system. Savannah State University.

Table 3.1: Summary of 21 bonnethead sharks tagged with acoustic transmitters and tracked within the array of hydrophones surrounding Beaufort Inlet, NC. Shark IDs marked with an asterisk are sharks that returned in 2017. Capture location indicates where fish were originally caught for this study: Beaufort Channel (BC), Morehead City Channel (MHCC), Northeast Middle Marsh (NEMM), Offshore of Shackleford Banks (OSSB), North River Channel (NRC). Days at liberty calculated as days between tagging date and date of last detection for 2016 or 2017, for sharks returning in 2017 days between first and last detection for that year are added to reach total days at liberty.

Shark ID	Capture location	Tagging date	Sex	Fork length (mm)	Total detections	Stations visited	Days at liberty
NC01	BC	06/24/16	F	800	2843	15	74
NC02	BC	07/14/16	F	925	138	21	6
NC03*	MHCC	07/16/16	F	825	3785	23	73
NC04	MHCC	07/16/16	F	855	68	9	4
NC05	MHCC	07/16/16	F	885	2495	29	52
NC06	MHCC	07/16/16	F	955	3042	24	49
NC07	MHCC	07/16/16	F	NA	3527	13	49
NC08	MHCC	07/16/16	F	885	2529	30	48
NC09*	MHCC	07/16/16	F	845	3581	14	133
NC10	MHCC	07/16/16	F	785	1953	11	27
NC11	NEMM	08/15/16	F	830	2405	24	38
NC12	NEMM	08/15/16	F	870	81	10	2
NC13	NEMM	08/22/16	F	895	1057	26	14
NC14	NEMM	08/22/16	F	815	316	9	27
NC15	NEMM	08/22/16	F	865	541	31	15
NC16	OSSB	08/23/16	M	715	45	5	3
NC17	NRC	08/25/16	F	835	528	21	21
NC18*	NRC	08/25/16	F	865	837	33	43
NC19*	NRC	08/26/16	F	930	112	2	28
NC20*	NRC	08/26/16	F	850	1842	45	113
NC21	MHCC	08/03/17	F	860	2698	13	36

Table 3.2: Summary of 16 bonnethead sharks tagged with acoustic transmitters and tracked within the array of hydrophones surrounding Wassaw Sound, GA. Shark IDs marked with an asterisk are sharks that returned in 2016 or 2017. Capture location indicates where fish were originally caught for this study: Bull River (BR), Priest Landing (PL), West Tybee Cut (WTC), West Romerly Entrance (WRC), East Romerly Entrance (ERC). Days at liberty calculated as days between tagging date and date of last detection for 2015 or 2016, for sharks returning in 2016 and 2017 days between first and last detection for that year are added to reach total days at liberty.

Shark ID	Capture Location	Tagging Date	Sex	Fork length (mm)	Total Detections	Stations Visited	Days at Liberty
GA1*	BR	6/9/2015	F	820	11248	1	197
GA2	BR	6/9/2015	F	790	4988	1	77
GA3	BR	6/9/2015	F	840	816	2	76
GA4	PL	6/10/2015	F	830	245	2	78
GA5*	WTC	6/10/2015	F	900	4502	6	395
GA6	WTC	6/10/2015	F	890	51	1	28
GA7	WRC	6/10/2015	F	900	2239	4	56
GA8	ERC	6/10/2015	F	890	3400	1	84
GA9	WTC	6/16/2016	F	820	13	2	1
GA10	ERC	6/16/2016	F	780	0	0	0
GA11	BR	8/3/2016	F	880	258	2	24
GA12	PL	8/3/2016	F	700	25	1	30
GA13	WTC	8/4/2016	F	830	2484	4	100
GA14*	WTC	8/4/2016	F	880	2168	3	54
GA15	WRC	8/4/2016	F	880	1827	2	57
GA16	WRC	8/4/2016	F	800	8940	6	89

Table 3.3: Summary of ocean excursions for 21 sharks tracked acoustically within the array of hydrophones surrounding Beaufort Inlet, NC. Excursions were identified as detections occurring outside of Beaufort Inlet. Duration was quantified as the time elapsed between last detection within the inlet, prior to detection outside, and the first detection within the inlet, after being detected outside. Value is shown as mean $\pm$ 1 SE.

Shark ID	Number of excursions	Mean duration (hr)
NC01	17	7.4 ± 3.5
NC02	0	NA
NC03	16	3 ± 0.7
NC04	1	78
NC05	21	3.7 ± 1
NC06	8	1 ± 0.3
NC07	30	1.6 ± 0.3
NC08	11	1.7 ± 0.4
NC09	19	5.1 ± 3.7
NC10	6	2.8 ± 1.2
NC11	15	3.2 ± 1
NC12	0	NA
NC13	7	12.2 ± 8.8
NC14	1	239.6
NC15	3	23.2 ± 22.6
NC16	1	48
NC17	1	168.1
NC18	1	3.4
NC19	0	NA
NC20	4	8.1 ± 1.9
NC21	4	7.3 ± 2.6

Table 3.4: Summary of detections for bonnethead sharks tagged within the NC array, received from other acoustic telemetry arrays. State codes are as follows: SC – South Carolina, GA – Georgia, FLa – Florida. Date range calculated as date first detected outside array to date last detected outside array, with detections occurring more than one year from date of first detection outside array separated by a comma.

Shark ID	Detections outside	States visited	Date range
NC03	281	SC, GA	11/11/16 – 5/3/17
NC05	36	SC, GA, FLa	09/24/16 – 03/03/17
NC06	7	SC	09/18/16 – 09/19/16
NC07	212	SC, GA	09/22/16 – 04/10/17
NC08	407	SC, GA, FLa	09/07/16 – 05/06/17
NC11	28	SC, GA	10/02/16 – 11/12/16
NC12	186	SC, GA, FLa	09/12/16 – 12/29/16
NC13	62	SC, GA	09/13/16 – 12/08/16
NC17	41	SC	11/08/16 – 12/06/16
NC18	161	SC, GA	09/22/16 – 05/04/17
NC19	296	SC, GA, FLa	09/08/16 – 05/03/17
NC20	87	SC, GA, FLa	09/19/16 – 05/04/17
NC21	214	SC, GA, FLa	09/18/17 – 05/19/18

Table 3.5: Summary of detections for bonnethead sharks tagged within the GA array, received from other acoustic telemetry arrays. State codes are as follows: GA – Georgia, FLa – Florida. Date range calculated as date first detected outside array to date last detected outside array.

Shark ID	Detections outside	States visited	Date range
GA01	275	GA, FLa	09/10/15 – 04/25/16
GA04	1	FLa	01/11/17
GA05	385	GA, FLa	07/22/15 – 01/29/16
GA07	471	GA	06/13/16 – 09/09/15
GA08	29	GA	06/15/15
GA11	108	GA	11/16/2016 – 02/13/17
GA13	20	GA	09/02/16 – 11/24/16
GA14	35	GA	09/16/16 – 11/18/16
GA15	206	GA, FLa	08/09/16 – 09/09/16
GA16	354	GA	08/11/16 – 10/19/16

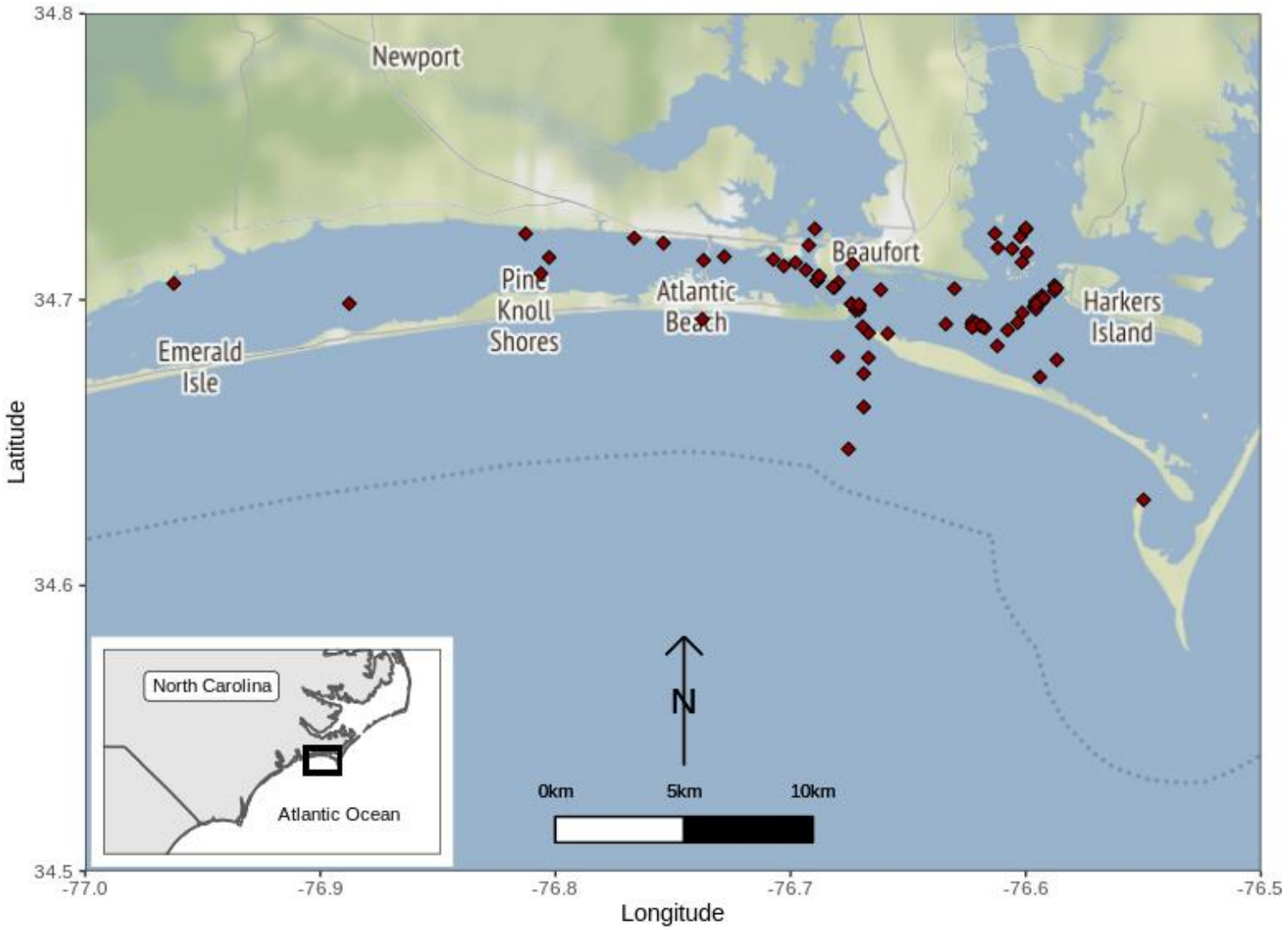

Figure 3.1: Map of study site in North Carolina. Red diamonds indicate locations of each of the 78 hydrophones in the NC array, used for tracking bonnethead shark movement during residency in 2016 and 2017.

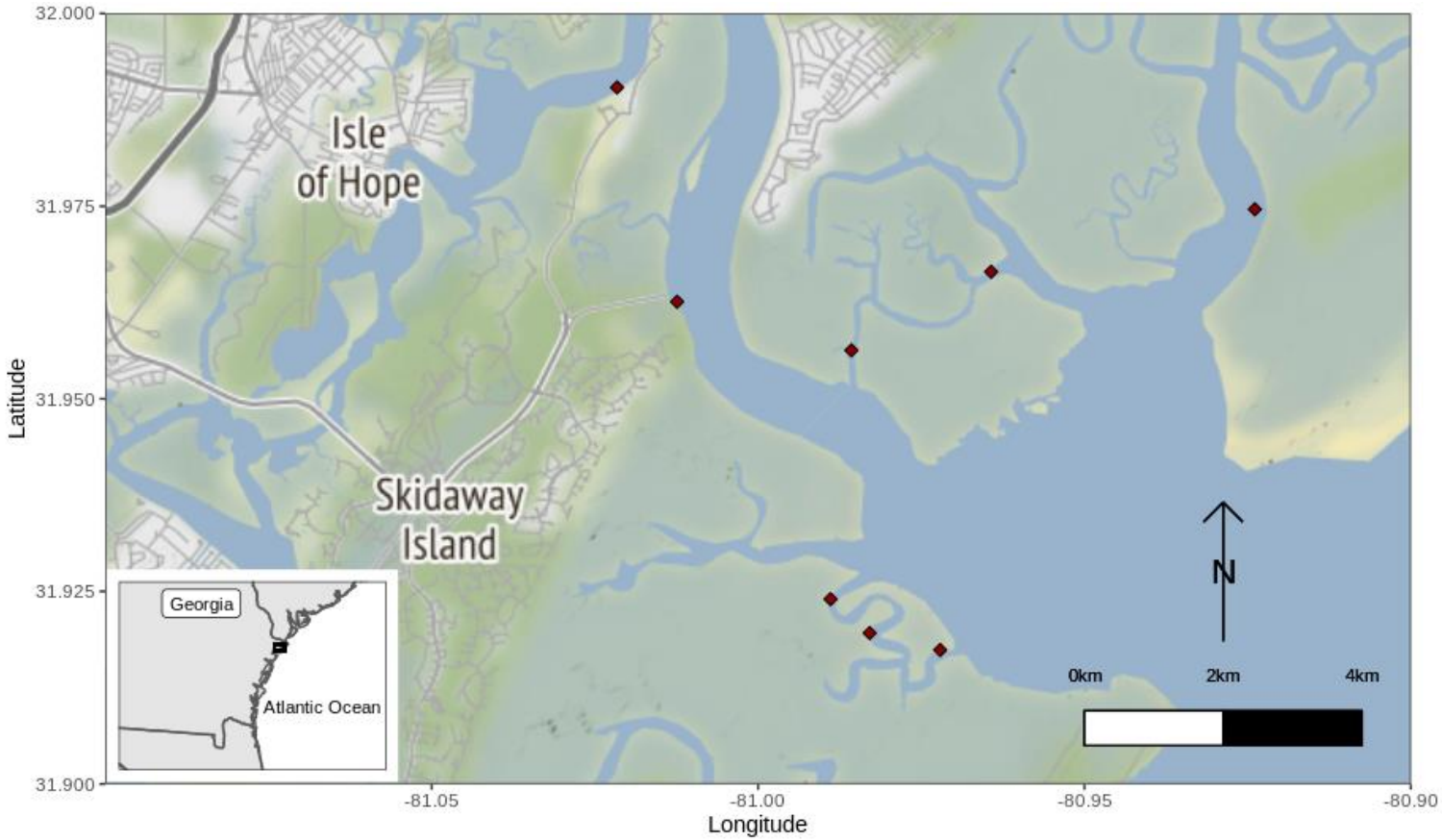

Figure 3.2: Map of study site in Georgia. Red diamonds indicate locations of each of the 8 hydrophones in the GA array, used for tracking bonnethead shark movement during residency in 2015, 2016, and 2017.

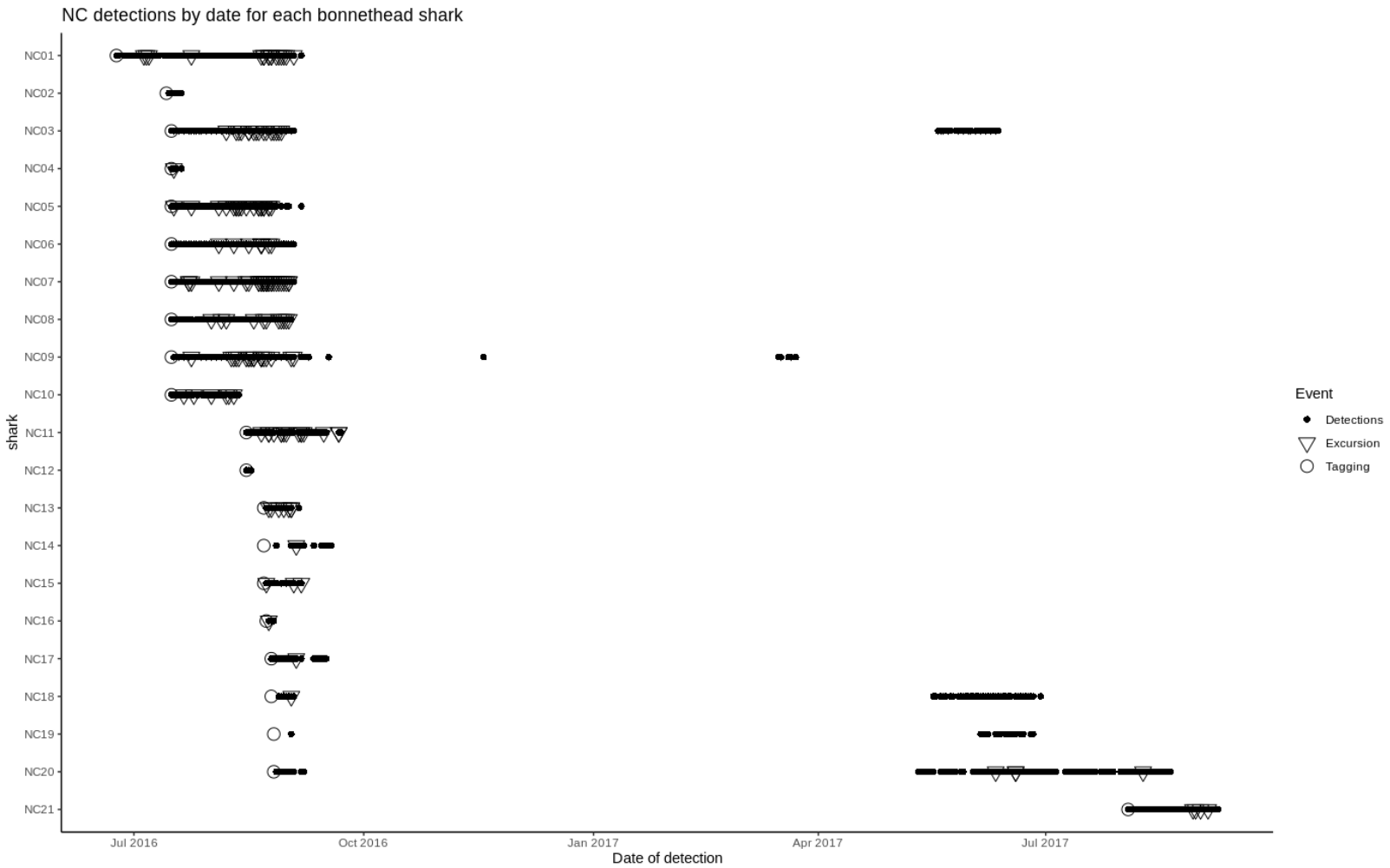

Figure 3.3: Abacus plot showing dates of all detections from each bonnethead shark tagged and detected in the NC array.

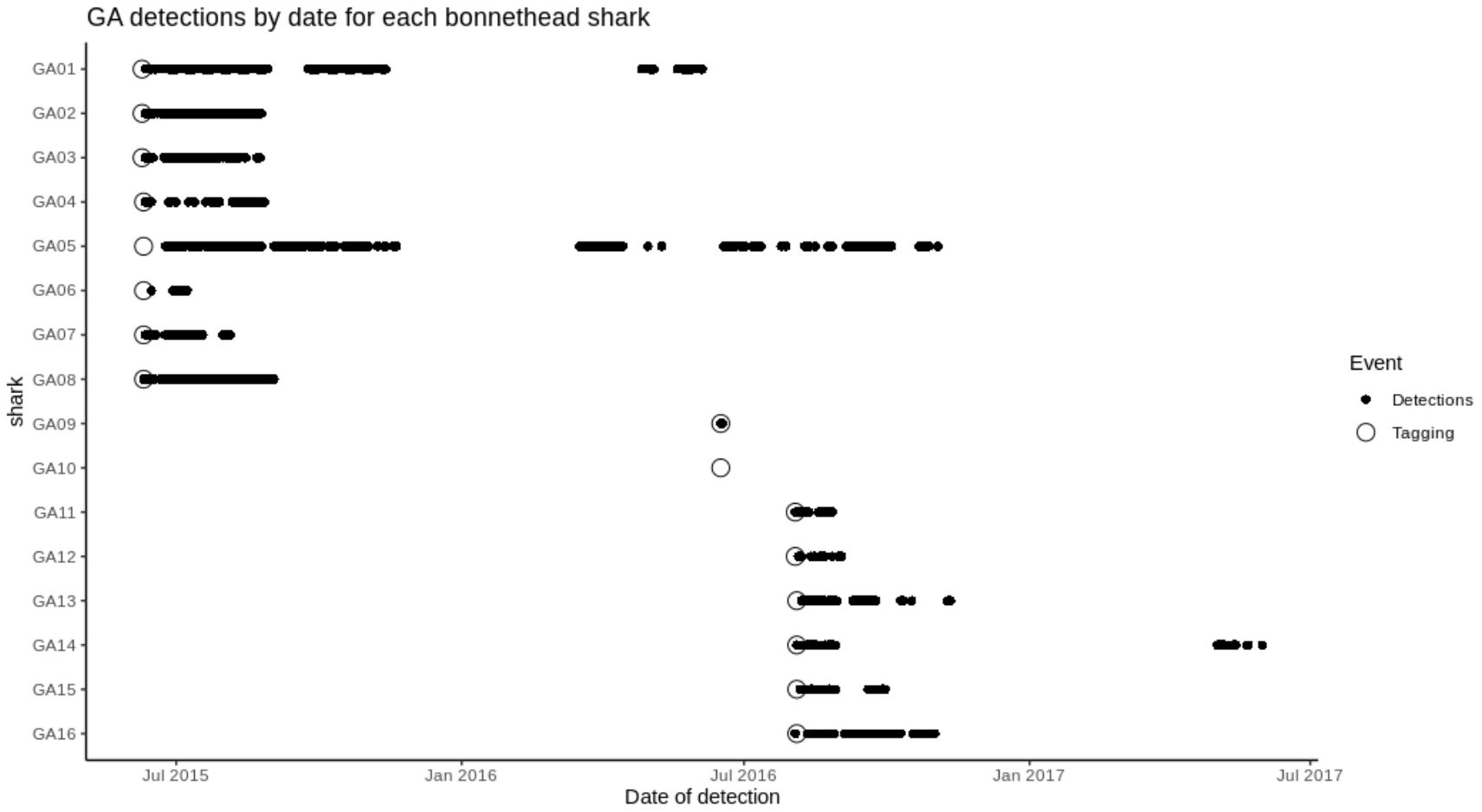

Figure 3.4: Abacus plot showing dates of all detections from each bonnethead shark tagged and detected in the GA array.

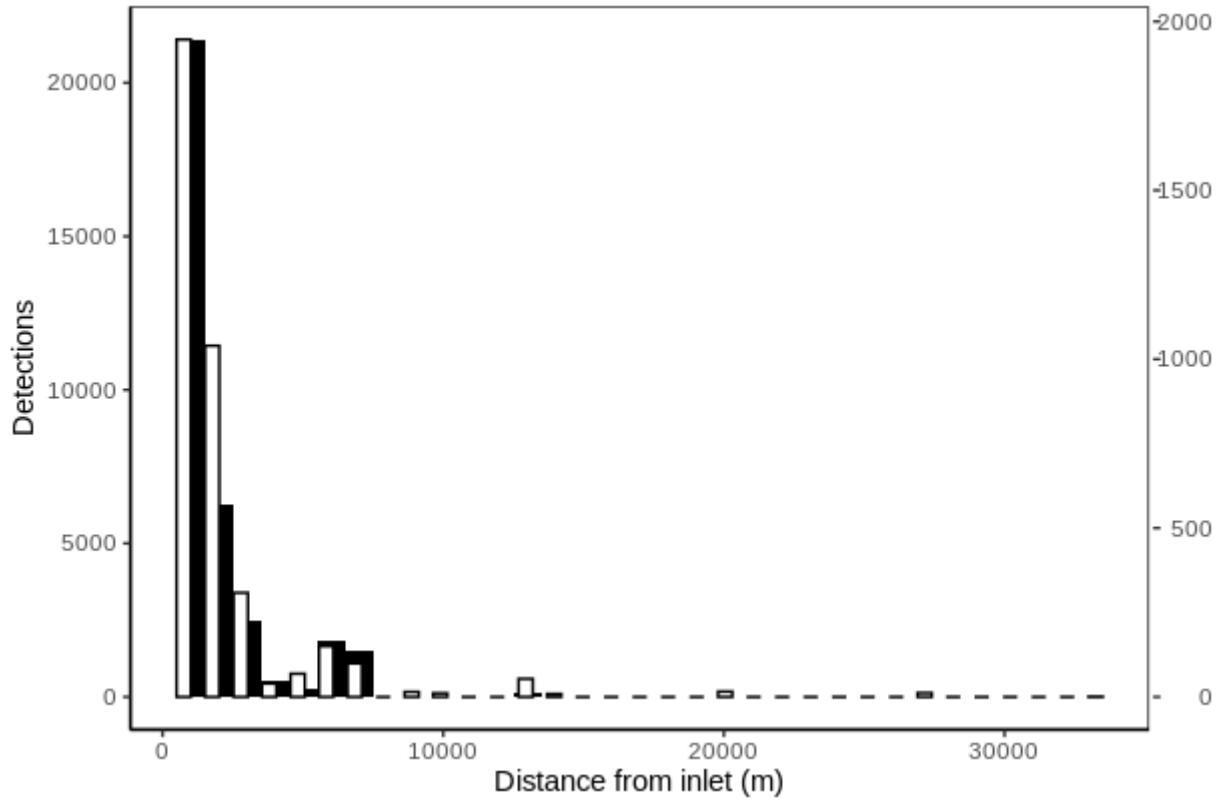

Figure 3.5: Number of detections of all bonnethead sharks tracked acoustically in the NC array (N = 21) by distance from Beaufort Inlet. Detections are aggregated in bins of 1,000 m. Black bars indicate raw detections, according to 1st y-axis scale. White bars indicate detections normalized by the number of hydrophones within each bin, according to 2nd y-axis scale.

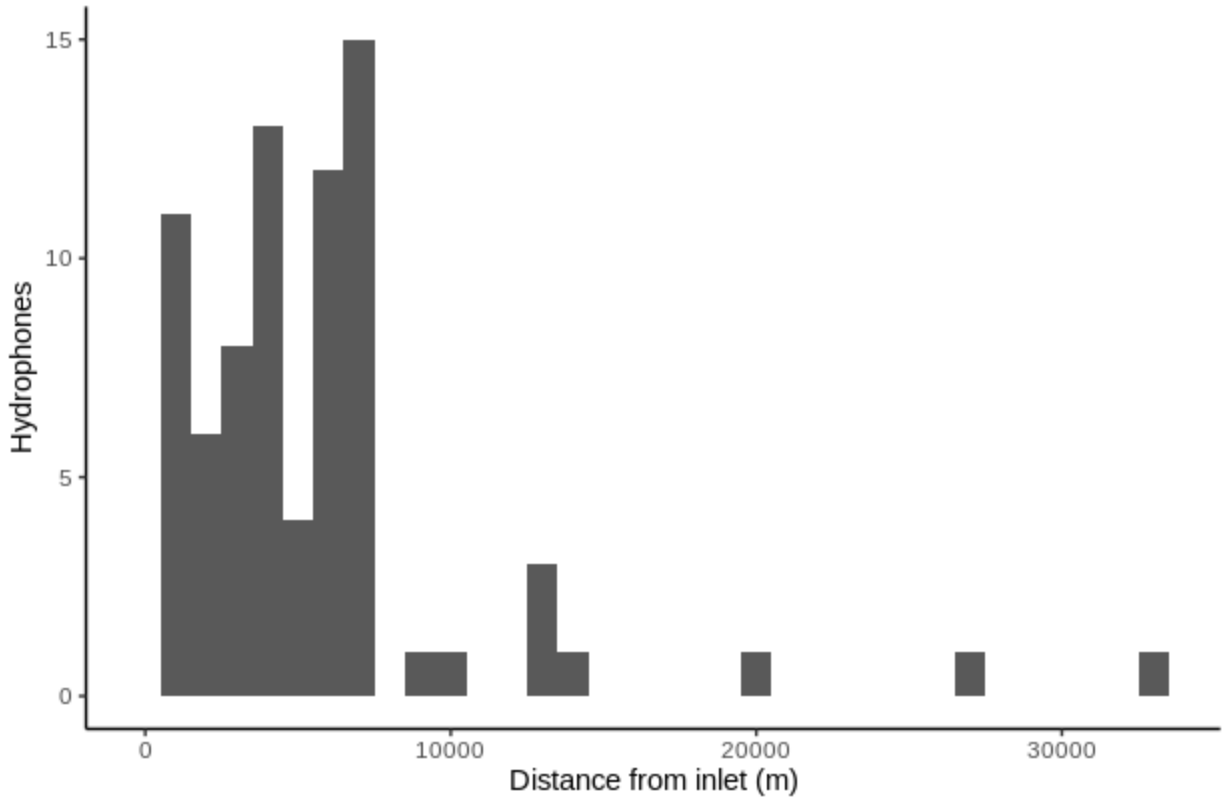

Figure 3.6: Number of hydrophones (total N = 78) by distance from Beaufort Inlet. Hydrophones were aggregated in bins of 1,000 m.

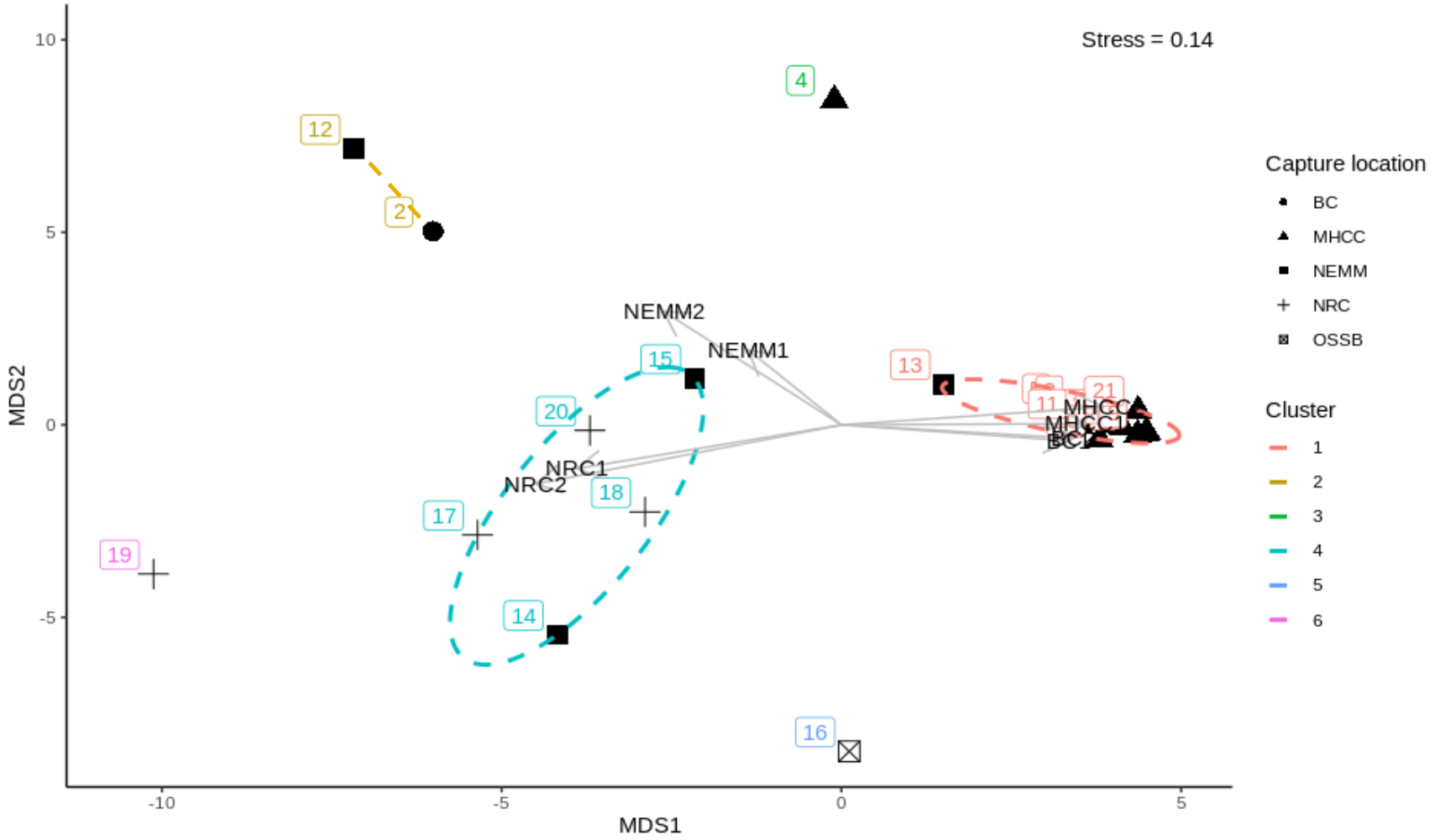

Figure 3.7: nMDS plot with each point representing one of the bonnethead sharks tracked acoustically within the NC array. Numbers represent shark IDs for individual bonnethead sharks and shapes represent capture locations. Group or clusters represent 10% similarity. Arrows show the weighted average scores for hydrophone stations ranked in the top 5%, based on correlation to ordination axes. Hydrophone label and capture location codes are as follows: BC – Beaufort Channel, MHCC – Morehead City Channel, NEMM – Northeast Middle Marsh, NRC – North River Channel, OSSB – Offshore of Shackleford Banks.

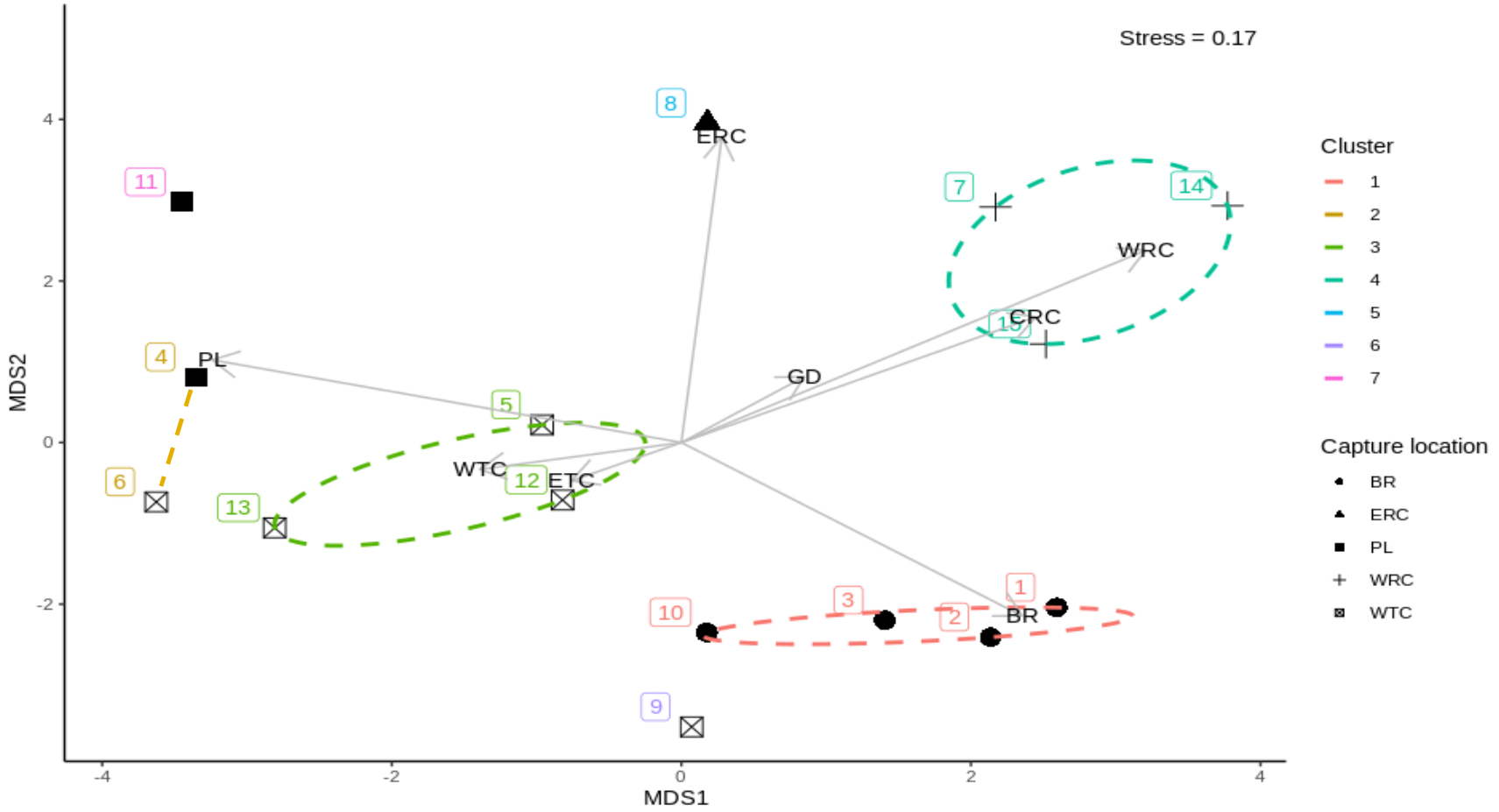

Figure 3.8: nMDS plot with each point representing one of the bonnethead sharks tracked acoustically within the GA array. Numbers represent shark IDs for individual bonnethead sharks and shapes represent capture locations. Group or clusters represent 10% similarity. Arrows show the weighted average scores for each hydrophone station. Hydrophone label and capture location codes are as follows: BR – Bull River, CRC- Central Rommerly Creek, ERC – East Rommerly Creek, ETC – East Tybee Cut, GD – Gas Dock, PL – Priest Landing, WRC – West Rommerly Creek, WTC – West Tybee Cut.

CHAPTER 4: SHARK DETECTION PROBABILITY FROM AERIAL DRONE SURVEYS WITHIN A TEMPERATE ESTUARY[1]

Introduction

Distribution and abundance estimates of sharks have typically been obtained from capture methods, such as netting or hook-and-line, often in combination with tagging studies, which together have guided our understanding of shark population dynamics and movement patterns (Kohler and Turner 2001). While valuable, there are challenges to interpretation of data gathered by these methods related to the relatively low density and high patchiness of sharks compared to other taxa, and the need to sample over relatively large areas to reduce uncertainty with respect to shark numbers (Peterson et al. 2017). Additionally, capture methods may be inappropriately invasive in some situations for sampling sharks (e.g., mortality of endangered species), which has inspired the use of less-invasive methods, such as photo identification (Bansemer and Bennett 2008). Aerial visual surveys have also been employed over large spatial scales for estimating shark distribution and abundance (Rowat et al. 2009).

Visual surveys via manned aircraft have also been utilized extensively to study other large marine animals. In the case of marine mammals and seabirds, aerial visual surveys, along with shipboard surveys, are perhaps the most widely used means of obtaining information on distribution and abundance globally (Buckland et al. 2001; Kaschner et al. 2012). With recent technological advances, the use of digital imagery has become competitive with visual methods in manned aerial surveys for these animals, resulting in similar to substantially larger estimates of abundance (Buckland et al. 2012; Koski et al. 2013). Importantly, the use of manned aircraft

has a number of logistical and scientific drawbacks, such as prohibitive cost, disturbances to wildlife, and the difficulty of covering smaller survey areas (Christie et al. 2016).

Recently, there have been considerable advances in the use of unoccupied aircraft systems (UASs), creating an attractive platform for both terrestrial and marine ecological surveys (Anderson and Gaston 2013). These UASs are advantageous with respect to aerial manned visual surveys due to the remotely controlled, smaller, and quieter aircraft, as well as the digital imagery component, which could potentially lead to more reliable, reviewable estimates. Marine mammal surveys, which have traditionally been carried out via manned aircraft for many species, have been conducted with UASs for several species, such as dugongs, seals and sea lions (Jones et al. 2006; Hodgson et al. 2013; Sweeney et al. 2015). UASs are also used in a broad range of ecological studies on marine mammals from estimating size or body condition of individuals to collecting exhaled breath condensate for DNA and hormonal analyses (reviewed in Johnston 2019). Surveys for seabirds and sea turtles appear to benefit from the use of drones, particularly with respect to time and/or costs when compared to ground- or water-based counts (McClellan et al. 2014; Rees et al. 2018). Finally, Kiszka et al. (2016) examined shark and ray densities by drone surveys in shallow-water reef systems off Moorea, French Polynesia, demonstrating the potential value of this approach to survey for sharks and showing how the technology was not limited to only those species that are required to surface for respiration.

The bonnethead shark, *Sphyrna tiburo*, is a small coastal shark species often found in estuaries, shallow bays, and channels, where pupping females are most common (Compagno et al. 2005). Bonnetheads are also commonly found in high densities, with multiple individuals encountered within an area of 50 m^2 (Myrberg and Gruber 1974). The resulting patchiness in their distribution makes UASs an attractive survey platform. Drones are easy to operate over

mesoscale ranges (< 3 km) and at low altitude (< 100 m), making them potentially useful to monitor bonnethead distributions and habitat use in shallow-water estuarine habitats. Due to the widely varying environmental conditions found in temperate estuaries, determining the effects of particular environmental variables on detection rates of sharks from drone surveys is important for understanding the efficacy of this approach in estimating patterns of distribution and abundance. There is also mounting interest in utilizing drones in nearshore waters for public safety to help minimize interactions between larger sharks and humans, and thus understanding potential limitations of this approach in different environmental contexts also has very practical applications (Colefax et al. 2019).

Visibility bias, which results from observers missing animals, has been a fundamental problem in the use of observer-based surveys, particularly in aerial surveys (Caughley 1974). The missing animals are either potentially visible to observers, but not seen (perception bias) or are concealed, often by turbid water (availability bias), although these two biases are difficult to separate in practice (Marsh and Sinclair 1989; Pollock et al. 2006; Barlow 2015). In mid-Atlantic estuaries, turbidity extremes due to frequent resuspension of sediment and plankton by wind and tides have obvious, large effects on light penetration throughout the water column (Kirby-Smith and Costlow 1989). We designed a series of field experiments using shark decoys photographed from overhead by drones to test effects of environmental parameters on visibility bias. Given the aforementioned effect of turbidity on potential visibility bias, even in shallow water columns, we hypothesized that the interaction between turbidity and decoy depth would have the greatest effect on detection probability.

Materials and Methods

Shark Decoys

To investigate the utility of UASs in surveying bonnethead sharks, we deployed decoys that were fashioned to have the appearance of bonnetheads from overhead. The decoys (N = 9) were cut from plywood using the outline from a ~ 1 m bonnethead shark that did not survive the transition to captive display at the North Carolina Aquarium at Pine Knoll Shores (NC Aquarium). This particular specimen was a gravid female and thus representative of the size range of bonnetheads typically found within the Newport River Estuary, North Carolina. The plywood decoys were epoxied (Nos. 105 & 207, West System®, Michigan, USA) to resist water damage. Decoys were then sanded and spray-painted to mimic the shark's countershading pattern from above using a combination of colors: Nos. 86014, 68181, 84230, and 63000, Valspar®, Minnesota, USA. To confirm that the decoys had the appearance of bonnetheads, one was placed in a holding tank at the NC Aquarium with a live bonnethead while photos were taken from overhead with Cannon Powershot S110 digital cameras used during drone surveys (Figure 4.1). Finally, one decoy was made to have the shape of a more generic shark species, an Atlantic sharpnose, *Rhizoprionodon terraenovae*. This was accomplished by simply trimming the "rostrum" of the bonnethead-shaped decoy to produce a conical snout (i.e., without cephalophoil), thereby allowing us to assess the potential of identifying decoys as bonnetheads or non-bonnetheads. Decoys were positively buoyant, and had to be anchored during deployment by 20-cm lines at the head and caudal region, which were connected to standard bricks that rested on the seabed.

Drone Flights

Bonnethead sharks are commonly found within the Newport River Estuary, a shallow water body (< 3 m average depth), so decoys were placed in two flight areas in shallow waters surrounding Pivers Island in Beaufort, NC, on five separate days during the fall of 2015 as well as in the spring and fall of 2016 (Figure 4.2). Selected quadrats (0.0001 degrees latitude x 0.0001 degrees longitude, approximately 10 m x 10 m) within our flight areas targeted a depth range of 0-2 m. Within the flight areas, we haphazardly positioned decoys across the available range of depths. Depth measurements (to the nearest 0.1 m) were taken using transect tape for each decoy that was deployed (8-9 decoys per flight day) at the time of deployment. GPS coordinates (decimal degrees) were also recorded for each decoy.

Each day, environmental variables cloud cover and secchi disk depth were recorded. Cloud cover was recorded as a categorical variable, with either not cloudy (no clouds visible overhead on the days we conducted the surveys) or cloudy (cloud cover > 37% overhead on the days we conducted surveys, based on NOAA definition of partly cloudy), using the Weather Underground Forecast Android phone application, which used data from the Dakota station (KNCBEAUF23), approximately 2 km from our flight areas (Weather Underground 2011). Secchi depth was measured once within the flight area immediately before or after deploying decoys, using a 20 cm secchi disk, which was lowered by a string with marks every 0.1 m into the water until the disk was no longer visible, at which point the depth measurement was recorded. Mean wind speed was also recorded for each flight using Weather Underground data (Weather Underground 2011). Each day, to the extent possible, we scheduled 3 flights (1 per spectral filter, see following paragraph) at low, mid, and high tide to make full use of the local tidal amplitude (~ 1 m) and expand our depth interval coverage (Table 4.1). Depth measurements for decoys in

subsequent flights were recorded as the sum of the original depth measurement and change in tidal height, estimated from NOAA water level data for the Beaufort, Duke Marine Lab, NC station (8656483), less than 0.5 km from our flight areas (NOAA 2018).

A total of 30 UAS flights were conducted using a fixed wing drone (eBee, senseFly®, Switzerland), equipped with either a Cannon IXUS 127 HS or Cannon Powershot S110 digital camera with one of three spectral filters: Regular (RGB), Red Edge (RE), and Near Infrared (NIR). Flight missions were designed and automated using the flight management software included with the eBee (eMotion, senseFly®, Switzerland). Each flight area (approx. 0.8 km^2) was divided into eBee overpass transects that were 400-m-long and 25-m-apart. Flight altitude was 60 m, flight speed was 13 m s^{-1}, and flights lasted about 15 minutes. eBee cameras captured a downward-facing image roughly every four seconds along each transect with an on-the-ground resolution of < 2.7 cm/pixel. Individual footprint area for digital images ranged from 4,200 – 8,478 m^2.

Image Assessments

Images were indexed for factor levels using four continuous variables: time of day (< 10:30am, 10:30 – 1:30 pm), , mean wind speed (< 4 m s^{-1}, 4 – 8 m s^{-1}, > 8 m s^{-1}), secchi depth (< 1 m, 1 – 1.5 m, > 1.5 m) and decoy depth (< 0.6 m, 0.6 – 1 m, > 1 m). Images were also indexed by two categorical variables: filter (RGB, RE, NIR) and cloud presence (cloudy, not cloudy). For continuous variables, values were discretized into two- or three – level classifications, based on natural breaks in the data, which was done because the limited range of values observed during the 30 UAS flights didn't allow for full exploration of these variables. This index was used to construct a matrix of 43 photographs, containing 0-9 shark decoys. Across the 43 photos, there

were 144 bonnethead decoys and 15 non-bonnethead decoys, representative of the full spectrum of combinations of factor levels (36 unique combinations, largely driven by multiple depths within any single photo) present within the days of sampling, with at least 2 replicates for each level of each factor. The matrix was then utilized to construct a PDF file containing the 43 images for distribution to be scored. Images were sent out to a group of fisheries and estuarine scientists (N = 15) who volunteered to score each photo for presence of sharks. Without being provided any prior information regarding the number or identity of decoys that were deployed in the field of view of each image, each scorer was asked to place symbols directly on top of where they thought sharks were in each image, with separate symbols denoting bonnethead or Atlantic sharpnose sharks. Scorers were also given the option to place a mark in a box denoting no sharks were present in the image. To standardize scoring efforts, a quadrant grid denoting maximum zoom frame as well as a 5-minute time limit per photograph were specified.

We used a hierarchical coding system to evaluate the series of possible outcomes for each decoy and/or image after scoring. For images that contained decoys, each decoy was assigned a code of 0 if not detected, or a code of 1 if detected (symbol correctly placed). For a symbol to be considered correctly placed it could not be more than one body length away from the decoy (per instructions to scorers). Any symbol placed at a greater distance than 1 m from any decoy was considered a false detection. For decoys that were detected, a second layer of coding was applied to indicate if the species identification was correct (0 – incorrect, 1 – correct). Finally, images that contained no decoys were only evaluated for the number of false detections in each image.

Data Analysis

Detection probability (number of times detected/number of scorers) was calculated for each decoy, a metric for the probability of detection by the "average" observer, which was the value that all subsequent tests were applied to, except in the case of false detections. To examine the range of detection probabilities, mean detection probability and standard error was computed across all decoys (across factor-levels) using the R package *psych* (Revelle 2017). The effects of 5 parameters on detection probability were further explored via the Mann-Whitney U test (two-level) or Kruskal-Wallis H test (three-level) among factor-level groupings: time of day, filter type, cloud presence, wind, and decoy depth, using the R package *coin* (Hothorn et al. 2008). Because wind and tide conditions changed across survey flights on each flight day, which would affect turbidity, and we failed to sample this variable frequently enough, we decided to exclude secchi depth from our analyses. These non-parametric rank-sum tests were utilized because detection probabilities could not be assumed to be normally distributed within groupings. We considered p values, patterns of detection probability and variances to evaluate strength of evidence for environmental conditions on detection probability (sensu Murtaugh 2014).

We used regression tree analysis (in R package *rpart* Therneau et al. 2015) to rank the relative importance of environmental factors in explaining the variance in detection probabilities. In addition to their flexibility (i.e., non-parametric), these models have strengths in their robustness as well as their relative ease of use and interpretation, complementing traditional statistical techniques (De'Ath and Fabricius 2000). We considered 5 factors and chose continuous input for numerical variables (time of day, depth, and wind speed) as this provided more informative (i.e., variance reducing) splits of detection probabilities, along tree branches. We pruned the tree using the 1– SE rule (as in Breiman et al. 1984).

To determine if detected sharks could be reliably identified as bonnethead or non-bonnethead, misidentification rates (number of times incorrectly identified/number of scorers who detected decoy) were calculated for all decoys detected by at least one scorer. Misidentification rates were segregated by species (bonnethead or non-bonnethead) to determine if misidentified decoys would lead to "class 1" or "class 2" misidentification. In this context, "class 1" would be the misidentification of a bonnethead as a non-bonnethead (Atlantic sharpnose), which would lead to a bias of underestimation of bonnethead abundance; whereas "class 2" would be the misidentification of a non-bonnethead as a bonnethead and lead to a bias of overestimation of bonnethead abundance. These rates were then aggregated by factor-level to look at effects of environmental parameters on misidentification. These groupings were also compared using non-parametric rank sum tests.

False detections were summed across scorers for each image, aggregated by factor-level and compared using non-parametric rank sum tests to examine possible environmental effects on perceiving sharks when they were not actually present, excluding decoy depth as we had no way to determine at what depth a falsely identified decoy was perceived. All statistical analyses and plotting of data were conducted in R (R Core Team 2016), using the following packages: *diplyr* (Wickham and Francois 2016), *tidyr* (Wickham 2017), *ggplot2* (Wickham 2009), and *rpart.plot* (Milborrow 2017).

Results

Detection probability for all 159 individual decoys ranged from 0 (never detected) to 1 (always detected), with an overall mean value of 0.27 ± 0.03 (mean and standard error). Mean detection probabilities for environmental factor combinations ranged from 0 to 0.96 (Table 4.2).

For the 73 decoys that were detected by at least one observer, individual misidentification rates also ranged from 0 (correctly identified by all scorers who detected) to 1 (misidentified by all scorers who detected), with an overall mean value of 0.24 $\pm$ 0.03 SE. Mean false detections for individual images ranged from 0 to 0.4, with an overall mean value of 0.04 $\pm$ 0.01 SE across 15 inspections of each photo.

Mean detection probability was negatively related to decoy depth ($X^2 = 49.61$, df = 2, $p < 0.001$), from 0.55 $\pm$ 0.05 SE at depths less than 0.6 m to 0.03 $\pm$ 0.02 SE at depths greater than 1 m (Figure 4.3). Mean detection probability increased from 0.14 $\pm$ 0.04 SE in the early morning period (before 10:30 am) to 0.38 $\pm$ 0.04 SE in the mid-day period (10:30am to 1:30 pm; $Z = -4.34$, $p < 0.001$) (Figure 4.3). Overall mean detection probability was higher on not cloudy days, 0.40 $\pm$ 0.08 SE compared to 0.26 $\pm$ 0.04 SE on cloudy days, although not well supported statistically ($Z = 1.5$, $p = 0.134$) (Figure 4.3). Conversely, mean detection probability trended lower with increasing mean wind speed, from 0.4 $\pm$ 0.08 SE at winds below 4 m s^{-1} to 0.14 $\pm$ 0.06 SE at winds above 8 m s^{-1}, although due to the high overall variability in the data, we failed to detect a statistically consistent difference ($X^2 = 3.08$, df = 2, $p = 0.215$) (Figure 4.3). The only factor that did not affect mean detection probability was filter ($X^2 = 0.67$, df = 2, $p = 0.713$) (Figure 4.3).

Higher detection probabilities (0.55 $\pm$ 0.05 SE) were associated with shallow depths (< 0.72 m). Within the shallow depths, the highest detection probabilities (0.78 $\pm$ 0.05 SE) were associated with low wind speed (< 4.2 m s^{-1}). At higher wind speeds ($\geq$ 4.2 m s^{-1}), there were also relatively high detection probabilities (0.62 $\pm$ 0.14 SE) associated with the shallowest depths (< 0.35 m). Detection probabilities were lower (0.22 $\pm$ 0.06 SE) when depths were intermediate

(< 0.72 m, ≥ 0.35 m), and with high wind speed (≥ 4.2 m s^{-1}). The lowest detection probabilities (0.05 ± 0.01 SE) were associated with the deepest depths (≥ 0.72 m) (Figure 4.4).

Misidentification rates yielded no clear patterns among factor-level comparisons or between 'species': time of day (class 1: Z = 0.99, p = 0.320/ class 2: Z = 0.09, p = 0.932), filter (class 1: X^2 = 1.08, df = 2, p = 0.582/ class 2: X^2 = 0.22, df = 2, p = 0.896), cloud presence (class 1: Z = 0.95, p = 0.342/class 2: Z = 0.26, p = 0.798), wind (class 1: X^2 = 1.6, df = 2, p = 0.450/ class 2: X^2 = 0.09, df = 2, p = 0.958), and decoy depth (class 1: X^2 = 0.92, df = 2, p = 0.631/ class 2: Z = -0.09, p = 0.932). We also failed to detect any clear patterns or meaningful differences in false detections by factor-levels: time of day (Z = 0.76, p = 0.450), filter (X^2 = 1.63, df = 2, p = 0.442), clouds (Z = 0.79, p = 0.427), and wind (X^2 = 1.47, df = 2, p = 0.478).

Discussion

By deploying shark decoys across multiple environmental contexts in a temperate estuary we demonstrated that UAS surveys, with the ability to target smaller areas with greater precision and at higher sampling frequencies relative to manned aircraft, may have potential for answering specifically targeted ecological questions about sharks in this and similar environmental systems. The main factor influencing detection probabilities in our study was decoy depth, constraining surveys to shallow water to reliably detect sharks. This is likely due to visibility bias from turbidity, as increases in turbidity increase the rate of light attenuation throughout the water column (Brown 1984), presumably leading to greater concealment of decoys at depth. Robbins et al. (2014) used shark decoys that were slowly raised from depths of at least 5 m until they became visible to estimate the depth at which the decoy could be seen from aerial surveys conducted via manned aircraft. In that study, water turbidity measurements were taken across

flight days using a secchi disk and were deeper than the average depth at which the decoys were observed, suggesting turbidity may not be the only factor affecting visibility bias (Robbins et al. 2014). Our study suggests time of day, wind, and cloud cover might be additional factors affecting visibility bias.

The comparison of time of day (morning vs. mid-day) showed significant differences in detection probability, with mean detection probability during mid-day over two times as high as during the morning. This result was somewhat surprising as we had hypothesized that the high solar altitude at mid-day would create more glare when photos were taken from overhead, thereby increasing visibility bias as decoys become concealed beneath the glare. Total solar irradiance reaches a maximum at noon and the reflectance of incident solar radiation increases with increasing zenith angle of incidence (Kirk 1994). This means that while there might be more glare from overhead during mid-day solar angles, there is also more light available and greater penetration into the water, which could increase visibility. There was a notable effect of wind on detection probabilities during mid-day, however, with high winds leading to mean detection probabilities less than half of those at lower winds; this could possibly be explained by the increased scattering of light at the surface and thus lower availability and penetration of light in the water column. The availability and penetration of light into the water also likely explains the increased detection probabilities on days with fewer clouds in the sky.

If a decoy was detected, it generally could be identified as a bonnethead or not in ~75% of cases, insensitive to environmental conditions at each decoy. Misidentification rates also do not appear to vary across bonnethead and non-bonnethead decoys, which means that biases towards overestimation and underestimation of bonnethead sharks would be driven mainly by imbalances in abundance of bonnethead vs. non-bonnethead species. Likewise, environmental variability

does not appear to significantly alter the possibility of a decoy being spotted where it does not actually exist. These results suggest that the main obstacle to reliable estimation of species abundance from aerial drone surveys is visibility bias due to shark depth, and the likely underestimation of true shark abundance in temperate estuaries based solely on aerial surveys.

While our secchi depth measurements provided a description of the range of visibility across our flight days, the frequency at which they were taken (once per flight day) was not sufficient to provide a proxy for turbidity that could be correlated with each of our survey flights, not to mention the potential for spatial differences across our flight areas. Nonetheless, our minimum secchi depth value (0.7 m) roughly coincides with the first split decision in our regression tree (0.72 m decoy depth). There is roughly a 5% chance that a decoy would be spotted at depths greater than 0.7 m; this is not surprising considering that this depth was the visibility minimum for our flight days.

Our study is bounded by some constraints that guide the foci of our broader conclusions regarding the role of UASs in shark surveys. Due to our focus on bonnethead sharks, we only included decoys of small sharks (~1 m), which could have an effect on detection probabilities. In addition, we chose to use still images rather than video, which, especially in the case of surveying living sharks, could potentially influence rates of detections and/or false detections. We also were unable to test for the effects of different types of substrate beneath our decoys on the detection probability. Presumably, different colors/textures would influence visibility bias depending on how they contrasted with the shark's countershading pattern, however it should be noted that in tropical high-transparency water, benthic characteristics had no effect on shark decoy detectability from drone surveys (Hensel et al. 2018). While our study was experimental in terms of our control of decoy placement, it was observational in terms of susceptibility to

unpredictable environmental changes, which limited our sample sizes for some environmental variables. Finally, mainly due to our study focusing on one UAS platform (fixed wing), the flight altitude was a variable we kept constant, which could certainly have an effect on detection probabilities due to changes in visibility and image resolution at increased altitudes.

In summary, our decoys demonstrated that drone surveys for sharks in a turbid, temperate estuary, such as the Newport River Estuarine System, probably only work in very shallow water (< 0.7 m). Because turbidity increases the rate of attenuation of light at depth, visibility bias of sharks is increased, particularly at depths that exceed the minimum visibility or secchi disk depth. Wind could be a mechanism that exacerbates this visibility bias as it causes further resuspension of solids and alters reflection and refraction of light at the surface. Increasing solar altitude, while potentially causing increased glare in photographs taken from overhead, also leads to increased light availability and penetration in the water column, which could positively affect the detection of sharks from UAS surveys. Our results are in agreement with Kiszka et al. (2016), who suggested that UASs are particularly attractive for investigating population trends and habitat use patterns where visibility enables animal detection from surface to bottom of the water column. As interest in this approach to monitor sharks in coastal environments for public safety is increasing, it is important to understand the limitations across different coastal environments, some of which can be quite turbid. We agree with Pollock et al. (2006), who suggest that standardized protocols and strict ceilings on acceptable survey conditions can reduce variation in detection probabilities. We suggest that in temperate estuarine systems, which can have high turbidity, UAS surveys may need to be restricted to areas where the depth is shallower than the visibility minimum.

ENDNOTES

[1]This chapter previously appeared as an article in the Journal of Unmanned Vehicle Systems. The original citation is as follows: Benavides, M. T., F. J. Fodrie, and D. W. Johnston. 2020. Shark detection probability from aerial drone surveys within a temperate estuary. Journal of Unmanned Vehicle Systems 8(1):44–56.

REFERENCES

Anderson, K., and K. J. Gaston. 2013. Lightweight unmanned aerial vehicles will revolutionize spatial ecology. Frontiers in Ecology and the Environment 11(3):138–146.

Bansemer, C. S., and M. B. Bennett. 2008. Multi-year validation of photographic identification of grey nurse sharks, Carcharias taurus, and applications for non-invasive conservation research. Marine and Freshwater Research 59(4):322–331.

Barlow, J. 2015. Inferring trackline detection probabilities, g(0), for cetaceans from apparent densities in different survey conditions. Marine Mammal Science 31(3):923–943.

Breiman, L., J. H. Friedman, R. A. Olshen, and C. I. Stone. 1984. Classification and regression trees. Chapman & Hall, Boca Raton, FL.

Brown, R. 1984. Relationships between suspended solids, turbidity, light attenuation, and algal productivity. Lake and Reservoir Management 1(1):198–205.

Buckland, S., D. Anderson, K. Burnham, and J. Laake. 2001. Introduction to distance sampling. Oxford University Press, Oxford.

Buckland, S. T., M. L. Burt, E. A. Rexstad, M. Mellor, A. E. Williams, and R. Woodward. 2012. Aerial surveys of seabirds: the advent of digital methods. Journal of Applied Ecology 49(4):960–967.

Caughley, G. 1974. Bias in aerial survey. The Journal of Wildlife Management 38(4):921–933.

Christie, K. S., S. L. Gilbert, C. L. Brown, M. Hatfield, and L. Hanson. 2016. Unmanned aircraft systems in wildlife research: current and future applications of a transformative technology. Frontiers in Ecology and the Environment 14(5):241–251.

Colefax, A. P., P. A. Butcher, D. E. Pagendam, and B. P. Kelaher. 2019. Reliability of marine faunal detections in drone-based monitoring. Ocean & Coastal Management 174:108–115.

Compagno, L., M. Dando, and S. Fowler. 2005. Sharks of the world. Princeton University Press, Princeton, New Jersey.

De'Ath, G., and K. E. Fabricius. 2000. Classification and regression trees: a powerful yet simple technique for ecological data analysis. Ecology 81(11):3178–3192.

Hensel, E., S. Wenclawski, and C. Layman. 2018. Using a small, consumer grade drone to identify and count marine megafauna in shallow habitats. Latin American Journal of Aquatic Research 46(5):1025–1033.

Hodgson, A., N. Kelly, and D. Peel. 2013. Unmanned aerial vehicles (UAVs) for surveying marine fauna: a dugong case study. PLoS ONE 8(11):e79556.

Hothorn, T., K. Hornik, M. A. van de Wiel, and A. Zeileis. 2008. Implementing a class of permutation tests: the coin package. Journal of Statistical Software 28(8).

Johnston, D. W. 2019. Unoccupied aircraft systems in marine science and conservation. Annual Review of Marine Science 11(1):439–463.

Jones, G. P. I., L. G. Pearlstine, and H. F. Percival. 2006. An assessment of small unmanned aerial vehicles for wildlife research. Wildlife Society Bulletin 34(3):750–758.

Kaschner, K., N. J. Quick, R. Jewell, R. Williams, and C. M. Harris. 2012. Global coverage of cetacean line-transect surveys: status quo, data gaps and future challenges. PLoS ONE 7(9):e44075.

Kirby-Smith, W. W., and J. D. Costlow. 1989. The Newport River Estuarine System. Available from the University of North Carolina Sea Grant, Beaufort, N. C. UNC Seagrant College Publication UNC-SG-89-04.

Kirk, J. T. O. 1994. Light and photosynthesis in aquatic ecosystems. Cambridge University Press, Cambridge, England.

Kiszka, J. J., J. Mourier, K. Gastrich, and M. R. Heithaus. 2016. Using unmanned aerial vehicles (UAVs) to investigate shark and ray densities in a shallow coral lagoon. Marine Ecology Progress Series 560:237–242.

Kohler, N. E., and P. A. Turner. 2001. Shark tagging: a review of conventional methods and studies. Environmental Biology of Fishes 60:191–223.

Marsh, H., and D. F. Sinclair. 1989. Correcting for visibility bias in strip transect aerial surveys of aquatic fauna. The Journal of Wildlife Management 53(4):1017–1024.

McClellan, C. M., T. Brereton, F. Dell'Amico, D. G. Johns, A.-C. Cucknell, S. C. Patrick, R. Penrose, V. Ridoux, J.-L. Solandt, E. Stephan, S. C. Votier, R. Williams, and B. J. Godley.

2014. Understanding the distribution of marine megafauna in the English Channel region: identifying key habitats for conservation within the busiest seaway on Earth. PLoS ONE 9(2):e89720.

Milborrow, S. 2017. rpart.plot: Plot “rpart” models: An enhanced version of “plot.rpart.” https://cran.r-project.org/package=rpart.plot.

Murtaugh, P. 2014. In defense of P values. Ecology 95(3):611–617.

Myrberg, A. a, and S. H. Gruber. 1974. The behavior of the bonnethead shark, Sphyrna tiburo. Copeia 1974(2):358–374.

NOAA. 2018. Water Levels - NOAA Tides & Currents. https://tidesandcurrents.noaa.gov/waterlevels.html?id=8656483.

Peterson, C. D., C. N. Belcher, D. M. Bethea, W. B. Driggers, B. S. Frazier, and R. J. Latour. 2017. Preliminary recovery of coastal sharks in the south-east United States. Fish and Fisheries 18(5):845–859.

Pollock, K. H., H. D. Marsh, I. R. Lawler, and M. W. Alldredge. 2006. Estimating animal abundance in heterogeneous environments: an application to aerial surveys for dugongs. The Journal of Wildlife Management 70(1):255–262. John Wiley & Sons, Ltd.

QGIS Development Team. 2018. QGIS geographic information system. Open source geospatial foundation project. http://qgis.osgeo.org.

R Core Team. 2016. R: A language and environment for statistical computing. http://www.r-project.org.

Rees, A., L. Avens, K. Ballorain, E. Bevan, A. Broderick, R. Carthy, M. Christianen, G. Duclos, M. Heithaus, D. Johnston, J. Mangel, F. Paladino, K. Pendoley, R. Reina, N. Robinson, R. Ryan, S. Sykora-Bodie, D. Tilley, M. Varela, E. Whitman, P. Whittock, T. Wibbels, and B. Godley. 2018. The potential of unmanned aerial systems for sea turtle research and conservation: a review and future directions. Endangered Species Research 35:81–100.

Revelle, W. 2017. psych: procedures for personality and psychological research. https://cran.r-project.org/package=psych.

Robbins, W. D., V. M. Peddemors, S. J. Kennelly, and M. C. Ives. 2014. Experimental evaluation of shark detection rates by aerial observers. PLoS ONE 9(2):e83456.

Rowat, D., M. Gore, M. G. Meekan, I. R. Lawler, and C. J. A. Bradshaw. 2009. Aerial survey as a tool to estimate whale shark abundance trends. Journal of Experimental Marine Biology and Ecology 368(1):1–8.

Sweeney, K. L., V. T. Helker, W. L. Perryman, D. J. LeRoi, L. W. Fritz, T. S. Gelatt, and R. P. Angliss. 2015. Flying beneath the clouds at the edge of the world: using a hexacopter to supplement abundance surveys of Steller sea lions (Eumetopias jubatus) in Alaska. Journal of Unmanned Vehicle Systems 4(1):70–81.

Therneau, T., B. Atkinson, and B. Ripley. 2015. rpart: recursive partitioning and regression trees. https://cran.r-project.org/package=rpart.

Weather Underground. 2011. Weather Underground: forecasts. https://play.google.com/store/apps/details?id=com.wunderground.android.weather.

Wickham, H. 2009. ggplot2: Elegant graphics for data analysis. http://ggplot2.org.

Wickham, H. 2017. tidyr: easily tidy data with “spread()” and “gather()” functions. https://cran.r-project.org/package=tidyr.

Wickham, H., and R. Francois. 2016. diplyr: A grammar of data manipulation. https://cran.r-project.org/package=dplyr.

Table 4.1: Summary of environmental conditions and flight times for each flight date. Times are either reported in Eastern Daylight Time (EDT) or Eastern Standard Time (EST).

Flight date	Cloud cover	Wind speed (m s^{-1})	Secchi depth (m)	Approximate local flight times
22 Oct 2015	N	2-5	1.24	9:30, 12:30, 16:00 EDT
11 Mar 2016	Y	4-9	1.6	10:00, 12:00 EST
16 May 2016	N	2-5	1.15	10:40 EDT
29 Sep 2016	Y	3-5	0.7	8:30, 11:30 EDT
27 Oct 2016	Y	4	0.97	13:00 EDT

Table 4.2: Summary of treatment factor-level combinations with mean and standard error computed across all decoys within each treatment.

Treatment	Time of day	Filter	Clouds	Mean wind speed (m s^{-1})	Secchi depth (m)	Decoy depth (m)	Mean detection probability	Standard error
1	< 10:30 am	NIR	N	< 4	1 - 1.5	< 0.6	0.17	0.17
2	10:30 am - 1:30 pm	NIR	N	< 4	1 - 1.5	< 0.6	0.87	0.11
3	< 10:30 am	RE	N	< 4	1 - 1.5	< 0.6	0.56	0.28
4	10:30 am - 1:30 pm	RE	N	< 4	1 - 1.5	< 0.6	0.87	0.13
5	< 10:30 am	NIR	N	< 4	1 - 1.5	0.6 - 1	0.00	0.00
6	10:30 am - 1:30 pm	NIR	N	< 4	1 - 1.5	0.6 - 1	0.24	0.21
7	< 10:30 am	RE	N	< 4	1 - 1.5	0.6 - 1	0.00	0.00
8	10:30 am - 1:30 pm	RE	N	< 4	1 - 1.5	0.6 - 1	0.00	0.00
9	10:30 am - 1:30 pm	NIR	N	< 4	1 - 1.5	> 1	0.02	0.02
10	10:30 am - 1:30 pm	RE	N	< 4	1 - 1.5	> 1	0.00	0.00
11	10:30 am - 1:30 pm	RGB	Y	> 8	> 1.5	< 0.6	0.18	0.09
12	< 10:30 am	RGB	Y	4 - 8	> 1.5	0.6 - 1	0.01	0.01
13	10:30 am - 1:30 pm	RGB	Y	> 8	> 1.5	0.6 - 1	0.05	0.03
14	< 10:30 am	NIR	Y	4 - 8	> 1.5	0.6 - 1	0.03	0.03
15	< 10:30 am	RE	Y	4 - 8	> 1.5	0.6 - 1	0.12	0.12
16	< 10:30 am	RGB	Y	4 - 8	> 1.5	> 1	0.00	0.00
17	10:30 am - 1:30 pm	RGB	Y	> 8	> 1.5	> 1	0.23	0.23
18	< 10:30 am	NIR	Y	4 - 8	> 1.5	> 1	0.05	0.05
19	< 10:30 am	RE	Y	4 - 8	> 1.5	> 1	0.00	0.00
20	10:30 am - 1:30 pm	RGB	N	< 4	1 - 1.5	< 0.6	0.96	0.02
21	10:30 am - 1:30 pm	RGB	N	< 4	1 - 1.5	0.6 - 1	0.0667	0.0667
22	< 10:30 am	RGB	Y	4 - 8	1 - 1.5	0.6 - 1	0.67	0.33
23	< 10:30 am	RGB	Y	4 - 8	1 - 1.5	> 1	0.01	0.01
24	< 10:30 am	RE	Y	4 - 8	1 - 1.5	0.6 - 1	0.67	0.33
25	< 10:30 am	RE	Y	4 - 8	1 - 1.5	> 1	0.00	0.00
26	< 10:30 am	NIR	Y	4 - 8	1 - 1.5	0.6 - 1	0.64	0.32
27	< 10:30 am	NIR	Y	4 - 8	1 - 1.5	> 1	0.05	0.04
28	10:30 am - 1:30 pm	RGB	Y	4 - 8	< 1	< 0.6	0.80	0.20
29	10:30 am - 1:30 pm	RGB	Y	4 - 8	< 1	0.6 - 1	0.07	0.05
30	10:30 am - 1:30 pm	RE	Y	4 - 8	< 1	< 0.6	0.92	0.06
31	10:30 am - 1:30 pm	RE	Y	4 - 8	< 1	0.6 - 1	0.10	0.08
32	10:30 am - 1:30 pm	NIR	Y	4 - 8	< 1	< 0.6	0.68	0.14
33	10:30 am - 1:30 pm	NIR	Y	4 - 8	< 1	0.6 - 1	0.11	0.08
34	10:30 am - 1:30 pm	RGB	Y	4 - 8	1 - 1.5	< 0.6	0.51	0.18
35	10:30 am - 1:30 pm	NIR	Y	4 - 8	1 - 1.5	< 0.6	0.26	0.12
36	10:30 am - 1:30 pm	RE	Y	4 - 8	1 - 1.5	< 0.6	0.51	0.20

Figure 4.1: Photograph of live bonnethead (bottom left corner) and bonnethead decoy (slightly off-center) taken at the North Carolina Aquarium at Pine Knoll Shores.

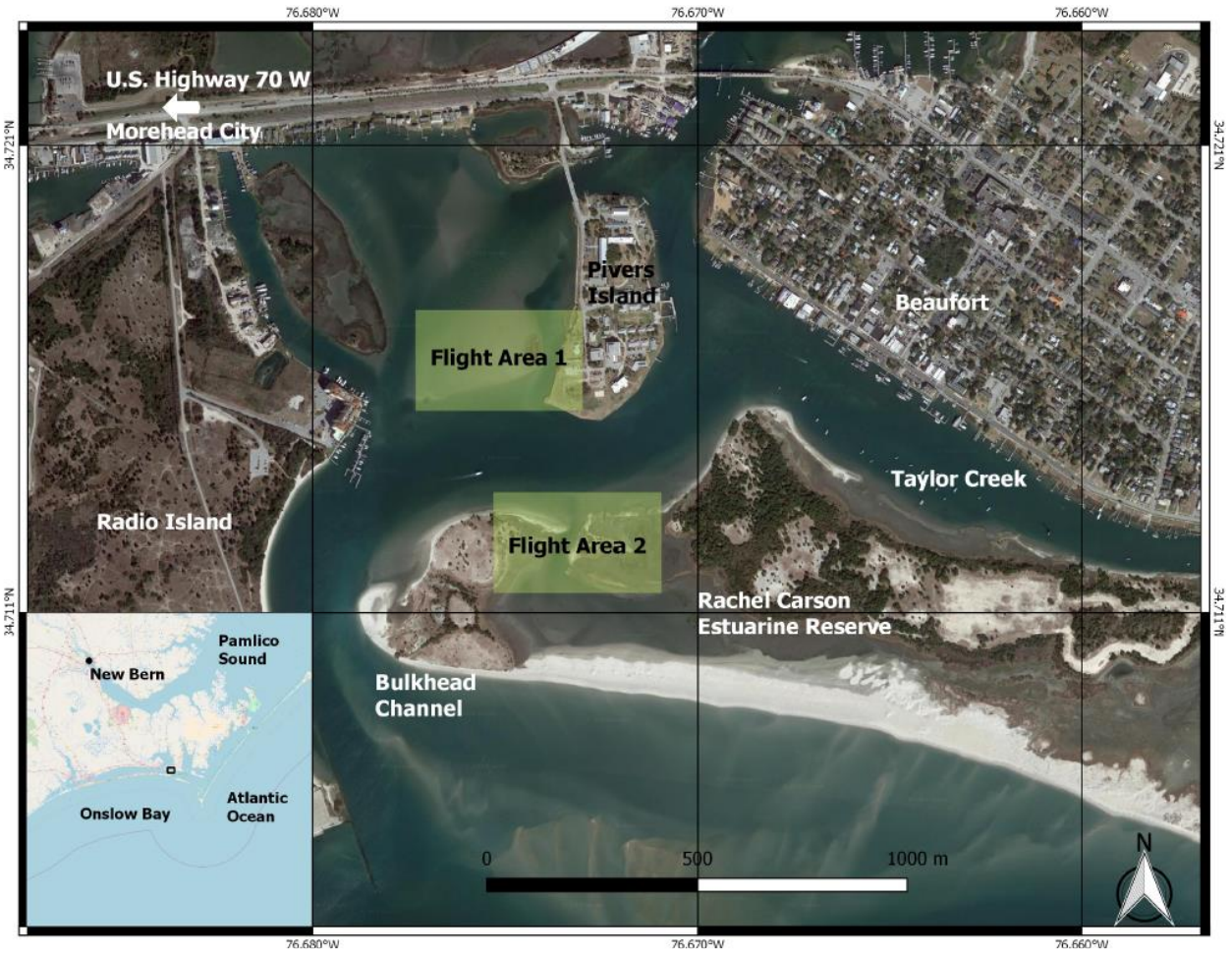

Figure 4.2: Map of study area in Eastern North Carolina with flight areas highlighted in yellow. Map was created using QGIS (QGIS Development Team 2018). Map data: © 2018 Google; © OpenStreetMap contributors.

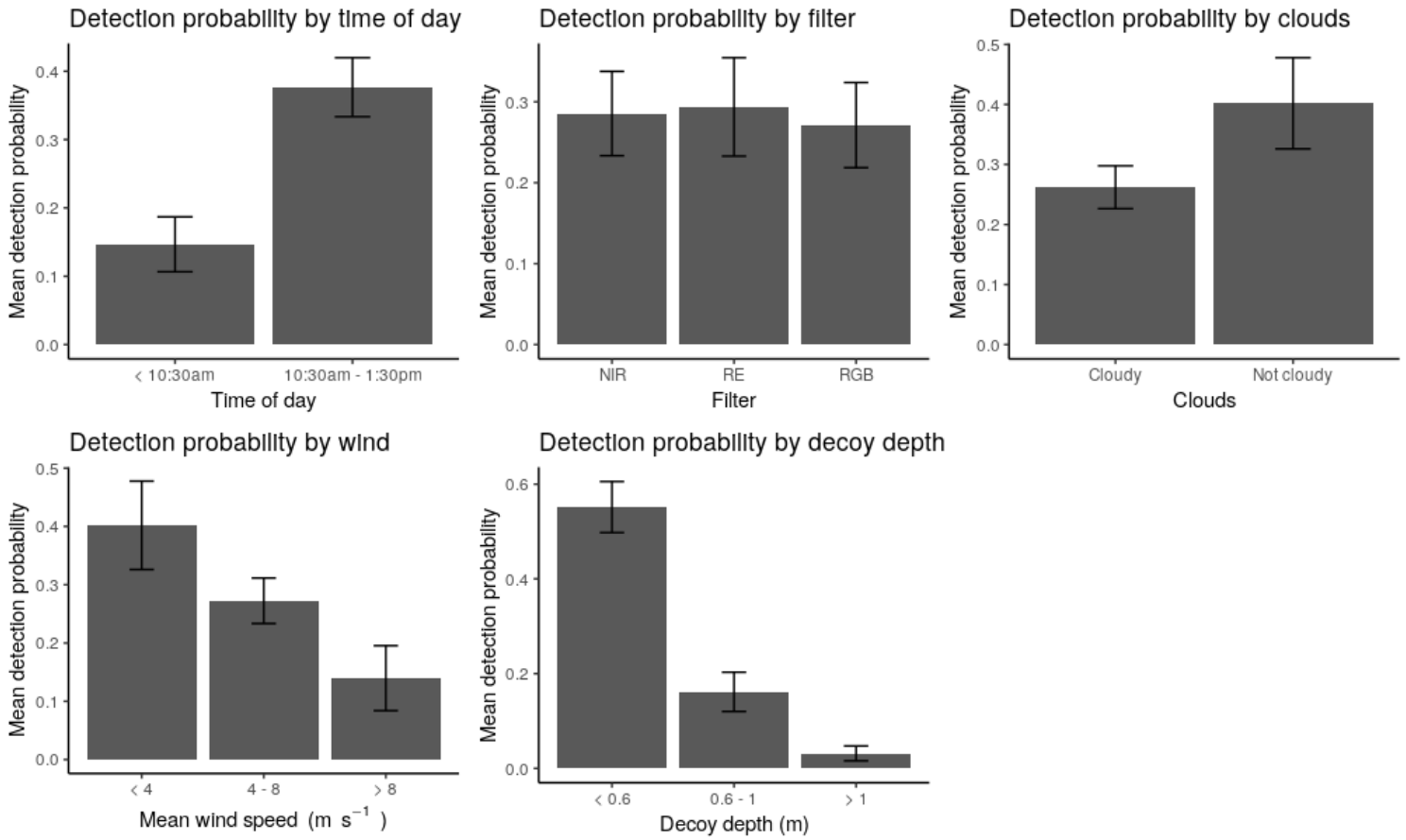

Figure 4.3: Factor-level comparisons for detection probabilities related to each of the 5 factors. Data are presented as mean detection probability + 1 SE.

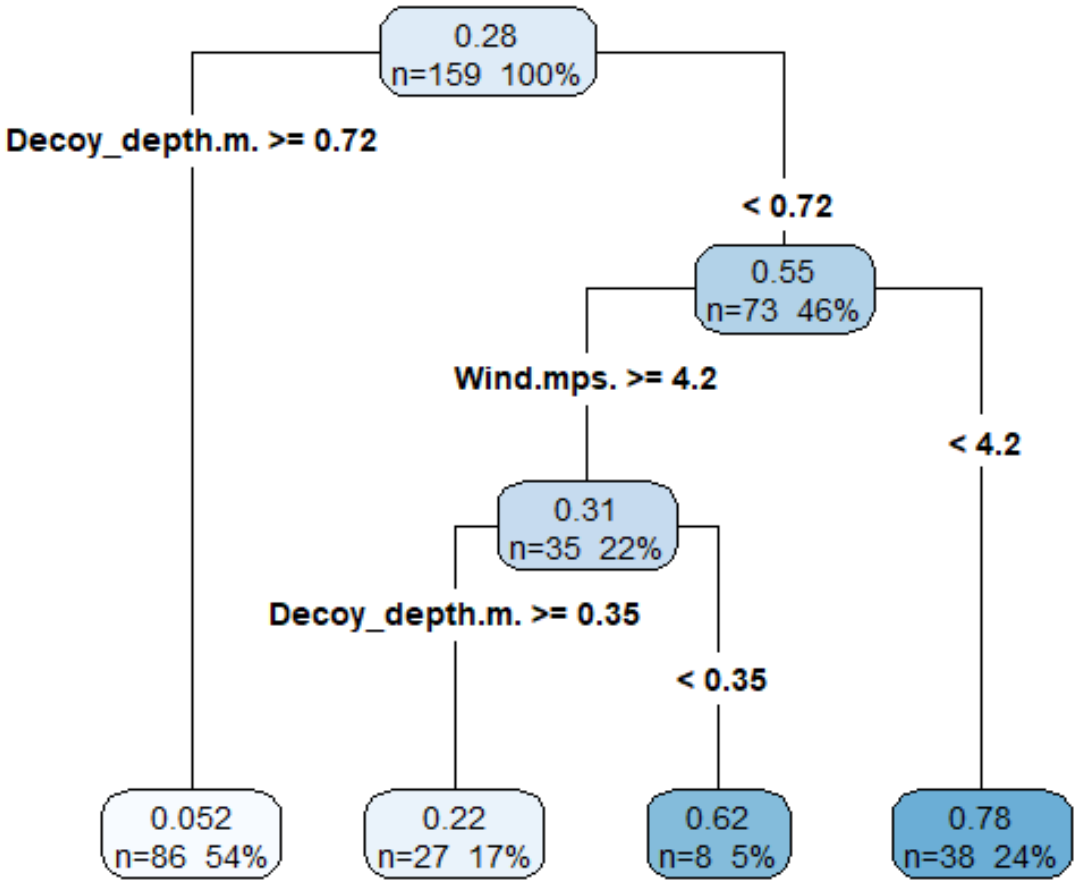

Figure 4.4: Regression tree showing split decisions as well as mean detection probability (#.##) at each node and leaf. Also shown are the number of cases in each node as a raw number (n) and percentage (%) out of 159 total decoys in images.